Standard spines and 3-manifolds

Carlo Petronio

February 10, 1999

Contents

Preface

In recent years invariants of three-dimensional manifolds and links embedded in three-manifolds have attracted considerable attention from mathematicians and physicists, in particular after the discovery that notions and techniques from theoretical physics and algebra can be used in the apparently less-structured field of low-dimensional dimensional topology to produce very deep new results. In general the starting point of the definition and existence theorem of an invariant is a presentation for the objects in the class under consideration, and a calculus for this presentation. More precisely one has a class of "concrete" objects (e.g. finite graphs with some additional structure and property), a rule to associate a three-manifold (or a link in a three-manifold) to each object, and a set of moves such that if two objects define the same three-manifold (or link) then they are obtained from each other by a finite sequence of these moves. To mention two examples of this scheme, we have the presentation of links in the three-sphere by planar projections with the Reidemeister moves, and the surgery presentation of closed oriented three-manifolds with the Kirby calculus. In this work I provide a calculus for compact three-manifolds with boundary based on standard spines, and discuss related questions; in particular I introduce a general framework for the definition of invariants based on this calculus.

I briefly sketch now the results obtained in this work and refer the reader to the introductions of the various chapters for more detailed descriptions and comments.

A standard spine of a connected three-dimensional compact PL manifold with non-empty boundary is a purely two-dimensional subpolyhedron which is a deformation retract of the manifold, has singularities which are stable in nature and has non-singular components which are discs (in other words, all the topology lives "near" the singularity). Standard spines have been known to exist and completely determine their manifold for about thirty years, after Casler's original work. Moreover about ten years ago Matveev and Piergallini have found a calculus for standard spines (in the sense mentioned above). In Chapter I of this thesis I introduce a presention of standard spines by means of finite planar graphs with some additional structure, and discuss the resulting calculus. The idea of this presentation is actually quite easy: one just embeds in the three-space the singular set of the spine "as planarly as possible", and then he reads the way the discs are glued to the singular set by means of permutations attached to the edges. For the case of oriented spines and the oriented calculus (which are new and introduced in Chapter I as well), the presentation becomes particularly nice. I call o-graphs the graphs (with additional structure) by which I present compact oriented three-manifolds with boundary.

O-graphs are a particularly easy way to present standard spines, which in turn are a very nice way to present three-manifolds (at least from my point of view), because they allow to visualize very well the manifold they define (remark in particular that a standard spine determines a decomposition of its manifold as a union of closed three-balls glued to each other along two-balls contained in the boundary). This makes o-graphs a rather versatile tool for facing topological and geometric questions concerning three-manifolds. An example of this fact is provided in Chapter II, where I describe an algorithm which associates to an o-graph of a manifold bounded by tori the system of Thurston's hyperbolicity equations for the manifold.

Chapter III is devoted to the relations between the o-graph presentation and other presentations. In particular I provide an algorithm which translates a surgery presentation of a closed oriented three-manifold into an o-graph of the punctured manifold, and an algorithm which translates such an o-graph into a Heegaard splitting of the manifold (this, together with Rourke's "constructive" proof of existence of surgery presentations, gives a circular diagram of translations of presentations into one another). I also show how to construct an o-graph of a link complement in the three-sphere and how to perform a connected sum of o-graphs.

Chapter IV contains the definition of two classes of invariants associated to the presentation by o-graphs. They are called bracket invariants because they mimic the definition of the bracket of a link projection in that they satisfy linear skein relations. The definition of the bracket is a rather natural one because o-graphs have considerable formal analogies with link projections. Bracket invariants are polynomials whose computation relies on tools of computer algebra and is therefore algorithmic (even though complexity is apparently overwhelming after the first few trivial cases). Since the Turaev-Viro invariants appear as bracket invariants, these theoretically computable invariants are indeed non-trivial. I should also mention that the Turaev-Viro invariants are presently the only non-trivial examples of bracket invariants. I could say that the bracket approach provides a general framework into which some algebraic theory must be placed to obtain actual invariants of three-manifolds: the theory of quantum symbols is contained in the framework, and the hope is that some other theory will give new invariants. Chapter IV also contains the proof that, under a very natural assumption, bracket invariants are multiplicative under connected sum, and the discussion of some computer experiments.

It should be mentioned that Chapter I and part of Chapter IV (in particular the definition of bracket invariants) are essentially drawn from a paper of mine and Prof. Benedetti [Be-Pet2], whereas Chapters II and III and the remaining part of Chapter IV (in particular the definition of hyperlocal bracket invariants and the proof that the Turaev-Viro invariants are of this type) are original with this thesis. I also want to mention that our use of o-graphs as a versatile tool for facing questions about three-manifolds and their invariants has continued beyond this thesis, and has led in particular to a note [Be-Pet3] concerning the recent proof of Justin Roberts of the known fact that the Turaev-Viro invariant is the squared module of the Reshetikhin-Turaev-Witten invariant.

I wish to thank the people who have helped me during the writing of this thesis and earlier in my professional life. In particular I express my gratitude to Prof. Edoardo Vesentini, under the supervision of whom I moved my first steps in the mathematical community, and who has always been, and still is, a very precious source of advice. I also want to mention my colleagues and close friends Chiara de Fabritiis, Marco Manetti and Mario Tessitore for the beautiful years spent together at the Scuola Normale Superiore, and for the mutual help we have always given each other. Thanks also go to the Scuola Normale Superiore itself for having provided such a stimulating mathematical environment. I am indebted to Prof. David Epstein for the friendful help he gave me during the year I spent as a visitor at the University of Warwick.

More strictly related to this work is my gratitude towards Prof. Michel Boileau and Prof. Hugh Morton, who accepted to report on it and provided helpful suggestions and remarks. I also thank Carlo Traverso, Francesco Amoroso, Barry Trager and Patrizia Gianni for their help in carrying out the computer experiments referred to in Chapter IV. I am grateful to Jeff Weeks for some interesting discussions concerning ideal triangulations of cusped hyperbolic manifolds (even if this did not influence very much the thesis itself). I acknowledge the Fondazione F. Severi, Arezzo, Italy, for the generous grant by which I was supported during the writing of this thesis. Finally, I wish to thank my advisor and friend Riccardo Benedetti, with whom this work has been thoroughly discussed (and partially co-produced). Talking of mathematics (and other things) with him has been a constant source of pleasure during this work.

This thesis is dedicated to my wife Elisa.

Chapter I

Graphic presentation

In this chapter we provide a presentation for compact oriented 3-manifolds with non-empty boundary up to orientation-preserving homeomorphism via a calculus on suitable finite (planar) graphs with extra structure ("decorated graphs"). We call our graphs "o-graphs" to emphasize that they also encode orientation. Closed manifolds are included in our presentation by removal of a 3-ball.

Decorated graphs have an intrinsic geometric counterpart, as they are actually obtained by considering standard spines of the manifold and extra structure on them ("decorated spines"). The calculus on graphs is derived from the Matveev-Piergallini moves on standard spines ([Ca], [Mat2], [Mat3], [Pi]) which we re-examine and adapt to our setting (in particular in Section 1 we establish an oriented theory). To discuss these ideas we will use both the point of view of decorated graphs and of decorated spines: the former is suitable for automatic approaches and the latter gives a better insight to the geometric situation.

A comparison with the presentation of closed 3-manifolds via surgery on framed links in S^3 and the corresponding Kirby calculus [Ki], [Fen-Rou] allows us to single out peculiarities of our graphic calculus. If one represents links by generic projections there are formal analogies between the two presentations, in particular both are supported by quadrivalent planar graphs with simple normal crossings and both express the change of orientation on manifolds by a simple involution on the set of graphs. The main differences are that edge-colours are taken in $\mathbb{Z}$ for framed links and in $\mathbb{Z}_3$ for us, and that our moves are local and *finite*, while the Kirby move depends on the number of strands involved, which can be arbitrarily many.

There exists another graphic calculus for 3-manifolds essentially based on the Matveev-Piergallini calculus, called the calculus on 3-gems (graph encoded 3-manifolds) [Ka-Li], [Fer-Gag], [Li-Man]. O-graphs and 3-gems are different objects and the topological constructions by which manifolds are associated to them are different. Moreover presentations via o-graphs and via 3-gems have essentially different features which we shortly mention:

1. The input data of an o-graph does not need to satisfy any combinatorial condition, which is not the case for 3-gems; in particular, using o-graphs, we can enumerate (with repetitions) all (possibly disconnected) oriented compact 3-manifolds in which all the components have boundary by means of the following set:

$$\{(n,p,c):\ n\in\mathbb{N}, p \text{ partition of } \{1,...,4n\} \text{ into pairs}, c\in(\mathbb{Z}_3)^n\}.$$

   On the contrary it is not so direct (but of course also not so difficult) to give a complete list of all 3-gems, because one has to verify certain combinatorial conditions on the coloration.

2. In the presentation via 3-gems orientability (in particular, orientation) is encoded by a specific additional structure, whereas it naturally comes with the definition in the presentation via o-graphs;

3. Presentation via o-graphs contains the idea of embedding parts of the manifold in $\mathbb{R}^3$, which is useful in various contexts (see e.g. Section III.2).

In this work we will be mostly concerned with the oriented case, but we also provide a presentation for non-oriented manifolds.

* * *

For the reader's convenience we state the main result which we will establish in this chapter.

We start by introducing a few definitions. In the whole work by "graph" we will always mean a 1-dimensional simplicial complex, i.e. we accept circular edges (edges having coincident endpoints) and parallel edges (multiple edges having the same endpoints). Consider a finite planar quadrivalent graph Γ in which vertices are drawn as crossings, and assume that some vertices of Γ are marked. In the sequel given such a graph we will always call "edges" of Γ those obtained by ignoring the vertices which are not marked (in other words, edges are locally embedded segments which cross non-marked vertices in the natural way and have marked endpoints). Remark that edges might well not cover the graph.

We define an o-graph to be the datum of:

1. A finite planar quadrivalent graph Γ with some marked vertices, where Γ is edge-connected in the sense just stated (in particular there is at least one marked vertex, and the edges cover Γ);

2. An under-over specification (as in the usual projections of links) at each marked vertex of Γ;

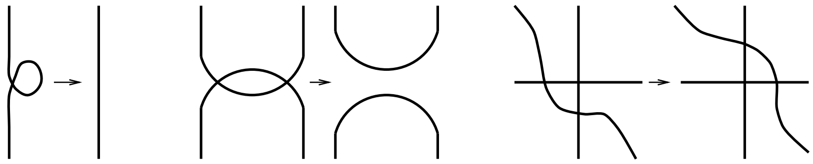

Figure I.1: These moves are called respectively $\mathrm{R_I}$, $\mathrm{R_{II}}$ and $\mathrm{R_{III}}$

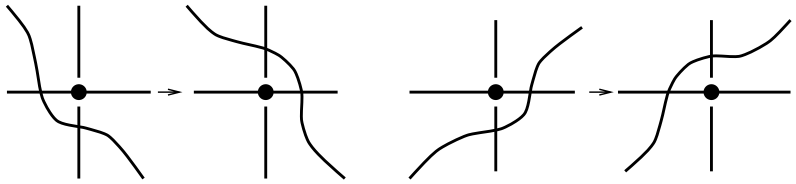

Figure I.2: These moves are called respectively $\mathrm{R'_{III}}$ and $\mathrm{R''_{III}}$

3. A colour chosen in $\mathbb{Z}_3$ attached to every edge of Γ.

We will always refer to Γ itself as an o-graph.

We will establish the following:

Theorem I.0.1. *To every o-graph there corresponds an oriented compact connected three-dimensional manifold with non-empty boundary well-defined up to orientation-preserving homeomorphism. Moreover:*

1. *Every such manifold is obtained from some o-graph with at least two marked vertices.*

2. *There exists an orientation-preserving homeomorphism between the manifolds associated to two o-graphs with at least two vertices if and only if the two o-graphs, regarded up to isotopies of the plane, are obtained from each other by a finite sequence of moves as shown in Figg. I.1 to I.4, and inverses of these moves.*

3. *Let an oriented manifold be associated to an o-graph. The same manifold with the opposite orientation is associated to an o-graph obtained as follows from the original one:*

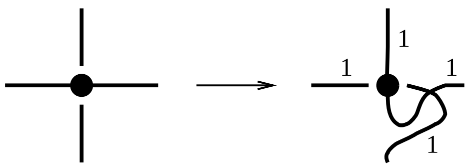

Figure I.3: This move is called C. Here the convention is that to a certain edge it is equivalent to attach a colour i or many colours whose sum modulo 3 is i; in other words multiple colours can be summed up

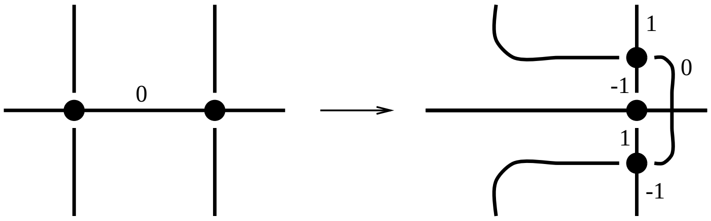

Figure I.4: This move is called MP. Same convention as above about sums of colours

(a) At every marked vertex reverse the under-over specification.

(b) Change the colour of every edge to its inverse (in $\mathbb{Z}_3$).

The topological construction which underlies Theorem I.0.1 (in other words, the strategy of its proof) is the following: given an o-graph Γ we define a standard polyhedron P, where the singular set of P is Γ itself and a neighbourhood of this singular set is embedded in $\mathbb{R}^3$ in a way prescribed by the colours of Γ. It turns out that P is in a natural way an *oriented* standard polyhedron (in a sense defined below) and therefore is a standard spine of an oriented manifold. Moreover every embedding in $\mathbb{R}^3$ of the neighbourhood of the singular set of an oriented standard polyhedron is encoded by some o-graph. Planar isotopy and the moves shown in Figg. I.1 to I.3 relate to each other any two o-graphs of the same oriented standard polyhedron, whereas the move of Fig. I.4 translates in terms of o-graphs the *oriented* Matveev-Piergallini move (defined below), which relates to each other any two standard spines of the same oriented manifold.

Theorem I.0.1 will be proved in Section I.3. The discussion in Sections I.1 and I.2 actually concerns also the case of non-oriented manifolds.

Let us remark that planarity of the graphs with which we represent manifolds is not a completely intrinsic fact, but we have decided to include this assumption in the definition of o-graphs because it allows us to deal with very concrete objects. The reader will see from the way these graphs are introduced that they should actually be considered only "locally planar" near marked vertices. However we also remark that planarity allows the easy description we have given for the move MP, while for locally planar graphs this would become more awkward.

I.1 Standard spines and orientation

In this section we state a few facts about standard polyhedra and spines of 3-manifolds. Some of these facts were known, and we recall them with minor differences. On the other hand we could not find in the literature the oriented version of this theory: we are going to establish it here.

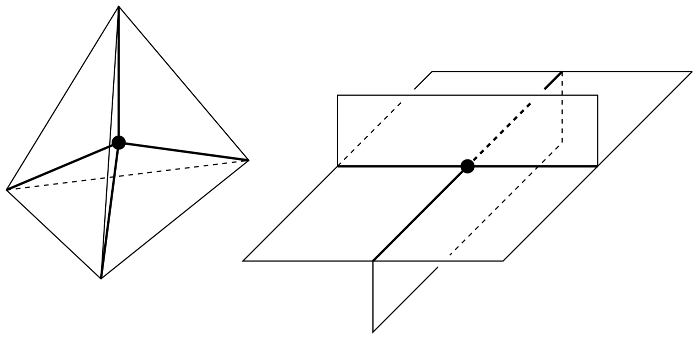

Figure I.5: Two descriptions of the neighbourhood of a vertex in a standard spine

Throughout this work we operate in the PL category, without further explicit mention: the basic notions, including that of collapse which we will need, can be found in [Rou-Sa]. A compact connected 2-dimensional polyhedron P is called quasi-standard if each point in it has a neighbourhood homeomorphic either to a plane, or to the union of three half-planes with common boundary line, or to the infinite cone over the 1-skeleton of a tetrahedron with vertex the barycentre of the tetrahedron (for further reference we show in Fig. I.5 such a set). The singular set $S(P)$ and the set of vertices $V(P)$ of a quasi-standard polyhedron are naturally defined. We say that P is standard if the components of $P \setminus S(P)$ are discs and the components of $S(P) \setminus V(P)$ are segments.

Lemma I.1.1. *A quasi-standard polyhedron P is standard if and only if the components of $P \setminus S(P)$ are discs and $V(P) \neq \emptyset$.*

Proof of I.1.1. If P is quasi-standard and the components of $P \setminus S(P)$ are discs then $S(P)$ is a connected graph (P is connected and a path in a disc can be pushed to the boundary, which is contained in the singular set); so $S(P) \setminus V(P)$ consists of segments if and only if $V(P) \neq \emptyset$. $\boxed{\text{I.1.1}}$

We call P a standard spine of a compact 3-manifold M if P is a standard polyhedron and there exists an embedding $i : P \to \mathrm{int}(M)$ such that M collapses onto $i(P)$. The following was established by Casler in [Ca] (see also [Mat1] for a generalization to all dimensions):

Theorem I.1.2. *Every connected compact 3-manifold with non-empty boundary admits a standard spine. Two 3-manifolds with homeomorphic standard spines are homeomorphic.*

According to this result if P is a standard spine of a manifold M we are allowed to define $M = \mathcal{M}(P)$. However $\mathcal{M}$ is not defined for all standard polyhedra (*cf.* Theorem I.1.6 below).

The following result was independently established by Matveev [Mat2], [Mat3] and Piegallini [Pi].

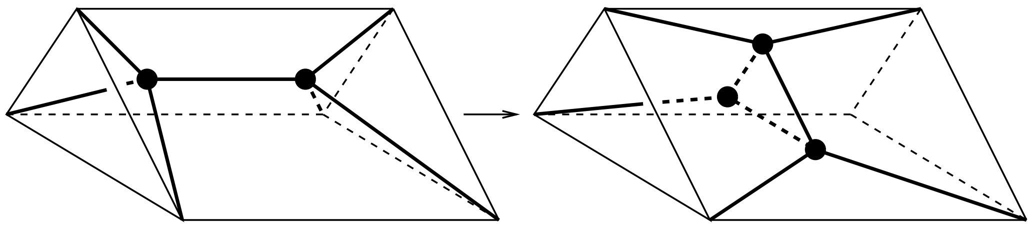

Figure I.6: The Matveev-Piergallini move; from this description it is evident that it depends only on an edge with distinct endpoints

Theorem I.1.3. *Every compact* 3*-manifold with non-empty boundary has a standard spine with at least two vertices. Standard spines with at least two vertices of homeomorphic manifolds are obtained from each other by a finite sequence of moves as shown in Fig. I.6, and inverses of it.*

Actually Matveev's result involves another move, but Piergallini's proof of sufficiency of the move of Fig. I.6 in presence of at least two vertices is correct. It is quite surprising that apparently all the authors who have used the Matveev-Piergallini calculus have ignored Piergallini's remark that essentially one move is sufficient (see [Ka-Li], [Tur-Vi]). For this reason we will reproduce with some detail, as an appendix to this section, Piergallini's proof that the second of Matveev's moves is actually deduced from the move of Fig. I.6.

We want to characterize standard polyhedra which are spines. Before stating the result (Theorem I.1.6) we need a few preliminaries.

Given a standard polyhedron we can cut out the discs close enough to the singular set so that what is left can be cut into finitely many pieces of "typical"' shape. The following long statement gives a precise definition of this procedure and collects all the properties we will use. The proof is straight-forward.

Lemma I.1.4. *Let P be a standard polyhedron, with $P \setminus S(P)$ consisting of d discs. There exist subpolyhedra $\mathcal{J}$ and $\mathcal{Y}$ of P such that:*

1. *$\mathcal{J}$ has d components $J_1, ..., J_d$ which are circles in $P \setminus S(P)$;*

2. *$P \setminus \mathcal{J}$ has $d+1$ components, one containing $S(P)$ and the other d homeomorphic to discs and contained one in each component of $P \setminus S(P)$;*

3. *$\mathcal{Y}$ is contained in the closure U of the component of $P \setminus \mathcal{J}$ which contains $S(P)$;*

4. *The components $Y_1, ..., Y_t$ of $\mathcal{Y}$ are "triods" (we call the cone over the discrete space consisting of* 3 *points a triod);*

5. *For $i = 1, ..., t$ we have:*

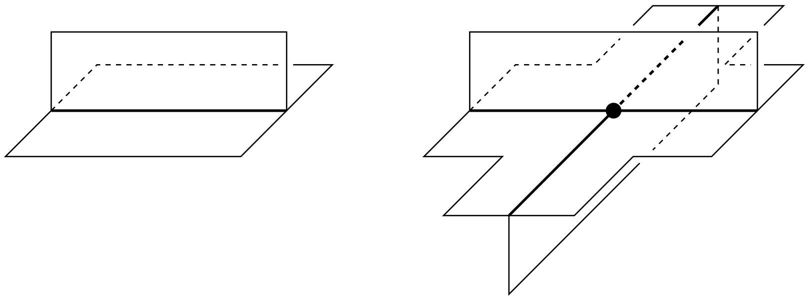

Figure I.7: Two "typical shapes" occurring in a standard polyhedron (the third shape is the disc)

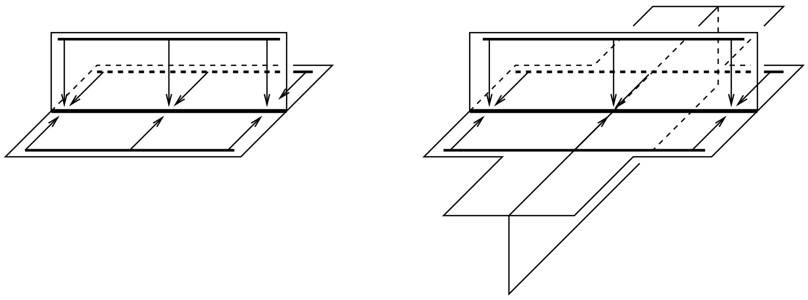

Figure I.8: Definition of a D_3-bundle on S^1 associated to a local embedding j; the thick line is a portion of j and the little arrows define the projection of the bundle

(a) $Y_i \cap V(P) = \emptyset$;

(b) $Y_i \cap S(P)$ *is the "centre" of* Y_i *(the only point removing which it falls into three pieces);*

(c) $Y_i \cap \mathcal{J}$ *consists of the three points which do not disconnect* Y_i;

6. *The closure of each component of* $U \setminus \mathcal{Y}$ *is homeomorphic to one of the spaces shown in Fig. I.7, and two such components intersect at most in a common* Y_i.

In the sequel will denote by D_3 the discrete space containing three points.

Lemma I.1.5. *To every local embedding* $j : S^1 \to S(P)$ *we can associate a* D_3*-bundle on* S^1 *denoted by* B_j *as explained in Fig. I.8.*

Proof of I.1.5. We only need to remark that, thanks to the symmetries of a typical neighbourhood of a vertex, when j crosses a vertex the situation can always be realized as shown on the right-hand side of Fig. I.8. $\boxed{\text{I.1.5}}$

The first part of the following result was established (in a different form) in [Mat1] and quoted in the present form in [Pi]. We include the proof for completeness and because the machinery is used elsewhere. As far as we know the second part was never observed before.

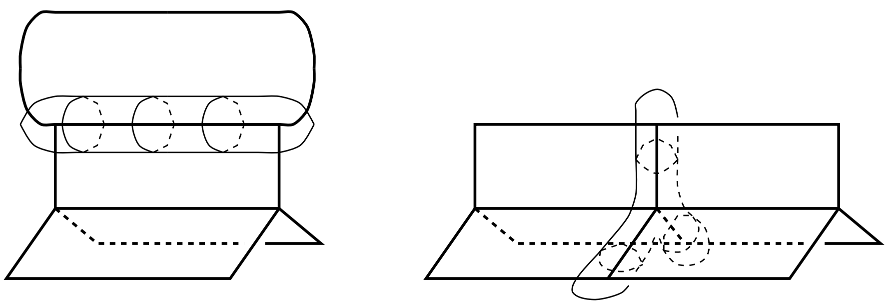

Figure I.9: The intersection of the neighbourhoods we have chosen

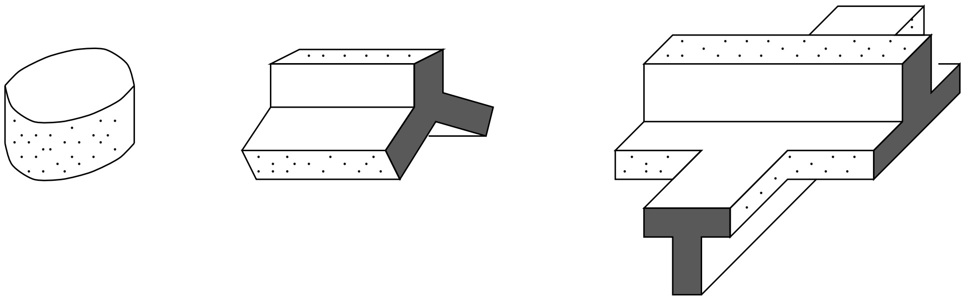

Figure I.10: The thick pieces which glue up to give a neighbourhood of P

Theorem I.1.6. *Let P be a standard polyhedron.*

(A) P is a standard spine of a manifold if and only if for any disc D of $P \setminus S(P)$, if $j : S^1 \to S(P)$ describes how D is attached to $S(P)$, then the D_3-bundle B_j is trivial.

(B) P is the standard spine of an orientable manifold if and only if for every embedding $j : S^1 \to S(P)$ the D_3-bundle B_j has 1 or 3 components.

Proof of I.1.6. (A) We start with the "only if" part. We can perform the construction of $\mathcal{J}$ and $\mathcal{Y}$ of Lemma I.1.4 within M. Let D_i be the closure of the i-th disc component of $P \setminus \mathcal{J}$ $(i = 1, ..., d)$; D_i is a closed disc embedded in $\mathrm{int}(M)$, so it has a neighbourhood W_i in M homeomorphic to a ball. For every component C_k of $U \setminus \mathcal{Y}$ we can find a neighbourhood V_k of C_k in M homeomorphic to a ball as well. Moreover we can arrange things in such a way that $W_i \cap V_k$ and $V_{k_1} \cap V_{k_2}$ are either empty or a ball, according as $D_i \cap C_k$ and $C_{k_1} \cap C_{k_2}$ are empty or not, while $W_{i_1} \cap W_{i_2}$ is always empty. When the intersection is not empty the local picture is as in Fig. I.9.

Now, operating within these balls, we can consistently thicken the D_i's and the C_k's, to obtain solid pieces as shown in Fig. I.10. By "consistently" we mean the following: remark first that the boundary of each solid piece in Fig. I.10 is divided into portions which can be white, black or dotted, and a dotted portion can be either an annulus or a strip; then "consistently" means that:

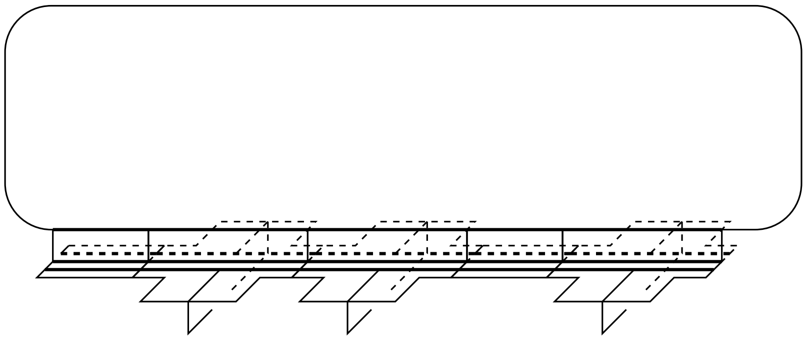

Figure I.11: Pieces glued around a disc

- the black portions are identified in pairs;
- every dotted strip is glued to two other dotted strips along the terminal segments;
- the strips glued together give annuli; each of these annuli is identified to some dotted annulus (the lateral surface of some cylinder).

Now fix i and let D_i be contained in the component D of $P \setminus S(P)$. We can say what it means for the D_3-bundle induced by the attaching function of D to be trivial: we abstractly glue the C_k's to ∂D_i, with each C_k appearing as many times as the number of components of $J_i \cap C_k$, taking into account the identifications along the Y_l's, as in Fig. I.11. (Remark that $J_i \cap C_k$ can have up to 6 components if C_k contains a vertex, up to 3 otherwise.) Then triviality is the condition that the thick lines close up to two circles (three including the boundary of the disc).

Let us return to the situation of a neighbourhood of P in M covered by nicely glued solid pieces as shown in Fig. I.10. We concentrate on the gluings involving the fixed disc D_i. If we give each of the pieces an arbitrary orientation and consequently orient the black portions of their boundary (see Fig. I.10) the following conditions are pairwise equivalent:

1. The dotted strips (Fig. I.10) glue up to a Möbius strip;
2. An odd number of identifications between black portions preserve the orientation;
3. The D_3-bundle is non-trivial.

Equivalences 1⇔2 and 2⇔3 are clear, and Not(1)⇒Not(3) implies the proof of “only if” in part A.

To establish “if” in part A, define a manifold M by gluing abstract solid pieces as in Fig. I.10 as prescribed by the gluings in P, which can be done because of implication Not(3)⇒Not(1) (the pieces are now abstract and not in

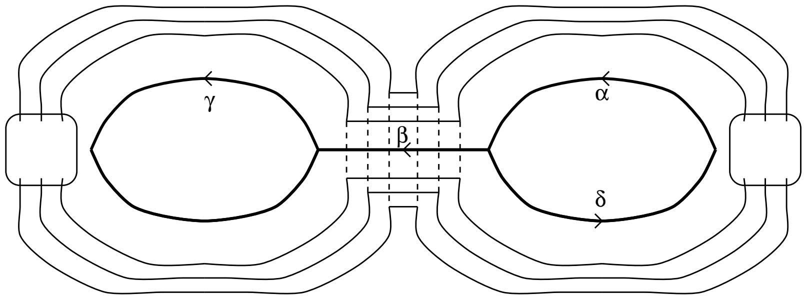

Figure I.12: Within the box on the left the strands are joined in such a way that the bundle on γ has 1 or 3 components, and the global bundle has 2 components, hence within the box on the right the strands must be joined so that the bundle on $\alpha\delta$ has 2 components

M, but the setting is the same). The result is a manifold which has standard spine P.

(B) Let P have the property that D_3-bundles induced on embeddings have either 1 or 3 components; we claim that the same property holds also for local embeddings. To see this, start with a local embedding j such that B_j has 2 components, and decompose j as $\alpha\beta\gamma\beta^{-1}\delta$, where γ is constant or an embedding of S^1 and α, β, δ are constant or local embeddings of $[0,1]$ in $S(P)$ (see Fig. I.12). The same figure also proves that if one cuts out $\beta\gamma\beta^{-1}$ the bundle still has 2 components, and the conclusion follows because one eventually reaches a circle.

Our claim is proved. We deduce from it that P is the spine of a manifold: the D_3-bundle induced by the attaching function of a disc has a global section (a circle contained in the disc), so it cannot have 1 component; then it has 3 components, i.e. it is trivial.

So we can prove equivalence in part B assuming in any case that P is the standard spine of a 3-manifold M. We think of M as being built up from pieces as in Fig. I.10. We recall that M is orientable if and only if there exists no loop $j : [0,1] \to M$ such that if the orientation is fixed at $j(0)$ and consistently followed along j, the orientation carried by $j(1)$ does not match the original one. Of course it is equivalent to confine oneself to embeddings of S^1 in $S(P)$. If one gives each non-cylindrical solid piece an arbitrary orientation and consequently orients the black portions of Fig. I.10, the following statements for an embedding $j : S^1 \to S(P)$ are pairwise equivalent:

1. The loop j reverses the orientation (in the above sense);
2. An odd number of the identifications between black portions met along j preserve the orientation;
3. The D_3-bundle B_j over S^1 has two components.

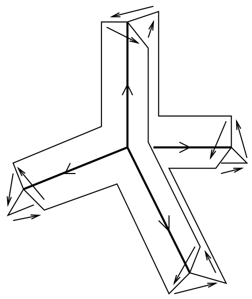

Figure I.13: At every vertex the orientations along the four edges must be in this situation. Recall that one can always reverse the direction of an edge and the order of the corresponding discs

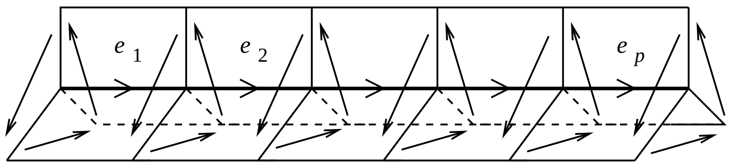

Figure I.14: A loop cut open at a vertex

Equivalences 1⇔2 and 2⇔3 are obvious, while 1⇔3 implies the conclusion of the proof of part B. $\boxed{\text{I.1.6}}$

We give now an intrinsic notion of orientation for a standard polyhedron. Fix P and $S = S(P)$. Remark that incident to every edge of S there are three germs of disc. We define an orientation of P along the edge as the choice of a direction for the edge and of a cyclic order for the three germs of discs, where a simultaneous reversal of the edge-direction and the disc-order is supposed to define the same orientation. At every edge there are exactly two orientations.

We define an orientation of P as the choice of an orientation of P along all the edges such that the compatibility condition shown in Fig. I.13 holds at every vertex. Of course P admits either no orientation at all or exactly two.

Lemma I.1.7. *A standard polyhedron P admits an orientation if and only if the D_3-bundle induced on every embedding of S^1 in $S(P)$ has either* 1 *or* 3 *components.*

Proof of I.1.7. It is sufficient to show that if $e_1, ..., e_p$ are edges whose union is a circle then there exists a consistent orientation along them if and only if the D_3-bundle on the circle does not have 2 components. Direct the e_i's consecutively. If v is the first vertex of e_1 then of course the bundle is trivial on $e_1 \cup ... \cup e_p \setminus \{v\}$, and we can orient P along the e_i's so that the compatibility holds at the vertices different from v. Looking at the definitions one has the situation of Fig. I.14, and then it is easily seen that the identification between

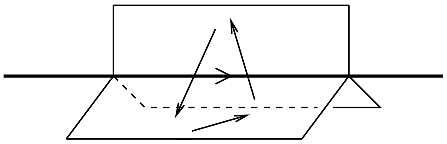

Figure I.15: The rule to orient a spine

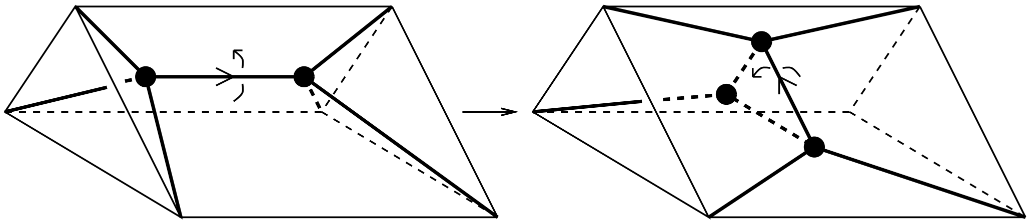

Figure I.16: The oriented Matveev-Piergallini move

the terminal triods preserves the cyclic order if and only if the resulting D_3-bundle does not have 2 components, whence the conclusion. $\boxed{\text{I.1.7}}$

Corollary I.1.8. *P is orientable if and only if it is the standard spine of an orientable manifold.*

This corollary is readily deduced from Lemma I.1.7 and Theorem I.1.6. But we have actually more: *there is a natural correspondence between orientations of the spine and orientations of the manifold.* This is obtained as follows. Let M be a manifold with a fixed orientation ω (we will denote it by M^ω). Let P be a standard spine of M and p be a point of some edge e of $S = S(P)$ and take a neighbourhood U of p in M and an orientation-preserving homeomorphism $\phi : U \to \mathbb{R}^3$. Define the orientation of P along e using ϕ and the usual left-handed screw rule in $\mathbb{R}^3$, as in Fig. I.15. If u is the unique orientation of P extending this one along e, we set $M^\omega = \mathcal{M}^\Omega(P^u)$. Of course one has $\mathcal{M}^\Omega(P^{-u}) = M^{-\omega}$. Remark that Fig. I.15 also provides the inverse rule: given an orientation of P, embed a neighbourhood of some point so that the situation is as in the figure, then define this embedding to be orientation-preserving and extend the orientation to M.

We define the oriented Matveev-Piergallini move on the set of oriented standard polyhedra in the natural way shown in Fig. I.16 (this is a natural choice as there are points whose neighbourhood the move does not alter, and we require that the orientation near them is preserved). The following result is an analogue of Theorem I.1.3 for the case of oriented manifolds.

Theorem I.1.9. *1. To every oriented standard polyhedron P^u there corresponds a connected oriented compact manifold with non-empty boundary $M^\omega = \mathcal{M}^\Omega(P^u)$.*

2. *For every connected oriented compact manifold M^ω with non-empty boundary there exists an oriented standard polyhedron P^u with at least two vertices such that $M^\omega = \mathcal{M}^\Omega(P^u)$.*

3. *Let $M_i^{\omega_i} = \mathcal{M}^\Omega(P_i^{u_i})$, $i = 1, 2$ where both P_1 and P_2 have at least two vertices. Then there exists an orientation-preserving homeomorphism of $M_1^{\omega_1}$ onto $M_2^{\omega_2}$ if and only if $P_1^{u_1}$ and $P_2^{u_2}$ are obtained from each other by a finite sequence of oriented Matveev-Piergallini moves and inverses of it.*

Proof of I.1.9. The first two assertions are readily deduced from Theorem I.1.3, Theorem I.1.6(B), Corollary I.1.8 and the above construction. We prove the third assertion.

Let $P_1^{u_1}$ be obtained from $P_2^{u_2}$ by only one oriented Matveev-Piergallini move. Then we know that $M_1^{\omega_1}$ and $M_2^{\omega_2}$ are homeomorphic, but maybe not as oriented manifolds. We think of P_1 and P_2 as embedded in the manifold, each inducing on the manifold an orientation as stated above. As we have remarked, in the oriented move there are points whose oriented neighbourhoods are unchanged, and then the two orientations on the manifold must be the same. The case of more than one move is easily settled.

Now let $M_1^{\omega_1} \cong M_2^{\omega_2}$ with orientation. Then $P_1^{u_1}$ and $P_2^{u_2}$ are obtained from each other by unoriented moves. We can think of these moves as taking place within the same oriented manifold, in such a way that for every move there is a portion of the spine which is unchanged under it. We give the intermediate spines the orientation defined by their embedding in the manifold. Then all the Matveev-Piergallini moves are oriented. $\boxed{\text{I.1.9}}$

We conclude this section with two appendices: the description of another way to present compact 3-manifolds with boundary (ideal triangulations) and the proof that the move of Fig. I.6 is actually sufficient in Theorem I.1.3.

We introduce now ideal triangulations and easily prove that this presentation is equivalent to that by standard spines. However it is remarkable that the equivalence of these presentations extends to ideal triangulations which do not define manifolds and standard polyhedra which are not spines.

By analogy with the hyperbolic case (see e.g. [Be-Pet1]) let us call a tetrahedron from which vertices have been removed an ideal tetrahedron. Assume we have finitely many copies of the ideal tetrahedron and instructions to glue the faces together in pairs through simplicial maps. The result X of the gluing has a natural PL topological structure: we will say that the combinatorial data define an ideal triangulation of X. We will denote by $\mathcal{T}$ the set of all ideally triangulated connected spaces (an element of $\mathcal{T}$ is the combinatorial data which define the space, *not* just the space), and by $\mathcal{T}_0$ the subset of $\mathcal{T}$ which contains

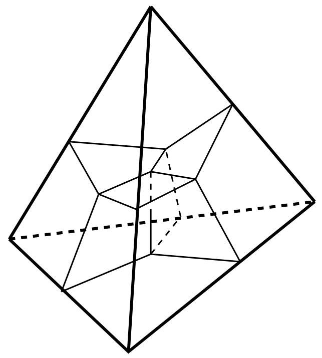

Figure I.17: Vertex-tetrahedron correspondence

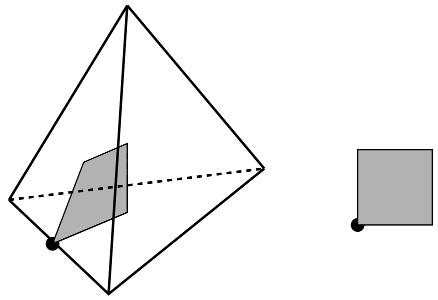

Figure I.18: These squares glue up to a disc

the spaces whose PL structure is a manifold structure (necessarily of dimension 3, of course).

We define now a function which to every element of $\mathcal{T}$ associates a 2-dimensional polyhedron. Inside the ideal tetrahedron we consider the 2-polyhedron shown in Fig. I.17; if we glue together various copies of the tetrahedron following the instructions given by $T \in \mathcal{T}$, the corresponding 2-polyhedra get glued, and we call $\phi(T)$ the result.

The next result will be used in Chapter II and in Section IV.5.

Proposition I.1.10. *The function ϕ defined via Fig. I.17 is a bijection of the set $\mathcal{T}$ of ideally triangulated spaces onto the set of standard polyhedra. Its restriction to the set $\mathcal{T}_0$ of ideally triangulated manifolds is a bijection onto the set of standard spines. Moreover if $M \in \mathcal{T}_0$ then $\phi(M)$ is the spine of a compact manifold with boundary whose interior is M.*

Proof of I.1.10. Given $T \in \mathcal{T}$, of course $P = \phi(T)$ is quasi-standard. We must check that it is standard, i.e. recalling Lemma I.1.1, that $P \setminus S(P)$ consists of discs. A component of this set is obtained from a finite union of squares as shown in Fig. I.18 by gluing together in pairs the edges incident to the marked vertices: the result is of course a disc.

To see that ϕ is a bijection we construct its inverse: to every singular vertex of a standard polyhedron P we associate an ideal tetrahedron as in Fig. I.17.

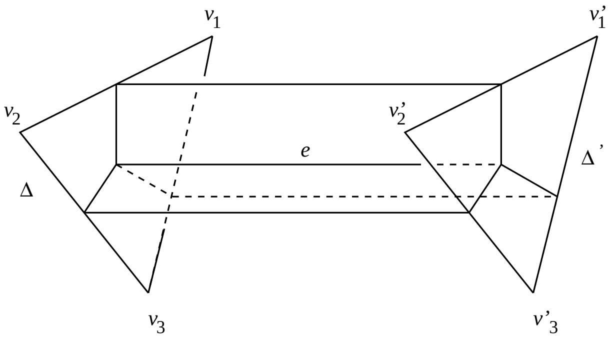

Figure I.19: The singular edge e prescribes that the triangles Δ and Δ' should be glued so that $v_i = v'_i$

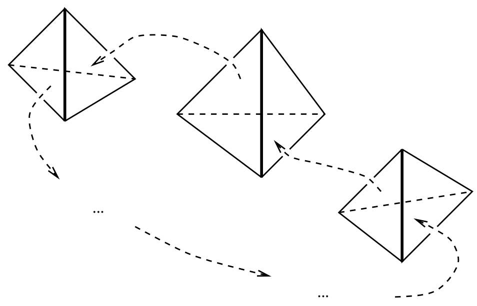

Figure I.20: The cycle of gluings around an edge

Gluings are defined by singular edges as suggested by Fig. I.19. It is easy to see that this indeed defines the inverse of ϕ.

For the second assertion we first explain the condition that $T \in \mathcal{T}$ defines a manifold. Let e_1 be an edge of one of the copies of the tetrahedron; let e_1 be contained in the faces F_1 and F'_1; let $g_1 : F'_1 \to F_2$ be the gluing function given by T; set $e_2 = g_1(e_1)$ and let F'_2 be the other face which contains e_2; proceed similarly until you find $e_{i+1} = e_1$; then

$$(g_i|_{e_i}) \circ \cdots \circ (g_2|e_2) \circ (g_1|_{e_1}) : e_1 \to e_1$$

can be either the identity or the reflection in the midpoint (see Fig. I.20). Then $T \in \mathcal{T}_0$ if and only if for all e_1 the result is the identity. In fact, in the glued space all points have links (in the PL sense) which are S^2, except perhaps midpoints of edges; the link of the midpoint of an edge is S^2 if the corresponding function is the identity, $\mathbb{P}^2$ otherwise.

Now from the proof of the first assertion it follows that glued edges in the space defined by T correspond to components of the smooth part of $\phi(T)$. Figure I.21 implies quite easily that the function associated to an edge is the identity if and only if the 3-points-bundle on the boundary of the corresponding disc is trivial. Thanks to Theorem I.1.6 the second assertion is proved.

For the last assertion, assume that an element T of $\mathcal{T}$ defines a manifold

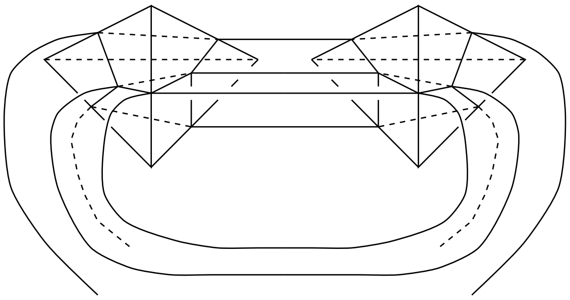

Figure I.21: The bundle on the boundary of a disc

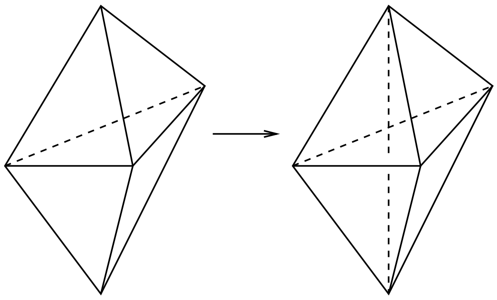

Figure I.22: This move relates any two ideal triangulations of the same manifold, provided that both involve at least two ideal tetrahedra

M. Then M is the interior of the compact manifold N obtained by truncating the tetrahedra near the vertices (the boundary of N is obtained by gluing the truncation triangles). We can collapse N onto $\phi(T)$ first within each tetrahedron, then on the common faces and lastly along edges, so $\phi(T)$ is a spine of N. $\boxed{\text{I.1.10}}$

From Theorem I.1.2 and Proposition I.1.10 we deduce that the interior of a compact manifold with boundary always admits an ideal triangulation. We just mention that the translation in terms of ideal triangulations of the Matveev-Piergallini move is as shown in Fig. I.22.

As announced, we now reproduce Piergallini's argument concerning sufficiency of the move of Fig. I.6 in Theorem I.1.3, adding some details which he omitted. For this purpose we introduce two other moves α and β on standard polyhedra as shown in Fig. I.23.

Remark I.1.11. 1. At every vertex there are three essentially different ways to apply α. This can be deduced from the fact that of the six regions originally incident to the vertex, a pair of opposite ones has the same number of vertices as before, while the other four have two vertices more than before. See also the more symmetric picture of α of Fig. I.24.

2. The move α and its inverse preserve the property of being a spine.

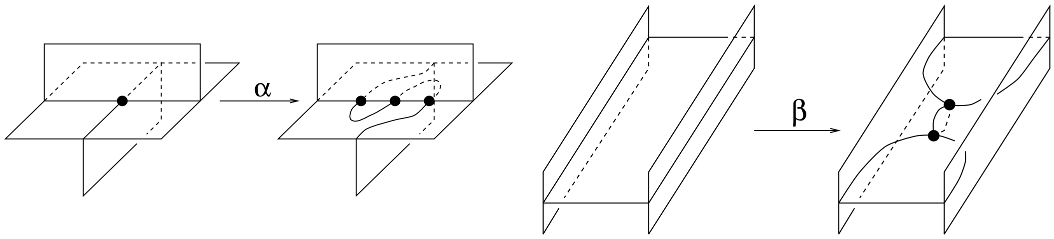

Figure I.23: Two moves on standard polyhedra

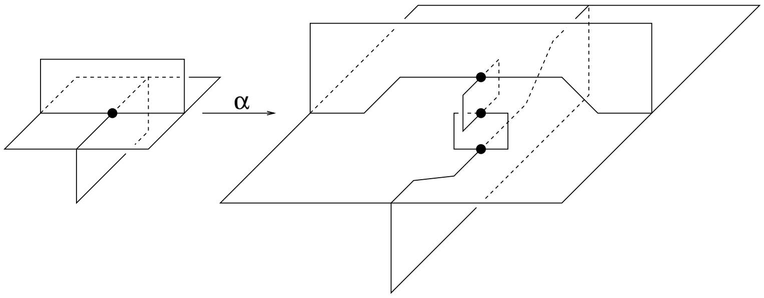

Figure I.24: A symmetric picture of α

3. For every region and every pair of (possibly coincident) edges of the region there are two essentially different ways to apply the move β. But if we have a spine we can insist that the regions which become adjacent after the move are those on the same component of the three-points-bundle on the boundary of the original region. In this case β is uniquely defined and it preserves the property of being a spine.

4. The inverse of β is not defined in general on standard spines, but when it is it preserves the property of being a spine.

5. The move α is a special case of the move β for spines.

For the sake of brevity in the rest of this section we will call γ the move of Fig. I.6. The result independently proved by Matveev and Piergallini is the following:

Proposition I.1.12. *Two standard spines of the same manifold are related by a finite sequence of moves α, γ and inverses of them.*

Following [Pi] we show how to prove Theorem I.1.3 assuming Proposition I.1.12.

Proposition I.1.13. *Two standard spines of the same manifold both with at least two vertices are related by a finite sequence of moves γ and inverses of it.*

Proof of I.1.13. We divide the proof in three steps.

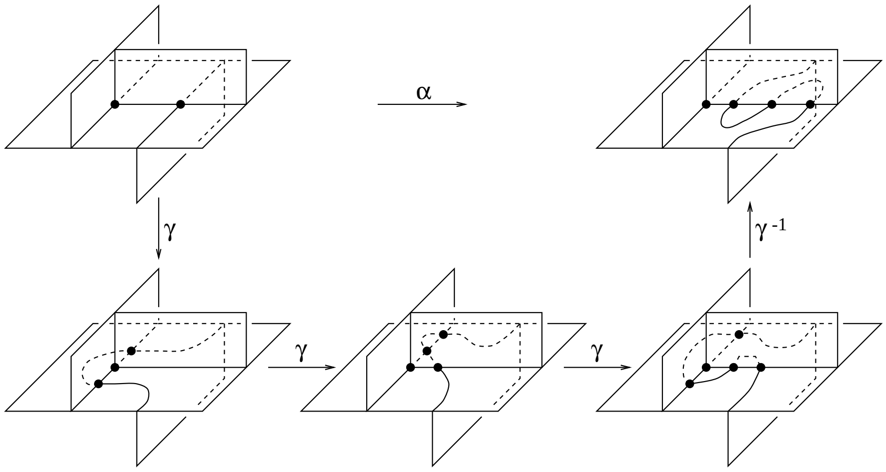

Figure I.25: γ implies α

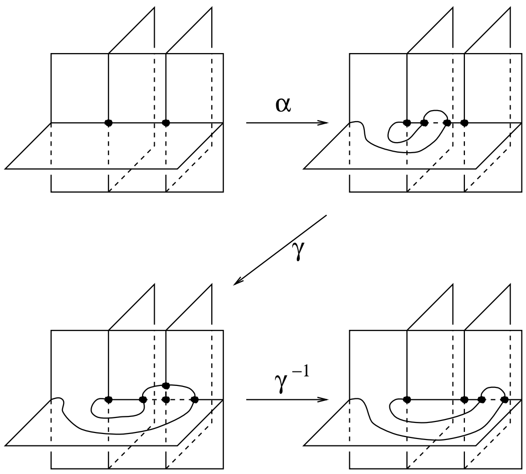

Figure I.26: γ implies β

If P has at least two vertices and $P \to Q$ via α then $P \to Q$ via a sequence of moves γ and inverses of it. To see this, we remark that all four edges originating from a certain vertex are equivalent from the point of view of applying α at the vertex (see Fig. I.24). Therefore it is not restrictive to assume that the situation is as in Fig. I.25, and then the same figure contains the proof of the first step.

If P has at least two vertices and $P \to Q$ via β then $P \to Q$ via a sequence of moves γ and inverses of it. From an iteration of the construction shown in Fig. I.26 it follows that Q is obtained by applying α on P (and hence in presence of more than one vertex) plus a sequence of moves γ and inverses of it. So the first step implies the second one.

To conclude the proof we must make do with the possibility that along our sequence of applications of α and γ there appears a spine with one vertex only.

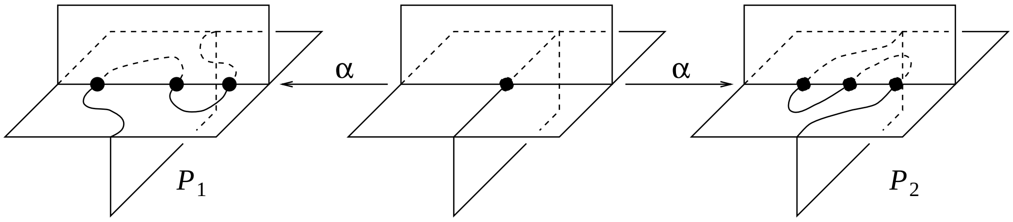

Figure I.27: Different applications of α

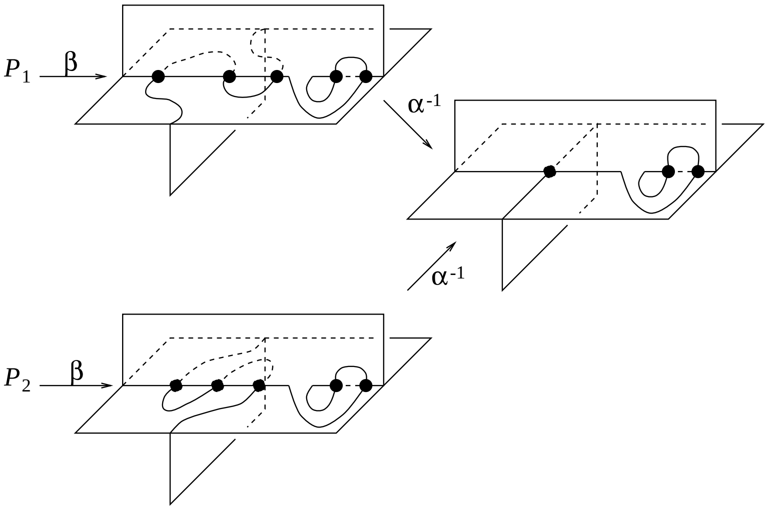

Figure I.28: How to deal with the case where a one-vertex spine appears

This must result from a move α^{-1} and only a move α can be applied to it. So the conclusion of the proof is deduced from the following third step:
Let P_1, P_2 be obtained by different applications of α at a certain vertex of P. Then $P_1 \to P_2$ via a sequence of moves γ and inverses of it. Thanks to what we know about α (see Fig. I.24 again) we can represent the situation as in Fig. I.27. Now we see from Fig. I.28 that P_1 and P_2 can be reduced to the same spine via applications of α's and β's always in presence of more than one vertex. Hence the first two steps imply the conclusion. $\boxed{\text{I.1.13}}$

I.2 Decorated spines and a graphic calculus for 3-manifolds: general case

As shown in the left-hand side of Fig. I.5 a vertex of a standard polyhedron has a neighbourhood with a totally symmetric description; to be precise such a neighbourhood has 24 symmetries (only 12 if there is an orientation and we want it to be preserved). However it is sometimes useful to consider the less symmetric description of the right-hand side of Fig. I.5; for instance we have used it in Fig. I.8 to define the 3-points-bundle induced on a singular loop. We can view in abstract terms the loss of symmetry at a vertex as a decoration of the vertex. Roughly speaking a decoration at a vertex is the choice of how to represent a neighbourhood of it as in the right-hand side of Fig. I.5. To specify this representation we must say which of the six discs is "over" (the opposite one will be "under") and how the adjacent four discs must be arranged on the horizontal plane.

Let us be more formal: we consider the following subset of $\mathbb{R}^3$:

$$E = ([-1,1]\times[-1,1]\times\{0\}) \cup ([-1,1]\times\{0\}\times[0,1]) \cup (\{0\}\times[-1,1]\times[-1,0]).$$

Let P be a standard polyhedron, let v be a vertex of P and recall that at v there are 6 germs of disc. We define a *decoration* of P at v as:

- The choice of a germ disc at v;
- The choice of an orientation for π, where π is the union of the four germs of discs adjacent to the chosen one (π is an open disc).

Given a decoration of P at v and a neighbourhood U of v in P we say a homeomorphism $\phi : U \to E$ is compatible with the decoration if:

- $\phi(D) = [-1,1]\times\{0\}\times[0,1]$ if D is the chosen germ of disc;
- $\phi|_\pi : \pi \to [-1,1]\times[-1,1]\times\{0\}$ preserves the orientation, where π is as above.

It is not hard to see that:

1. Every neighbourhood of v homeomorphic to E admits a homeomorphism compatible with the decoration;
2. Every neighbourhood of v contains some neighbourhood homeomorphic to E;
3. Two homeomorphisms of the same neighbourhood of v compatible with the decoration are obtained from each other by composition with an isotopy of $\mathbb{R}^3$ which preserves the horizontal plane $\mathbb{R}^2\times\{0\}$.

These facts mean that the formal definition of decoration really corresponds to the heuristic purpose it was meant for.

Remark I.2.1. At every vertex a standard polyhedron admits precisely 12 decorations.

We define a decoration of a standard polyhedron as the choice of a decoration at every vertex.

By definition a decoration of a standard polyhedron allows us to "canonically" embed in $\mathbb{R}^3$ neighbourhoods of the vertices. We consider now the problem of extending these embeddings to a neighbourhood of the singular set, which naturally leads to introducing a certain decorated planar graph. This discussion is very informal, but below we will provide precise statements.

Let P be a decorated standard polyhedron. We start with embeddings of neighbourhoods of the vertices compatible with the decoration, pushed apart by horizontal translations. Next, we extend the embedding to the whole singular set of P, with the requirement that the projection on the horizontal plane is generic. (Of course there is a considerable rate of arbitrariness in such an extension —we will take this into account.) Now we extend the embedding across an edge: we will have triods arriving from both endpoints, and we only need to be careful and match them correctly in the middle. It might not be possible to do this in $\mathbb{R}^3$ (we just work with $\mathbb{R}^4$ in this case, where $\mathbb{R}^4 \supset \mathbb{R}^3 \times \{0\} \cong \mathbb{R}^3$). Of course we do not have uniqueness (we could give either triod a complete twist before connection) but if we find an intrinsic method to number the three branches of each triod by $\{1, 2, 3\}$ we will have a well-defined permutation in $\mathfrak{S}_3$. Having found such a method our embedding will be essentially represented by a planar quadrivalent graph where some vertices are "fake", the others have some special decoration which allows us to recover the embedding, and the edges have a colour in $\mathfrak{S}_3$.

We will now formalize this construction. Since a graph defines a unique decorated standard polyhedron but the graph is not unique, it is convenient to start with graphs, show how they define standard polyhedra and then discuss non-uniqueness. Since we will use groups of permutations, we recall that the symbol $(i_1\, i_2\, \cdots\, i_k)$ denotes the function which maps i_j to i_{j+1} and i_k to i_1. We multiply two such symbols as functions, in the obvious way. For instance $(12)(13) = (132)$.

Let Γ be a finite connected quadrivalent graph embedded in $\mathbb{R}^2$ with normal crossings. Recall that by graph we mean a finite 1-complex. Assume that some vertices of Γ are marked, and define the edges of Γ as stated in the introduction by pretending that unmarked vertices do not exist: formally a (directed) edge is a local embedding $\alpha : [0, 1] \to \Gamma$ regarded up to (positive) change of parameter such that $\alpha(t)$ is marked exactly for $t = 0, 1$ and if $\alpha(t_0)$ is a crossing then $\alpha(t - \varepsilon)$ and $\alpha(t + \varepsilon)$ lie on opposite branches at the crossing for small $\varepsilon > 0$.

We define an s-graph to be the datum of:

1. A finite planar quadrivalent graph Γ with some marked crossings, where Γ is edge-connected (in the sense just stated);

2. An under-over specification (as in the usual projections of links) at each

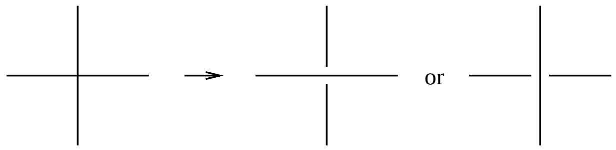

Figure I.29: How to loosen a crossing which is not marked

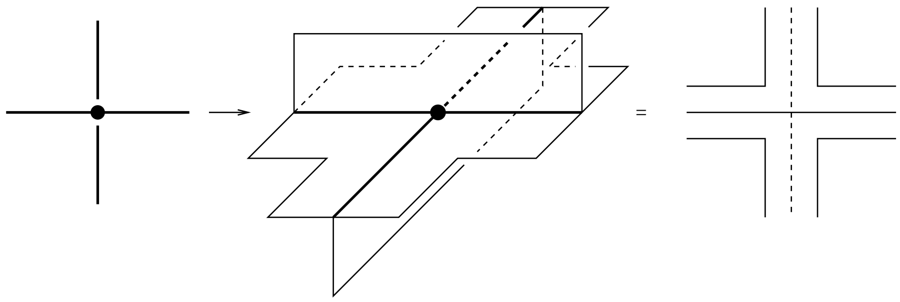

Figure I.30: For every marked vertex (left) we introduce a 3-dimensional object (centre) and a planar symbol for it (right)

marked vertex of Γ;

3. A direction for every edge of Γ;

4. A colour chosen in $\mathfrak{S}_3$ attached to every edge of Γ.

We will actually refer to Γ itself as an s-graph.

Formal procedure to recover a decorated standard polyhedron from an s-graph. Given an s-graph Γ the steps are as follows:

1. Embed $\mathbb{R}^2$ in $\mathbb{R}^3$ as $\mathbb{R}^2 \times \{0\}$, and for each vertex of Γ which is not marked choose an arbitrary way in $\mathbb{R}^3$ to loosen it (there are two such ways, see Fig. I.29).

2. For each marked vertex v select a small neighbourhood where Γ is a cross, and fit on it a subset of $\mathbb{R}^3$ as described in Fig. I.30. We also use a planar notation which on one hand is readily deduced from the s-graph and on the other hand easily implies the 3-dimensional situation.

3. For each edge we select a small segment which is far from all vertices and associate to it a subset of $\mathbb{R}^3$ as described in Fig. I.31. (Remark that for an end of an edge it is well-defined whether it is "over" or "under", so the definition makes sense.)

4. The objects defined in 2 and 3 terminate with T's which can be straight or upside-down. The choices we have made imply that we can extend the T's across the edges excluding the little segments, as shown in Fig. I.32,

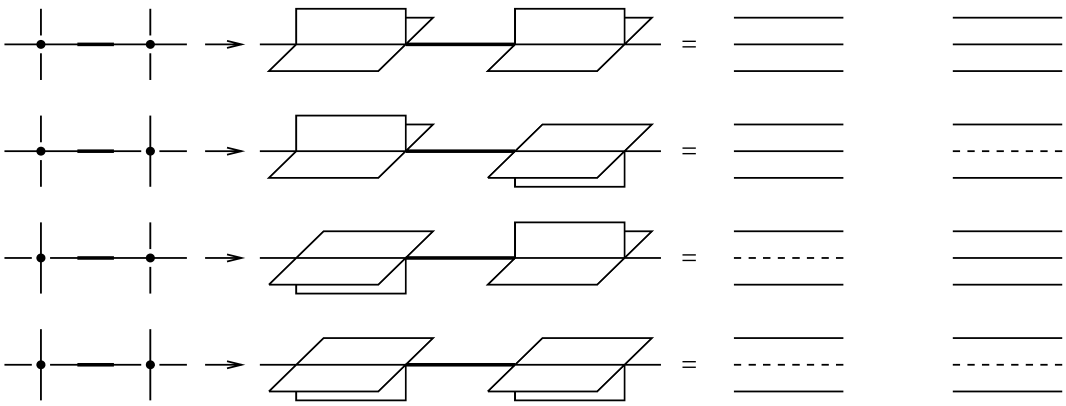

Figure I.31: Depending on the four possible cases for the endpoints of the edge (left) we introduce a 3-dimensional object (centre) and a planar symbol for it (right)

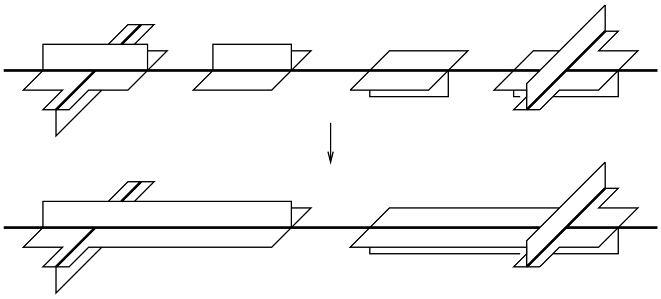

Figure I.32: An example of how to extend the T's across an edge

by allowing horizontal rotations and vertical translations (these are necessary if we meet a loosened crossing, as in Fig. I.33).

5. For each small segment we give a number 1, 2 or 3 to the three branches of each of the two T's involved as shown in Fig. I.34. Remark that this numbering depends on the direction of the edge and on whether the T is straight or upside-down. We move the T across the little segment in such a way that i on the right is joined to $\sigma(i)$ on the left. It is quite easy to see that this can be done in $\mathbb{R}^3$ if and only if $\mathrm{sgn}(\sigma) = +1$; otherwise

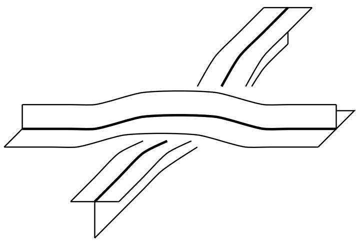

Figure I.33: How to deal with a loosened vertex

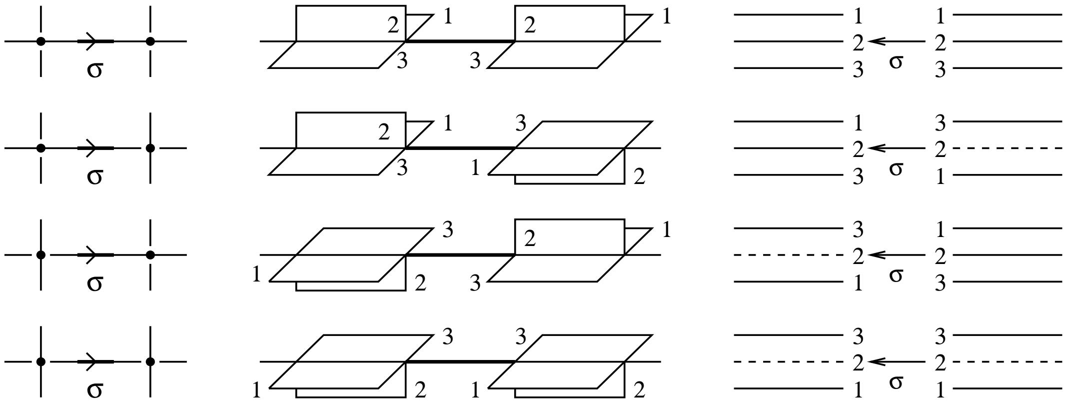

Figure I.34: How to label the branches of the T's and a symbolic planar description of the gluings to be performed (step 5)

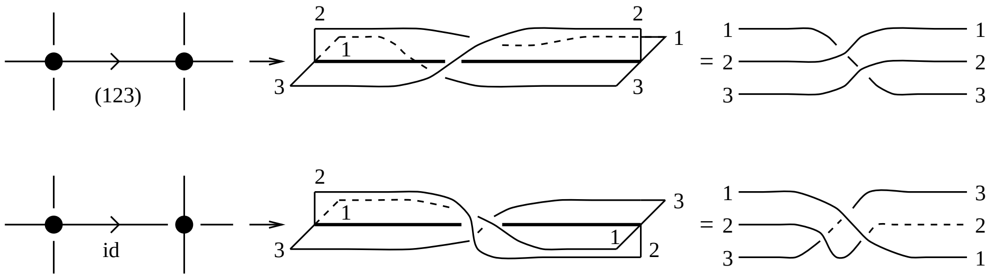

Figure I.35: Two examples where everything takes place in the three-space

we just need to add one more dimension. Some examples are shown in Figg. I.35 and I.36.

6. We have obtained a polyhedron in $\mathbb{R}^3$ or at worst in $\mathbb{R}^4$ which has four types of points, three of them being the same as in a quasi-standard polyhedron. Points of the fourth type have neighbourhoods homeomorphic to half-planes but not to planes. The set of all points of the fourth type is a union of disjoint circles, and we attach a disc to each of them following the boundary.

7. We have obtained a standard polyhedron and an embedding in $\mathbb{R}^4$ of a neighbourhood of its singular part. The restriction of this embedding to a neighbourhood of a vertex, after an isotopy in $\mathbb{R}^3$ which preserves the horizontal plane, is a homeomorphism with the set E defined at the beginning of the section. Hence we can choose the decoration of the vertex with which this homeomorphism is compatible. We have therefore a decorated standard polyhedron.

Lemma I.2.2. *If Γ is an s-graph the above-described procedure defines a unique decorated standard polyhedron $\mathcal{D}(\Gamma)$, and every decorated standard poly-*

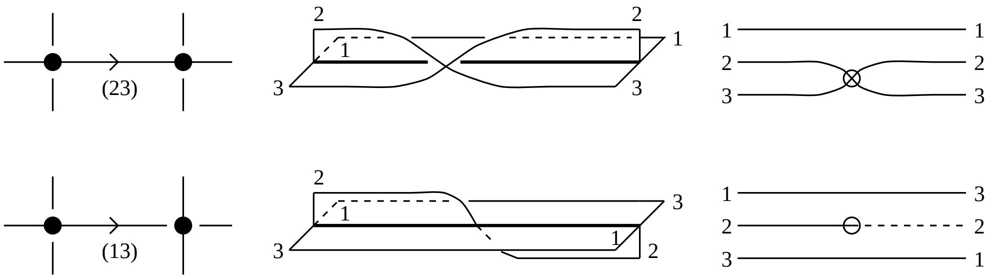

Figure I.36: In these examples there are strips which cross each other without meeting, thanks to the fourth dimension not shown in the picture. A symbolic planar picture describing the situation is also provided

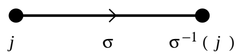

Figure I.37: If i is one of $\{j,\sigma^{-1}(j)\}$ then i' is the other one, while $s'=\mathrm{sgn}(\sigma)\cdot s$

hedron arises like this.

Proof of I.2.2. Steps 2, 3 and 4 are unique up to isotopy in $\mathbb{R}^3$ (or $\mathbb{R}^4$); step 5 is not unique in $\mathbb{R}^3$ (or $\mathbb{R}^4$) because we can give complete twists, but the associated abstract object is unique; steps 6 and 7 are intrinsically defined; different choices in step 1 of course lead to the same abstract object. So the above construction defines a unique polyhedron, which is standard by Lemma I.1.1.

The last assertion follows from the construction informally sketched above (start embedding near the vertices and extend). $\boxed{\text{I.2.2}}$

We will denote by $\mathcal{P}(\Gamma)$ the standard polyhedron obtained from $\mathcal{D}(\Gamma)$ by forgetting the decoration. Since we are interested in standard polyhedra as tools for studying 3-manifolds, we state the following:

Proposition I.2.3. *Let Γ be an s-graph. Then $\mathcal{P}(\Gamma)$ is the standard spine of a manifold if and only if the following holds: Pick the germ e of an edge at some vertex and an integer i in $\{1,2,3\}$, set $s=+1$ and replace the triple $\{e,i,s\}$ by $\{e',i',s'\}$ alternatively in the following two ways:*

1. *e' is the germ of the other end of the same edge and i',s' depend on the colour and direction of the edge, as described in Fig. I.37.*

2. *e' is one of the three other germs at the same vertex, $s'=s$ and e',i' are given in the various possible cases by Fig. I.38. In this figure we make the convention that when the direction of the edge is reversed the corresponding integer j must be replaced by $(1\,3)(j)$; it is easily checked that with this convention the four situations shown cover all possibilities.*

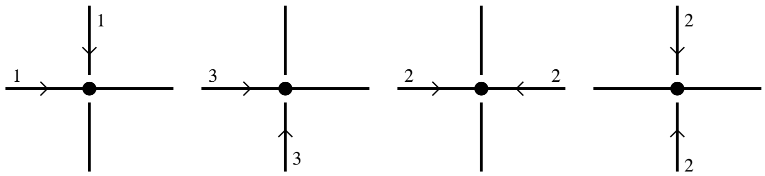

Figure I.38: The two pairs (germ-of-edge,integer-near-it) give $\{(e,i),(e',i')\}$

Then the condition is that the first time we have $\{e, i, s'\}$ *then we also have* $s' = +1$*, and this should happen for every initial choice of* e *and* i*.*

Proof of I.2.3. Using the procedure to recover $\mathcal{P}(\Gamma)$ from Γ one sees quite easily that this is exactly the condition that the 3-points-bundle over the boundary of every disc is trivial (see Theorem I.1.6). $\boxed{\text{I.2.3}}$

If $\mathcal{P}(\Gamma)$ is the standard spine of a manifold we call this manifold $\mathcal{M}(\Gamma)$.

We will discuss in the rest of this section the conditions under which two s-graphs define homeomorphic manifolds. There will be two intermediate steps corresponding to the questions:

1. When do two s-graphs define the same decorated standard polyhedron?
2. When do two s-graphs define the same standard polyhedron?

The final result will be a set of moves with which one obtains from a given s-graph all and only the s-graphs defining the same manifold. In the next section we will deal with the case of oriented manifolds.

First of all we look at s-graphs up to homeomorphisms of the plane isotopic to the identity, without comments.

Proposition I.2.4. *Given two s-graphs* Γ_1 *and* Γ_2 *there exists a decoration-preserving homeomorphism of* $\mathcal{D}(\Gamma_1)$ *onto* $\mathcal{D}(\Gamma_2)$ *if and only if* Γ_1 *and* Γ_2 *are obtained from each other by a finite sequence of the following moves:*

- *The "Reidemeister-type" moves* R_{I}, R_{II}, $\mathrm{R}_{\mathrm{III}}$, $\mathrm{R}'_{\mathrm{III}}$ *and* $\mathrm{R}''_{\mathrm{III}}$ *shown in Figg. I.1 and I.2 in the introduction. (We will refer to a finite combination of them and their inverses as an* R*-move.)*
- *The move* U *which consists in reversing the direction of an edge and changing its colour from* σ *to* $(13)\sigma^{-1}(13)$*.*

Proof of I.2.4. On considering the above construction, we can easily see that R-moves exactly recover arbitrariness for the embedding of a neighbourhood of the singular set (for an interpretation of R_{I} as a twist, see Fig. I.39). We also had arbitrariness in choosing the directions of the singular edges, and we can show that U describes the natural way to colour an edge after reversing the

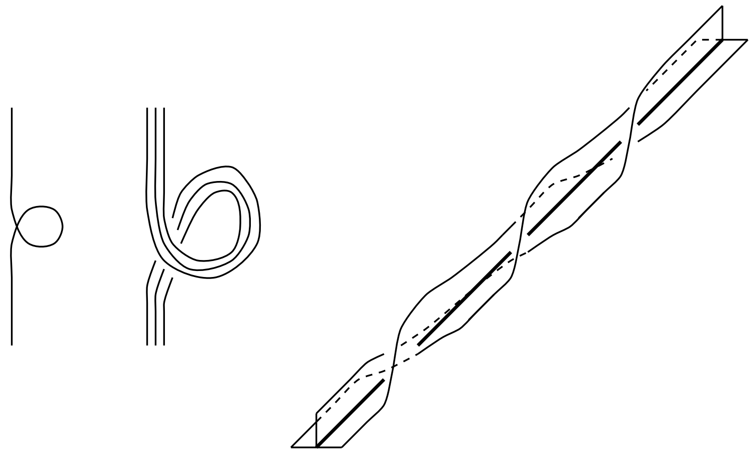

Figure I.39: Proof that $\mathrm{R_I}$ represents a twist in the embedding

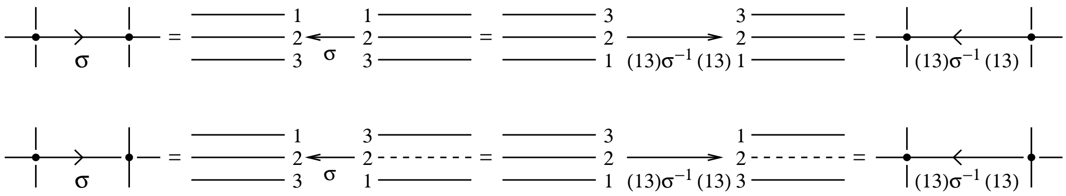

Figure I.40: Reversing the direction: two examples

direction, which implies the conclusion at once. We must distinguish the cases according as the endpoints of the edge are over or under. Figure I.40 refers to the cases where both the endpoints are over and where the first endpoint is over and the second one is under. The other cases are treated similarly. $\boxed{\text{I.2.4}}$

Remark I.2.5. The mapping $\mathfrak{S}_3 \ni \sigma \mapsto (13)\sigma^{-1}(13) \in \mathfrak{S}_3$ interchanges (12) and (23) and leaves the other elements unchanged.

From now on we will consider s-graphs up to moves R and U, i.e. we will view two s-graphs equivalent under them just as two different ways to draw the same object. With this convention an s-graph "is" a decorated standard polyhedron. Now, to discuss when $\mathcal{P}(\Gamma_1) = \mathcal{P}(\Gamma_2)$, we must see what is the effect on the s-graph of a change in the decoration of a vertex. This will result in the definition of new moves for s-graphs.

For the purpose of introducing these moves, we slightly extend the situation, by allowing the edges to be subdivided into finitely many subarcs, each with a direction and a colour. We introduce a product-move as follows: given two consecutive subarcs of an edge, we apply U (if necessary) to have them consecutively directed. Let the first subarc be decorated by σ and the second one by τ; the effect of the product-move is to remove the subdivision point between the arcs, direct the resulting arc in the obvious way and give it the

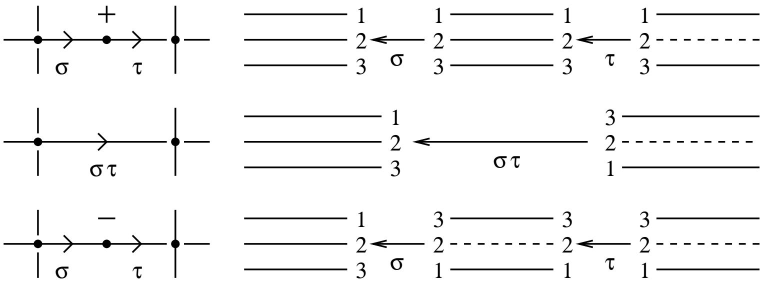

Figure I.41: An example of product. This picture shows that whatever geometric interpretation one chooses for the subdivision point (top and bottom) the result is the content of the product-move (centre)

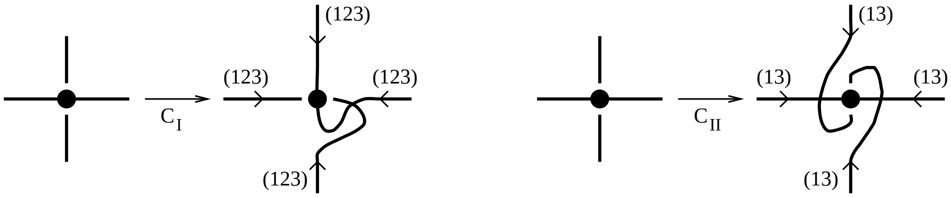

Figure I.42: The moves C_I and C_{II}

colour $\sigma\tau$. To check that this definition is completely natural see the example of Fig. I.41.

The moves we need, named C_I and C_{II} as they take place in the neighbourhood of a crossing, exploit the extension of the class of s-graphs which allows subdivisions. We think of the directions and colours of the edges involved as drawn outside the neighbourhood, so we do not deal with them. Both moves consist in adding four subdivision points near the vertex, joining these points to the vertex but not in the original way and then giving a certain direction and colour to the four arcs thus defined. The explicit description is given in Fig. I.42; we will always tacitly assume that they must be followed by product-moves so that subdivisions disappear.

Remark that the move C_{II} is unambiguosly defined at every vertex, while there are two ways to apply C_I: in fact before the move the figure is symmetric under rotation through angle π, and after the move it is not. One could specify how to apply the move by stating which branch must be over both before and after the move.

Proposition I.2.6. *Given s-graphs Γ_1 and Γ_2 (regarded up to isotopy and moves* R *and* U*), the standard polyhedra $\mathcal{P}(\Gamma_1)$ and $\mathcal{P}(\Gamma_2)$ are homeomorphic if and only if Γ_1 and Γ_2 are obtained from each other by a finite sequence of moves* C_I *and* C_{II}.

Proof of I.2.6. By Proposition I.2.4 we must discuss how the decoration of a standard polyhedron can be changed. Figures I.43 and I.44 show that both

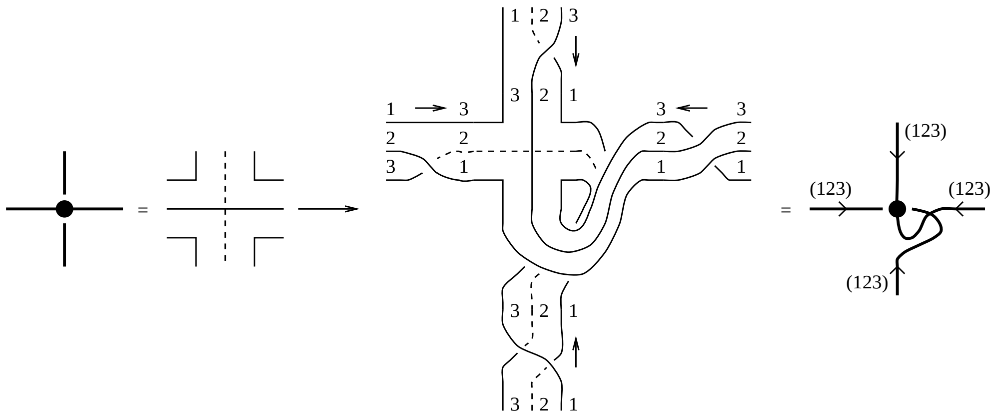

Figure I.43: Explanation of the move C_{I}

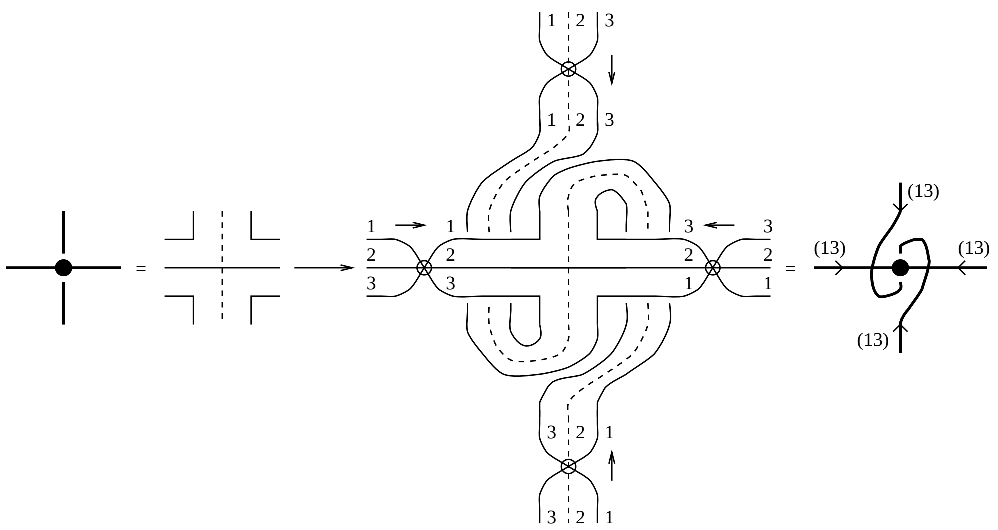

Figure I.44: Explanation of the move C_{II}

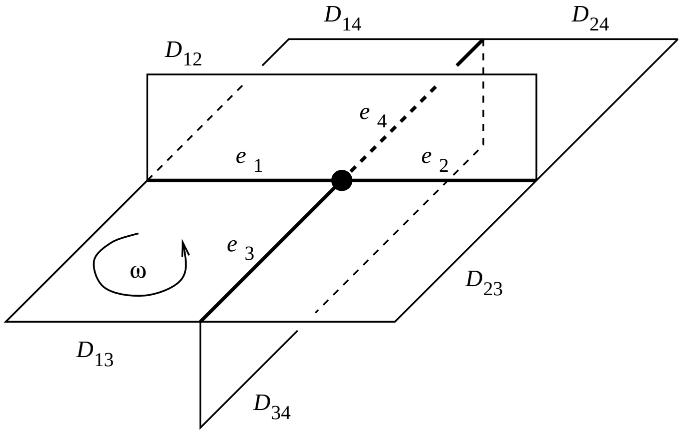

Figure I.45: Lettering conventions used to describe the effect of $\mathrm{C_I}$

the moves describe a modification of the embedding of a neighbourhood of a vertex, i.e. a modification of the decoration at the vertex. (In both the figures, to see that on the left there is the same object as on the right, check that the 12 external branches are joined in the same way inside.)

For the conclusion of the proof it is sufficient to check that the two changes of decoration induced by $\mathrm{C_I}$ and $\mathrm{C_{II}}$ generate all 12 possible decorations at a vertex. To see this it is sufficient to describe the situation in a more intrinsic way. We recall that an abstract decoration is the choice of a germ of disc and an orientation for the union of the four discs which are adjacent to it. Then the effect of $\mathrm{C_{II}}$ on the decoration is of course just to reverse the orientation.

For $\mathrm{C_I}$, consider an abstract decoration (D_{12}, ω), let e_1, e_2, e_3, e_4 be the germs of edges so that (e_1, e_3, e_2, e_4) are positively arranged with respect to ω, and D_{ij} is the germ of disc containing $e_i \cup e_j$ (see Fig. I.45). Then the effect of the two ways to apply $\mathrm{C_I}$ is to replace (D_{12}, ω) by (D_{24}, ω') or (D_{13}, ω''), where ω' extends $\omega|_{D_{14}}$ and ω'' extends $\omega|_{D_{23}}$.

It is therefore evident that we can obtain all 12 decorations. $\boxed{\text{I.2.6}}$

Remark I.2.7. By repeated composition of moves $\mathrm{C_I}$ and $\mathrm{C_{II}}$ at every vertex exactly 12 different situations (shown in Fig. I.46) can be produced. (In the figure we have deliberately isotoped and used R-moves so that $\mathrm{C_I}$ does not appear in the same form as in the definition.) This is obvious if one thinks of the intrinsic situation of decorated standard polyhedra (*cf.* the proof of I.2.6), but it is also not hard to prove it directly.

Proposition I.2.8. *The move* MP *defined in Fig. I.47 translates for s-graphs the Matveev-Piergallini move for an edge which has both the endpoints over and colour* id. *Moreover up to moves* R, $\mathrm{C_I}$ *and* $\mathrm{C_{II}}$ *every edge becomes like this.*

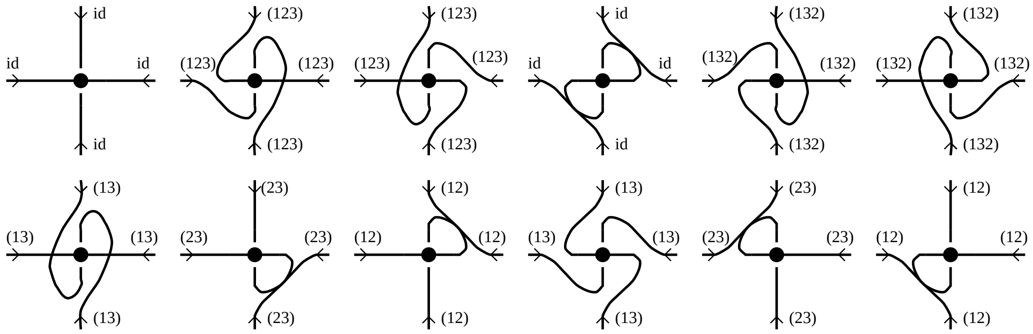

Figure I.46: The 12 different situations obtained at each vertex. Remark that the first 6 figures are those obtained using C_I only

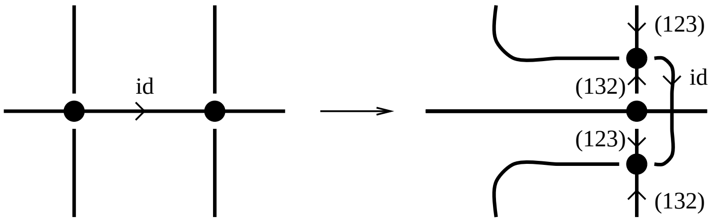

Figure I.47: The move MP

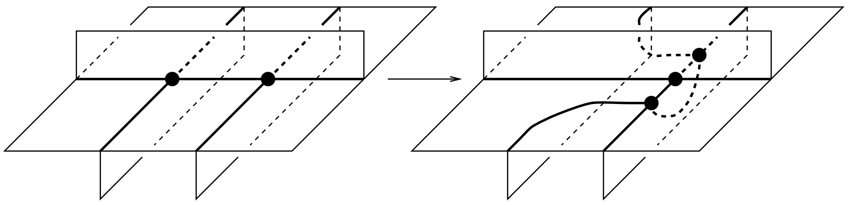

Figure I.48: A representation of the Matveev-Piergallini move on polyhedra

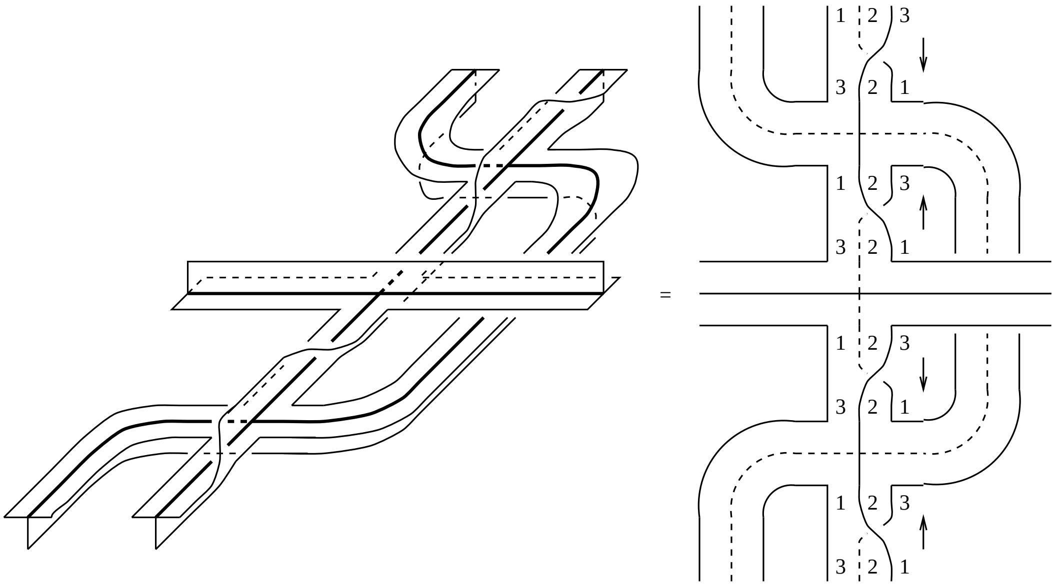

Figure I.49: This shows the effect of the Matveev-Piergallini move on a neighbourhood of the singular part. The planar representation is immediately translated to the move MP

Proof of I.2.8. The first assertion is proved by Figg. I.48 and I.49. The second assertion is easily deduced from Fig. I.46. $\boxed{\text{I.2.8}}$

As a consequence of Theorems I.1.2 and I.1.3, Propositions I.2.4, I.2.6 and I.2.8 we have the following:

Theorem I.2.9. *For every compact* 3*-manifold* M *with non-empty boundary there exists an s-graph* Γ *with* $M = \mathcal{M}(\Gamma)$*. If* Γ_1 *and* Γ_2 *are s-graphs with at least two vertices such that* $\mathcal{M}(\Gamma_1)$ *and* $\mathcal{M}(\Gamma_2)$ *are defined (see Proposition I.2.3), then* $\mathcal{M}(\Gamma_1)$ *and* $\mathcal{M}(\Gamma_2)$ *are homeomorphic if and only if* Γ_1 *and* Γ_2 *are obtained from each other by a sequence of moves* R, U, $\mathrm{C_I}$, $\mathrm{C_{II}}$, MP *and inverses of them.*

I.3 A graphic calculus for oriented 3-manifolds

In this section we specialize the construction of the previous one for oriented standard polyhedra, i.e. for standard spines of oriented manifolds. We first characterize the s-graphs which correspond to orientable manifolds.

Proposition I.3.1. *Let* Γ *be an s-graph. Then* $\mathcal{P}(\Gamma)$ *is orientable if and only if for every set of edges whose union is a circle the product of the signs of the corresponding colours is* $+1$.

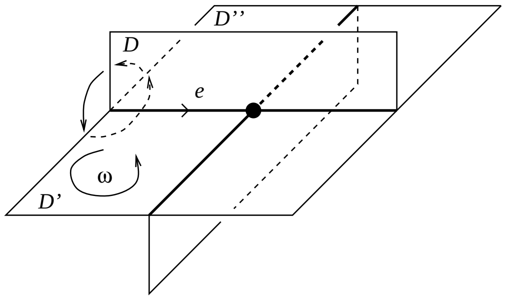

Figure I.50: A decoration compatible with the orientation

Proof of I.3.1. If one looks at the definition of the 3-points-bundle over a circle which is a union of edges, he easily sees that each edge with negative sign induces a transposition in the fibres, while an edge with positive sign induces a rotation. Therefore, the bundle has two components if and only if the product of the signs is -1, and the conclusion follows from Theorem I.1.6(B). $\boxed{\text{I.3.1}}$

We have stated this result as it could be useful when dealing with manifolds which are not a priori orientable. However we will show now that *oriented* manifolds admit a simpler representation. As in the previous section we start with an intrinsic definition of decoration and then we derive the graph representation.

We recall that a decoration for a standard polyhedron P at a vertex v is a pair (D, ω) where D is a germ of edge at v and ω is an orientation on the union π of the germs of discs adjacent to D. Let e be an edge of D, and direct e towards v. Let D' be the germ of disc on π on the right of e and D'' the germ of disc on π on the left of e (the notions of "right" and "left" involve ω and the direction of e). Now let P be oriented: we say the decoration is compatible with the orientation of P at v if the direction of e_1 and the cyclic order $D \to D' \to D'' \to D$ define the positive orientation of P along e_1. See Fig. I.50 to check that this is a natural choice.

Remark I.3.2. Given an oriented standard polyhedron exactly 6 decorations at each vertex are compatible with the orientation.

Proposition I.3.3. *Let Γ be an s-graph and let $\mathcal{D}(\Gamma)$ be the decorated standard polyhedron defined in Proposition I.2.4. There exists an orientation compatible with the decoration at each vertex if an only if all the colours in Γ have sign $+1$. Such an orientation, if any, is unique.*

Proof of I.3.3. We recall that Γ defines an embedding in $\mathbb{R}^3$ of a neighbourhood of each vertex, and the decoration is defined using these embeddings. Define the orientation near every vertex so that compatibility is respected. Consider an edge: it is not hard to see that the orientations near its endpoints match

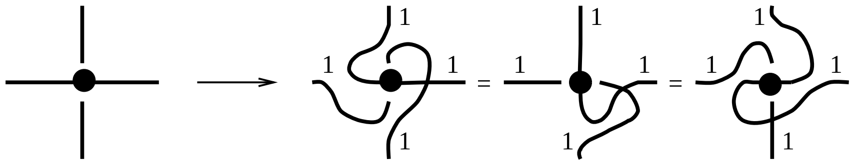

Figure I.51: Three descriptions of the move C which translates $\mathrm{C_I}$ for o-graphs

along the edge if and only if the colour the edge bears has sign +1, and the conclusion easily follows. $\boxed{\text{I.3.3}}$

Recalling Remark I.2.5 we have that for s-graphs as described in Proposition I.3.3 the direction of the edges is actually dispensable, and the colours belong to the subgroup of $\mathfrak{S}_3$ generated by $(1\,2\,3)$, which is isomorphic to $\mathbb{Z}_3$. Hence if we define an o-graph as an s-graph where are edges are not directed and the colours are taken in $\mathbb{Z}_3$ rather than in $\mathfrak{S}_3$ (see the introduction for a self-contained definition) using Proposition I.2.4 we have:

Proposition I.3.4. *Decorated oriented standard polyhedra with decoration compatible with the orientation correspond bijectively to o-graphs up to isotopy and moves* R.

As for s-graphs, from now on we consider o-graphs up to isotopy and moves R. Given an o-graph we denote by $\mathcal{P}^\Lambda(\Gamma)$ the oriented standard polyhedron P^λ defined by Γ in which the decoration is forgotten.

Proposition I.3.5. *Given o-graphs Γ_1 and Γ_2 there exists an orientation-preserving homeomorphism of $\mathcal{P}^\Lambda(\Gamma_1)$ onto $\mathcal{P}^\Lambda(\Gamma_2)$ if and only if Γ_1 and Γ_2 are obtained from each other by a finite sequence of applications of the move* C *defined in Fig. I.51.*

Proof of I.3.5. The move C is just the translation of $\mathrm{C_I}$ in the language of o-graphs. As in the proof of Proposition I.2.6 we only need to check that C generates the changes of decoration compatible with the orientation. This can be left to the reader (see also the next remark). $\boxed{\text{I.3.5}}$

Remark I.3.6. There are two ways to apply the move C at every vertex, and exactly 6 different situations can be produced by repeated applications. They are obtained from the first 6 diagrams of Fig. I.46 by omitting directions and writing i for $(1\,2\,3)^i$.

Proposition I.3.7. *If Γ is an o-graph and $P^\lambda = \mathcal{P}^\Lambda(\Gamma)$ then $P^{-\lambda} = \mathcal{P}^\Lambda(\Gamma')$, where Γ' is obtained from Γ by reversing the under-over specification at marked vertices and replacing each colour by its inverse in $\mathbb{Z}_3$.*

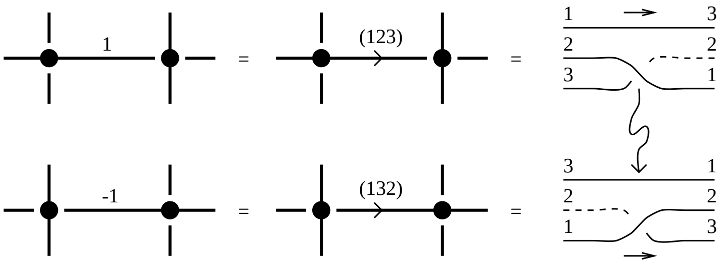

Figure I.52: The reflection in the horizontal plane replaces a colour by its inverse

Proof of I.3.7. Γ defines an orientation-preserving embedding in $\mathbb{R}^3$ of a neighbourhood of the singular part of P. We prove that replacing Γ by Γ' corresponds to composing the embedding with the reflection of $\mathbb{R}^3$ in the horizontal plane (of course this is sufficient). It is evident that the effect of the reflection on a vertex is to exchange under-arc and over-arc, while we show by an example in Fig. I.52 that the effect on colours is inversion in $\mathbb{Z}_3$. $\boxed{\text{I.3.7}}$

Now, we have the move MP which is readily translated in the language of o-graphs, as shown in Fig. I.4 of the introduction. We denote it by MP again.

Proposition I.3.8. *The move* MP *translates for o-graphs the oriented Matveev-Piergallini move for an edge which has both the endpoints over and colour* 0*. Moreover up to moves* R *and* C *every edge becomes like this.*

Proof of I.3.8. Recalling Proposition I.2.8 the first assertion is obvious, and the second one is readily checked using Remark I.3.6. $\boxed{\text{I.3.8}}$

We have eventually established the main result stated in the introduction. In fact Theorem I.0.1 summarizes Theorems I.1.2 and I.1.3 and Propositions I.3.4, I.3.5, I.3.7 and I.3.8.

Having proved the main result of the chapter, we discuss now two complementary facts. The first deals with the inverse of the move MP and the second with spines with one vertex.

We start by characterizing the situations where the inverse of the move MP can be applied after some application of moves C. This could have some relevance in automatic approaches. Given an o-graph let us define a triangle in it as a set of 3 edges every 2 of which share exactly one vertex. We say a triangle is in standard configuration if it looks as in Fig. I.53, namely the edges are simple, they bound a true triangle in the plane and, proceeding counterclockwise, they have the first endpoint under and the second endpoint over.

Lemma I.3.9. *Given a triangle in an o-graph, up to moves* C *at its three vertices (plus isotopy and moves* R*), it is always possible to transform it in standard configuration, and the colours in this standard configuration are uniquely determined.*

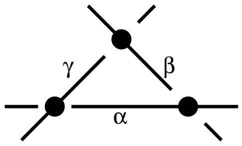

Figure I.53: Standard configuration of a triangle

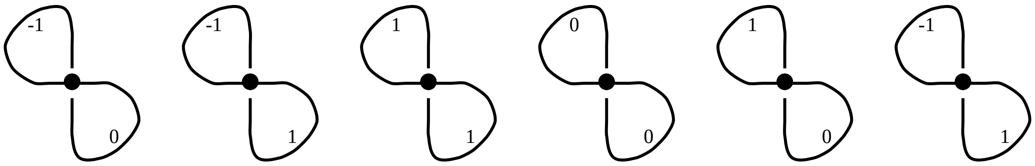

Figure I.54: Oriented spines with one vertex

The proof of this fact can be left to the reader. Remark that a similar result is false for s-graphs (there exist moves at vertices which preserve a standard configuration and perturb its colours). Hence the next Proposition I.3.10 does not apply to the non-oriented case (a variation of it would).

Proposition I.3.10. *One can apply the inverse of the move* MP *to a triangle if and only if this triangle has colours* $-1, -1, -1$ *in standard configuration.*

Proof of I.3.10. The are two ways to prove this result, both of which we sketch. First, remark that geometrically we can apply the inverse of the Matveev-Piergallini move if and only if the triangle, as a subset of the singular set of the spine, bounds a disc in the spine. Then one goes back to the proof of Proposition I.2.3 and analyses the special situation here.

Second, we know that every edge can be transformed so that the move MP directly applies to it. Then it is sufficient to find the standard configuration of the triangle directly produced by MP. $\boxed{\text{I.3.10}}$

Let us recall the reason why we have considered, when dealing with manifolds, only spines with at least two vertices: as we have seen in the first section, the single move we have taken into account (Fig. I.6) is not sufficient to generate the whole calculus is one accepts spines with one vertex. On the other hand, spines with one vertex are perfectly acceptable, and Piergallini lists them in [Pi]. Since he is only interested in once-punctured closed manifolds, he gives an incomplete list from the point of view of spines. We give a complete list here and check that also non-orientable manifolds arise from spines with one vertex.

Proposition I.3.11. *There are exactly* 6 *oriented standard polyhedra with* 1 *vertex, shown in Fig. I.54; the first two are spines of a punctured* S^3*, the next two are spines of a punctured* $L_{4,1}$*, the fifth is a spine of a punctured* $L_{5,2}$ *and the last is a spine of a twice punctured* S^3*, i.e. of* $S^2 \times [0,1]$. *There are exactly*

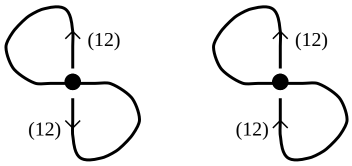

Figure I.55: Non-orientable spines with one vertex

2 *non-orientable standard polyhedra with one vertex which are standard spines of manifolds, shown in Fig. I.55; both have the Klein bottle as boundary and the first one is a spine of the Giesekind manifold (a hyperbolic non-orientable manifold —see [Mat-Fo]).*

Proof of I.3.11. For the oriented case, one remarks that using moves C every o-graph with one vertex can be transformed to one and only one of those of Fig. I.54. The analysis of what manifolds arise is left to the reader. One way to see that the first two and the next two will give the same manifold is to reverse the orientation.

For the non-orientable case, as an application of Proposition I.2.3 one immediately sees that both edges must have colour with negative sign, and that colours (1 3) are forbidden. An easy analysis on the moves at the vertex leads to the two cases of Fig. I.55.

One checks that the boundary is the Klein bottle and that the first manifold is the Giesekind one using the correspondence between spines and ideal triangulations given by Proposition I.1.10. $\boxed{\text{I.3.11}}$

Chapter II

Hyperbolicity equations of an o-graph

As a first application of the presentation of 3-manifolds via o-graphs we provide in this chapter an algorithm to test hyperbolicity directly on an o-graph. To be precise, if Γ is an o-graph which represents a 3-manifold M bounded by tori, the algorithm associates to Γ a finite system $\mathcal{S}$ of rational equations in finitely many variables which express hyperbolicity of the ideal triangulation of M corresponding to the o-graph as described in Proposition I.1.10. In particular:

- If $\mathcal{S}$ has a solution in the product of open upper half-planes then the interior $\mathrm{int}(M)$ of M has a complete hyperbolic structure of finite volume;
- If $\mathrm{int}(M)$ has such a structure then for some o-graph representing M the corresponding system $\mathcal{S}$ has a solution in the product of closed upper half-planes minus $\{0, 1\}$.

Actually, the system $\mathcal{S}$ will not be unique, because the algorithm involves certain choices, but the property of having a solution in open upper half-planes will not depend on the particular $\mathcal{S}$ produced.

Roughly speaking, the argument which is behind our algorithm is the following: we consider the ideal triangulation of $\mathrm{int}(M)$ given by Proposition I.1.10 and we look for a hyperbolic structure on $\mathrm{int}(M)$ with respect to which the tetrahedra of this triangulation are geodesic ideal tetrahedra in $\mathbb{H}^3$. Since ideal tetrahedra in $\mathbb{H}^3$ are parametrized by the upper half-plane the problem faithfully translates into a system of equations. However it is remarkable that our algorithm bypasses all 3-dimensional constructions: its implementation deals with planar graphs only, and also its proof essentially takes place on the boundary of M.

The reason why our algorithm might have some interest is that according to Thurston's hyperbolization theorem [Thu2], [Thu3], [Morg] (see also [Ja], [Hem] for the topological background) the interior of an irreducible 3-

manifold bounded by tori in general does have a complete hyperbolic structure, so it is a very natural question to try and construct it using an ideal triangulation. Moreover it is known [Ep-Pen] that for some triangulation this attempt "almost" succeeds (in the sense that moduli in $\mathbb{R} \setminus \{0, 1\}$ must be accepted —see [Pet] for an example). We also recall that in recent years there has been considerable interest in algorithmic approaches to hyperbolization of 3-manifolds (in particular link complements) using ideal triangulations [Ad-Hi-We], [Hen-We], [We].

We think that o-graphs could serve as a useful framework for constructing examples of hyperbolic manifolds: on the one hand it is obvious how to list all o-graphs explicitly and on the other hand the method to associate equations to the o-graph is very easy (much easier than the method for link complements). See also [Mat-Fo] for a discussion about this point which does not mention o-graphs.

The chapter is organized as follows: Section 1 contains the statement of the result. Section 2 briefly reviewes general facts concerning hyperbolicity of ideal triangulations of manifolds bounded by tori. In Section 3 we show how to recover the boundary directly from the o-graph, using an easy representation of surfaces by planar graphs. In Section 4 we look closely at the triangulation of the boundary derived from the ideal triangulation of the manifold, we show how to obtain the hyperbolicity equations and hence we conclude the proof of the main result.

II.1 The algorithm

In this section and in other parts of the chapter we will deal with planar graphs which have trivalent and quadrivalent vertices, where trivalent vertices are marked. By this we mean that quadrivalent vertices are fake: in other words the graph is a trivalent abstract one which is locally planar near vertices. By now the reader should be familiar with such a convention, and we do not insist on this point.

In the next statement we refer to the topology of the boundary of the manifold represented by an o-graph: we will show below in Proposition II.3.2 that it is quite easy to reconstruct it from the o-graph. Actually, Proposition II.3.2 is based on a construction which is strictly contained in that of the next result. We prefer to keep the statement shorter, and we leave it to the reader to put the two results together.

Theorem II.1.1. *Let Γ be an o-graph and let M be the associated compact oriented 3-manifold with boundary. Assume that ∂M consists of tori. Assign labels $z_1, \ldots, z_n$ to the vertices of Γ and construct a coloured trivalent graph Θ as shown in Figg. II.1 and II.2; the colouring consists of a symbol z_i or z_i' or z_i'' attached to each germ of edge, where z_i' and z_i'' stand respectively for*

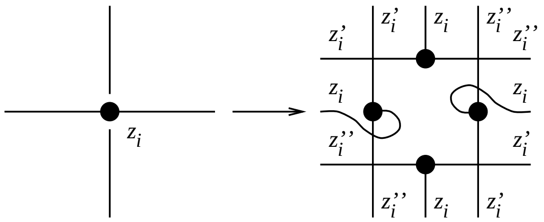

Figure II.1: Trivalent graph associated to an o-graph: first rule

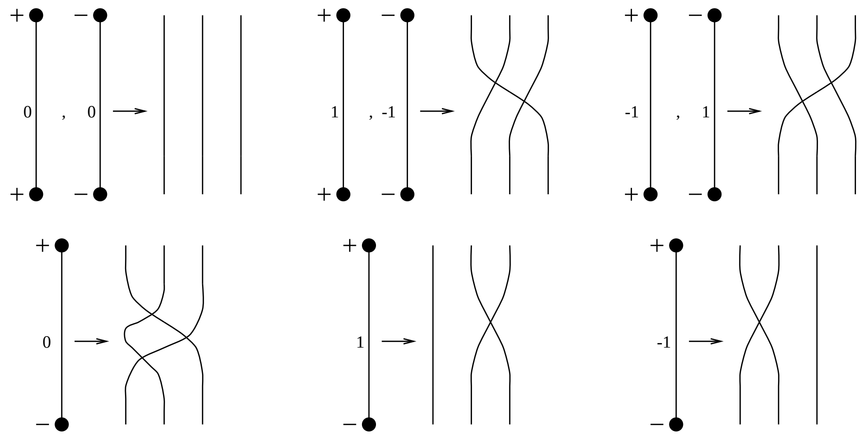

Figure II.2: Trivalent graph associated to an o-graph: second rule

the expressions $1/(1-z_i)$ *and* $1-1/z_i$. *Choose generators* $\gamma_1,...,\gamma_p$ *of* $H_1(\Theta)$, *where* γ_j *is a simplicial loop. For* $j=1,...,p$ *define rational expressions* $h(\gamma_j)$ *in* $z_1,...,z_n$ *as follows:*

1. *Fix an arbitrary starting point on* γ_j *and an initial expression* $u=1$.
2. *Follow* γ_j *and at every vertex you meet replace your expression* u *by the new expression* u' *shown in Fig. II.3.*
3. *When you are back to the intial point, set* $h(\gamma_j)=u$.

Consider the system of rational equations

$$\mathcal{S}: \;\; h(\gamma_j)=1 \qquad j=1,...,p.$$

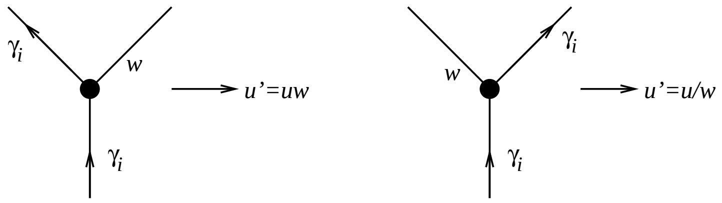

Figure II.3: How u changes through a vertex

Then $\mathcal{S}$ has a solution in a product of open half-planes if and only if $\mathrm{int}(M)$ *has a complete hyperbolic structure of finite volume with respect to which the tetrahedra of the ideal triangulation given by Proposition I.1.10 are isometric to geodesic ideal tetrahedra in $\mathbb{H}^3$. In particular the property that $\mathcal{S}$ has a solution in a product of open half-planes does not depend on the choice of the generators γ_j.*

Remark II.1.2.

1. The trivalent graph Θ of the statement might well be disconnected. We will actually see that its components naturally correspond to the boundary components of M.
2. The choice of simplicial generators for $H_1(\Theta)$ can be performed algorithmically. One proceeds separately for each component and exploits the following recursive procedure which gives generators of $H_1(G)$ for any connected graph G:
   (a) if G is a bouquet of circles, i.e. it has one vertex, take these circles;
   (b) if G has en edge e which joins distinct vertices, collapse e, apply recursion and reintroduce e in the obvious way.
3. In Fig. II.3 we have tacitly assumed that each γ_j is a local embedding. Of course to have a more formal statement we could either stipulate that the γ_j's are indeed local embeddings or give the rule that u is unchanged at vertices where γ_j returns on its steps. In the former case we would need to modify the γ_j's produced by the algorithm outlined above by getting rid of edges which are followed in one direction and immediately afterwards in the opposite direction.
4. With some effort and adding more structure to the input of a graph (e.g. a total order of the vertices and a direction on each edge) one can devise an algorithm which leads to a unique well-defined set of generators of the first homology group. In view of the last assertion of Theorem II.1.1 this effort is not worthwhile.

II.2 Hyperbolicity equations

In this section we assume that the reader is familiar with the basics of hyperbolic geometry —see e.g. [Thu1], [Be-Pet1]. We just recall that ideal tetrahedra in $\mathbb{H}^3$ up to orientation-preserving isometry are parametrized by euclidean triangles up to orientation-preserving similarity. If we mark a pair of opposite edges on the tetrahedron, i.e. a vertex on the triangle, the space of moduli is the open upper half-plane π^+. If we change the marking the moduli change in an easy way (see Fig. II.4 for an illustration of these facts; as usual $z' = 1/(1-z)$ and $z'' = 1 - 1/z$).

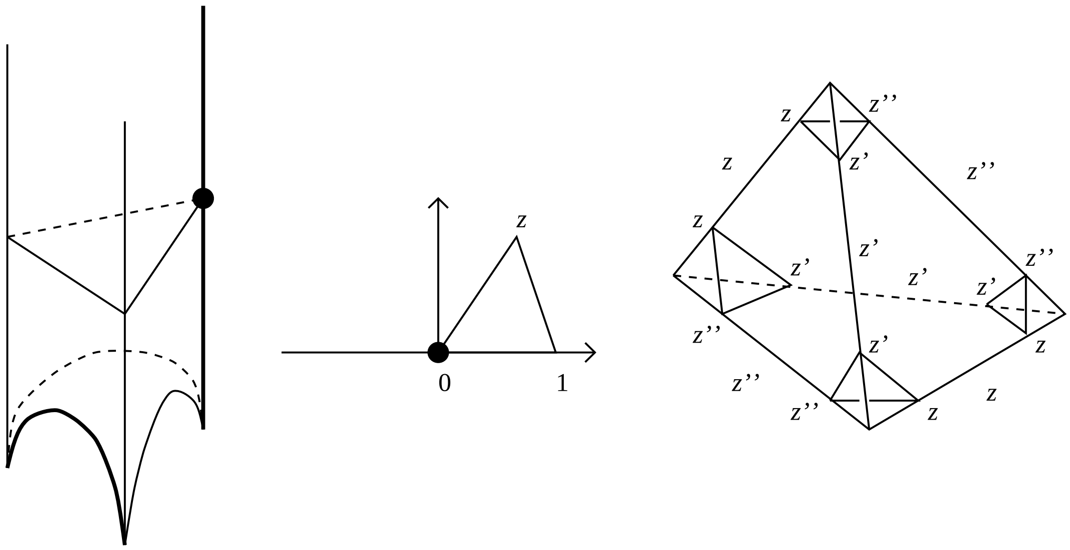

Figure II.4: Moduli for ideal tetrahedra and similarity triangles

Let M be a compact oriented 3-manifold with non-empty boundary whose interior has a fixed ideal triangulation. (We already know that these triangulations correspond bijectively to standard spines of M by Proposition I.1.10.) We want to endow $\mathrm{int}(M)$ with a complete hyperbolic structure of finite volume, which forces us to assume that ∂M consists of tori. We try to do this by realizing the tetrahedra as ideal ones in $\mathbb{H}^3$ and then extend the structure.

So, fix moduli for the various tetrahedra. If we realize the gluings by isometries we have a hyperbolic structure which we must extend to the edges and make complete. Remark that the boundary tori are now unions of similarity triangles (Fig. II.4) glued along edges by similarities.

Proposition II.2.1. *The hyperbolic structure of the tetrahedra extends to a global complete hyperbolic structure on* $\mathrm{int}(M)$ *if and only if on each torus of* ∂M *the above-defined decomposition into similarity triangles is compatible with a global euclidean structure.*

Proof of II.2.1. This fact can be seen as an application of the 3-dimensional version of Poincaré's polyhedron theorem (see [Ep-Pet] and the references quoted therein). We only need to remark that every edge (i.e. codimension-2 face) must hit the boundary: therefore the condition that the tetrahedra are properly glued around it is subsumed by the assumption that on the boundary the triangles are properly glued.

See also [Be-Pet1] for a direct proof of this result. $\boxed{\text{II.2.1}}$

So, given a torus subdivided into similarity triangles we want to be able to say whether the torus is globally euclidean. We have the following criterion:

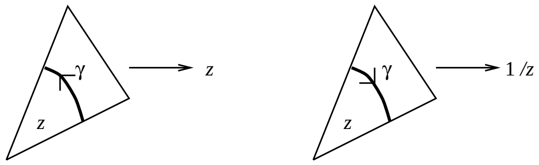

Figure II.5: Contribution of the intersection with a triangle (oriented as a subset of the plane)

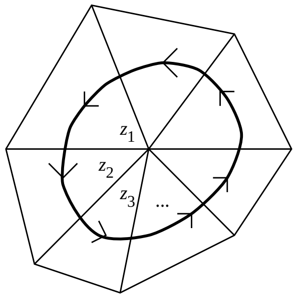

Figure II.6: Extension to the vertices of the similarity structure

Lemma II.2.2. *Let the torus be subdivided into triangles each having a fixed similarity structure given by some element of π^+. Let G be the 1-skeleton of the dual cellularization to this subdivision. If γ is a simplicial loop in G define a number $h(\gamma) \in \mathbb{C}_*$ as the product of a contribution for each triagle γ meets, as shown in Fig. II.5. Then h is a well-defined homomorphism on $H_1(G)$ and the torus supports a euclidean structure compatible with the similarity structure of the triangles if and only if $h(\gamma)$ is identically* 1.

Proof of II.2.2. The first assertion is obvious and we take it for granted.

We first claim that if $h(\gamma) \equiv 1$ then in particular we have a global similarity structure: to check compatibility at vertices we take loops around each of them (Fig. II.6). The hypothesis implies that the product of the moduli around each vertex is 1, and then the compatibility condition is that the sum of the arguments is always 2π and not $2\pi n$ with $n \geq 2$. Using the fact that the Euler characteristic of the torus is 0 we see that the triangles are twice as many as the vertices. So if at some vertex the sum of the arguments is more than 2π then the total sum of the arguments is more than π times the number of triangles. This is a contradiction and our claim is proved.

So we can prove the lemma assuming that we have a torus T with a similarity structure. We can associate to this structure a homomorphism (the holonomy) $H_1(T) \to \mathbb{C}_* \coprod \mathbb{C}$ well-defined up to conjugation. (Here $\mathbb{C}_* \coprod \mathbb{C}$ is the group of orientation-preserving similarities of the plane.) If we project to the factor $\mathbb{C}_*$ we have a well-defined homomorphism $\tilde{h} : H_1(S) \to \mathbb{C}_*$ and it can be shown (see e.g. [Be-Pet1]) that the torus is euclidean if and only if $\tilde{h} \equiv 1$.

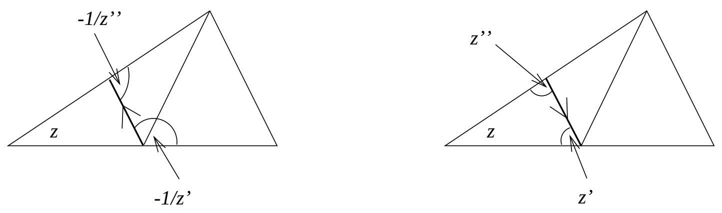

Figure II.7: These further subdivisions turn γ into a simplicial loop

The following rule of computation can be found in [Be-Pet1]: if γ is a simplicial loop then $\tilde{h}(\gamma)$ is the product of a contribution for every vertex v of γ; v contributes with minus the product of the moduli at v of the triangles which are on the right of γ at v. Now we can adapt this rule to loops in G, and show that actually the map h of the statement is just $\tilde{h}$ composed with the quotient map $H_1(G) \to H_1(T)$, whence the conclusion.

By simplicity, we refer to a loop γ which meets each triangle in one simple arc. We can assume that γ meets edges in their midpoints. Now we further subdivide the triangles (without changing the similarity structure) so that γ becomes simplicial, see Fig. II.7. In this figure we have also shown the moduli on the right of γ. The contribution of the edge in exam to $h(\gamma)$ is minus the product of these moduli, i.e. respectively:

$$-(-1/z')(-1/z'') = z \qquad - z'z'' = 1/z$$

and the proof is complete. $\boxed{\text{II.2.2}}$

The proof of the above result makes an essential use of the fact that the surface in question is a torus. However given any surface subdivided into similarity triangles, a homomorphism h can be defined as in the above statement, and one may wonder whether the assumption that $h \equiv 1$ forces the surface to be a torus. This is false, and a counterexample is given in Fig. II.8. This figure shows the surface of genus 2 subdivided into euclidean triangles (each triangle is drawn in the plane with its own similarity structure, and the moduli are shown). The homology group of the 1-skeleton of the dual cellularization has 5 generators, and it is quite easy to check that h is indeed 1 on them.

We conclude this section by recalling that in [Ep-Pen] it has been shown that a non-compact complete hyperbolic 3-manifold with finite volume is obtained by gluing together in pairs the faces of finitely many convex ideal geodesic polyhedra. If we cut the polyhedra into tetrahedra being careful that faces glued together are cut into triangles in the same way, we obtain a topological ideal triangulation which is isotopic to a geodesic ideal triangulation where some of the tetrahedra might have degenerated into quadrilaterals (two edges being the diagonals). This corresponds to taking moduli

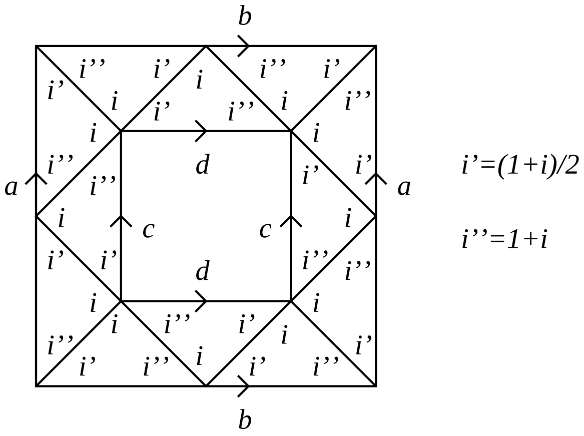

Figure II.8: A similarity triangulation of the genus 2 surface

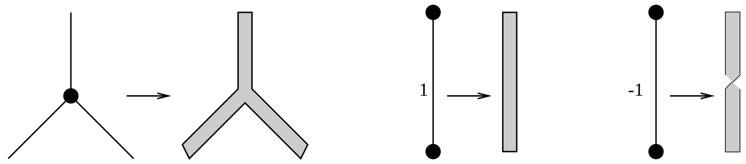

Figure II.9: How to construct the trivalent ribbon

in $\pi^+ \cup (\mathbb{R} \setminus \{0,1\})$ rather than in π^+ only. If we modify Lemma II.2.2 by allowing some triangles to have moduli in $\mathbb{R} \setminus \{0,1\}$, it is still true that if the torus is euclidean then $h \equiv 1$ (the converse is not quite true and we avoid discussing the matter in detail). So for the stated ideal triangulation we have a "generalized solution" of the equations $h \equiv 1$.

II.3 Recovering the boundary from the o-graph

We first quickly introduce a representation of surfaces by planar graphs and its oriented version. We use trivalent graphs with fake quadrivalent vertices, in the usual sense, where edges have colour $+1$ or -1. If Θ is such a graph we obtain a surface from it by first constructing a trivalent ribbon as shown in Fig. II.9 and then attaching a disc to every boundary component of the ribbon.

If we start with a graph with no edge-colour we introduce the colour $+1$ everywhere and repeat the construction: but now the ribbon (and hence the surface) has a well-defined global orientation (given by the local embedding in the plane).

Remark II.3.1. 1. The surface resulting from a graph Θ with edge-colours

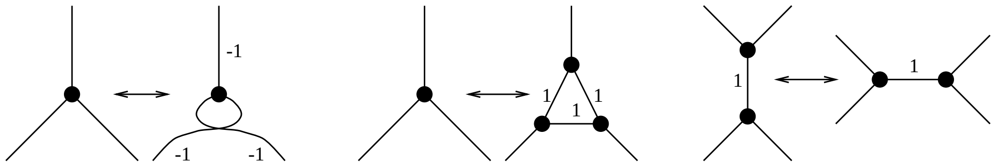

Figure II.10: Graphs defining the same surface are equivalent under these moves

is orientable if and only if in Θ the product of colours along closed circuits is always 1.

2. Every surface can be obtained from some Θ, and every oriented surface can be obtained from some Θ with no edge-colours.

3. Using [Pa] it is not hard to find a planar calculus for surfaces based on these representations. The moves to be taken into account in the general case are those of Fig. II.10 (plus those which express the fact that quadrivalent vertices are fake), and the first move is omitted in the oriented case. Moreover a graph of an orientable surface can be stransformed into one without edge-colours (i.e. all colours equal to $+1$) by moves of the first type.

4. Since we know that surfaces are completely classified, this presentation is not so interesting. However, even in the oriented case, the computation of the Euler characteristic is not local in Θ, and one essentially needs to reproduce the construction.

Proposition II.3.2. *Let Γ be an o-graph representing a 3-manifold M and let Θ be the graph associated to Γ as in Figg. II.1 and II.2 (disregarding the colours z_i, z_i', z_i''). Then the surface associated to Θ as described above in this section is the boundary of M.*

Proof of II.3.2. The standard polyhedron defined by Γ and the way M is reconstructed from it naturally induce a decomposition of ∂M into pieces of 3 types: "wide T's", strips, discs; the first two types of pieces are shown in Figg. II.11 and II.12, while discs appear as upper and lower caps of the solid discs $D^2 \times [0,1]$ glued in to obtain M. The same Figg. II.11 and II.12 (together with the discussion of the remaining cases, which we leave to the reader) prove that ∂M is represented by the graph Θ_0 which is obtained from Γ via the rules of Figg. II.13 and II.14. Now we must take into account the fact that in Fig. II.11 (and its translation Fig. II.13) part of the boundary has been embedded with the wrong orientation. By applying twice the first move of Fig. II.10 we can correct the orientation as shown in Fig. II.15. It is now easy to check that the result is the graph Θ with all coulours $+1$ described in the statement. $\boxed{\text{II.3.2}}$

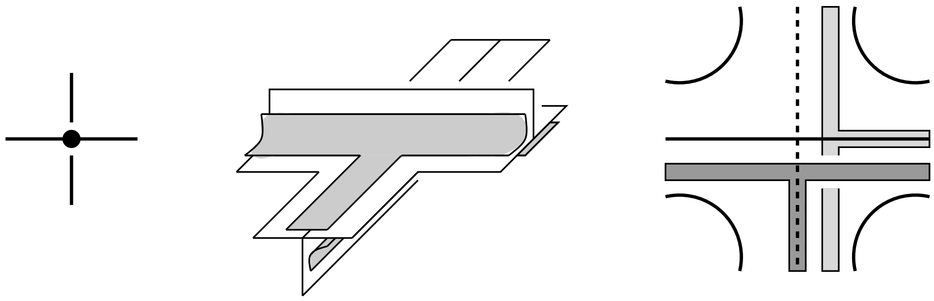

Figure II.11: "Wide T's" on the boundary

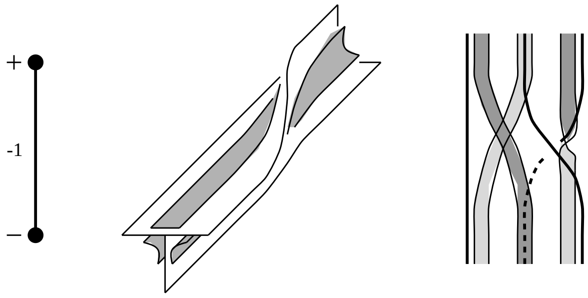

Figure II.12: Strips on the boundary

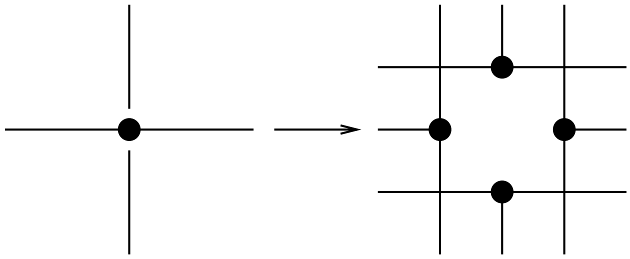

Figure II.13: A non-oriented representation of the boundary: first rule

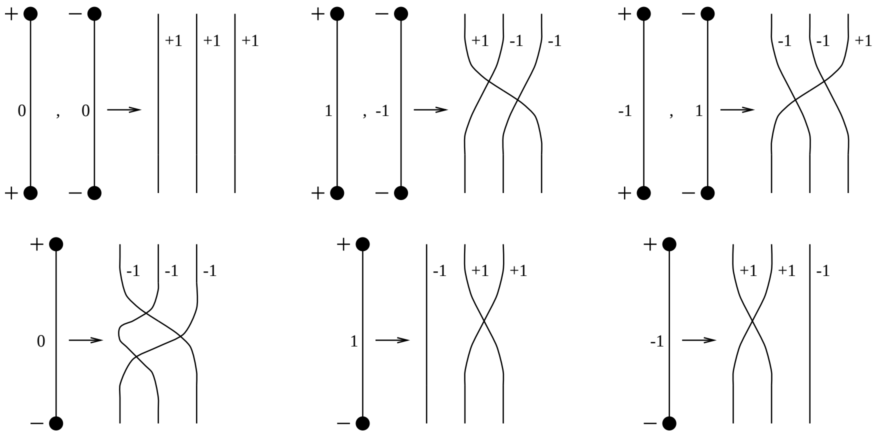

Figure II.14: A non-oriented representation of the boundary: second rule

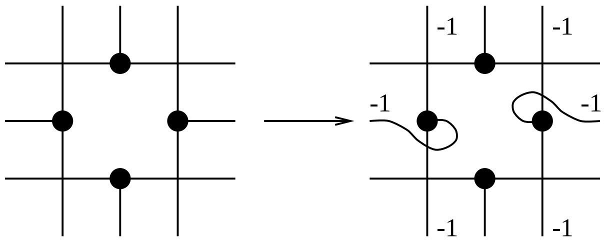

Figure II.15: Correcting orientation

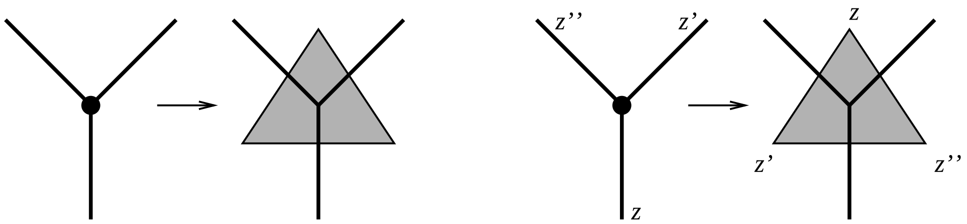

Figure II.16: Associating a triangle to a trivalent vertex

II.4 Triangulation of the boundary and proof of the main result

In this section we prove Theorem II.1.1. The argument is carried out in four steps, the first three of which are actually more general: they are developments of the representation of surfaces introduced in the previous section.

Triangulations of surfaces. We suggest another way to understand the representation of surfaces defined above. Let Θ be a planar trivalent graph with fake crossings. We can associate to every vertex of Θ a triangle in the plane as in the left-hand side of Fig. II.16. Now, an edge of Θ joins two edges of triangles, and we agree that it prescribes the orientation-reversing gluing of these two edges. The result of these gluings is the surface represented by Θ. (If there are edges with colour -1 then the corresponding gluings will preserve orientation.)

Similarity triangulations of surfaces. We can now push this method farther and assume that the three germs of edges at every vertex of Θ are coloured by numbers $z, z', z'' \in \pi^+$ with $z' = 1/(1-z)$ and $z'' = 1 - 1/z$, with z, z', z'' arranged in counter-clockwise order around the vertex. Then, as in the right-hand side of Fig. II.16, we can associate to the vertex a similarity triangle.

Computation of holonomy. Let Θ be as above (with colours z, z', z'' on germs of edges) and assume it represents a torus T. A simplicial loop γ in Θ can be seen as a loop in the 1-skeleton of the cellularization dual to the triangulation of T defined by Θ; if one goes back to Lemma II.2.2 and to the function h defined there, he sees that $h(\gamma)$ is computed exactly as in the statement of Theorem II.1.1. Moreover we have that h is a homomorphism, therefore T

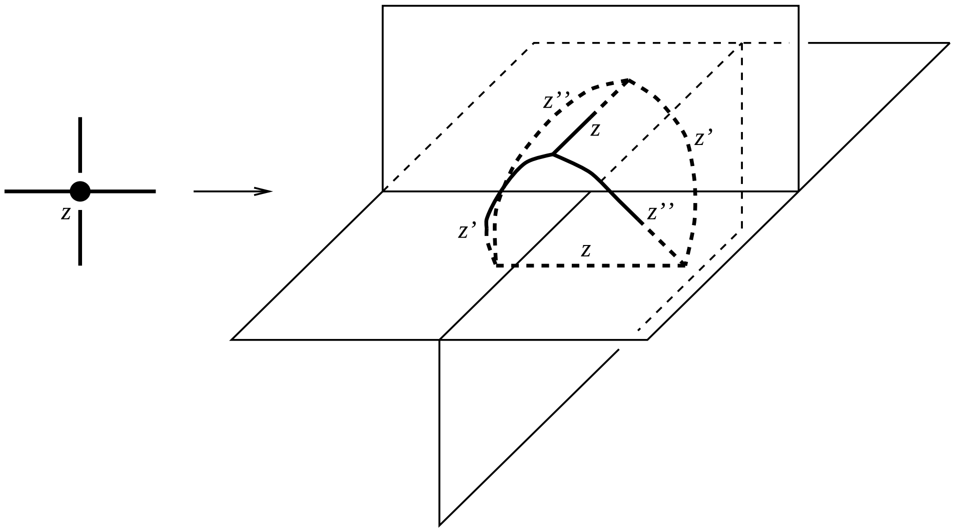

Figure II.17: Moduli of the tetrahedra in the decomposition

has a euclidean structure compatible with the decomposition into similarity triangles if and only if $h(\gamma) = 1$ when γ ranges in a set of generators of $H_1(\Theta)$.
Conclusion. Now fix the notation of the statement of Theorem II.1.1. Recalling Proposition I.1.10, to the i-th vertex of the o-graph there corresponds a tetrahedron in the associated decomposition of M. As shown in Fig. II.17 the variable z_i is the modulus for the identification of this tetrahedron with an ideal one. Now we have that ∂M is decomposed into similarity triangles, and it follows from Fig. II.18 that this decomposition is obtained from Θ in the abstract way explained earlier in this section. By simplicity in Fig. II.18 we are still showing two of the triangles with the wrong orientation, but the correction already shown in Fig. II.15 allows us to conclude.

Therefore the quations $h(\gamma) = 1$ are exactly those which express hyperbolicity in the sense of Proposition II.2.1. $\boxed{\text{II.1.1}}$

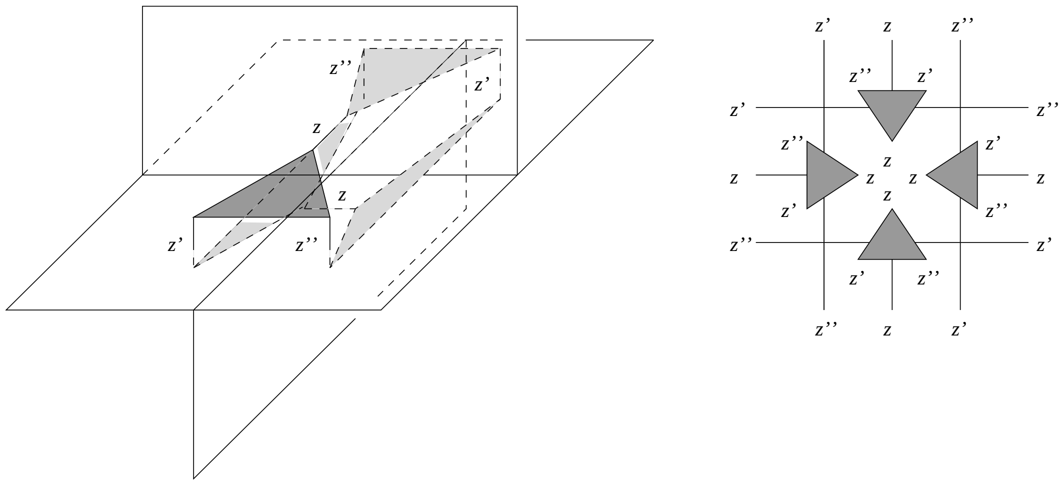

Figure II.18: Moduli of the triangles in the decomposition of the boundary

Chapter III

Constructions of graphic presentations

This chapter contains spare material whose aim is to convince the reader that presenting 3-manifolds by o-graphs is not only very simple, but also quite natural. In particular we show that certain natural operations as making punctures and taking connected sums are immediately translated in terms of o-graphs (Section 3). We provide algorithms (linear in terms of complexity, in a natural sense) which give o-graphs of manifolds presented by surgery (Section 1) and of link complements (Section 3). We also provide an algorithm which, given an o-graph of a once-punctured closed oriented manifold, produces a Heegaard diagram for the manifold (Section 2).

III.1 O-graph from surgery presentation

We assume the reader is familiar with the usual terminology of surgery presentation of 3-manifolds [Ki], [Fen-Rou], [Mort]. The statement and proof of the next result are slightly informal, because a completely precise treatment would be much longer and not much clearer.

Theorem III.1.1. *Let Γ be a link diagram and let M be the closed oriented 3-manifold obtained by Dehn surgery on Γ along the diagrammatic framing. Then the following steps 1-7 lead to an o-graph Γ' which represents M with one puncture.*

1. *We fix in the plane a box which contains a segment ℓ (dotted in the figures) and isotope Γ in the plane so that it is contained in the box, it has finitely many transversal intersections with ℓ and all its crossings lie on ℓ. (See below for various figures illustrating these conditions.)*

2. *Now we start constructing an o-graph bit after bit. Outside the box we operate as described in Fig. III.1.*

3. *We replace each component of* Γ *by a strip (with dashed margins in the figures) parallel to it. (In other words we are taking the ribbons defined by the diagrammatic framing. See the next point for special rules to be applied near* ℓ*, in particular at crossings.)*

4. *Near* ℓ *we operate as described in Figg. III.2 to III.4. (Observe the pairs of signs* $+$ *and* $-$ *which we introduce: they will serve for the rest of the construction.)*

5. *Inside each strip there are now finitely many* $+$*-pairs and* $-$*-pairs. We need to have at least three of each: if we have less we operate as in Fig. III.5 and/or Fig. III.6.*

6. *Now we will operate within each strip. We stipulate that any vertex which will arise because of strip-crossings will be a fake one. Therefore if we concentrate on one strip we can pretend it looks as in Fig. III.7. Without loss of generality we also assume that the sequence of signs has the form*

$$(-)^{h_0}(+)^{k_0} - +(-)^{h_1}(+)^{k_1}\cdots(-)^{h_p}(+)^{k_p}$$

with k_0 *and* h_1 *possibly* 0 *and all other* h_i*'s and* k_i*'s positive integers. Within the strip we then operate as described in Figg. III.8 to III.10. In all these figures colours not shown are* 0*. Figure III.8 gives the "general rule" for the case* $h_0 = 1$*,* $k_0 = 0$*,* $h_1 = 0$ *and* $k_1 = 1$ *(and* $p = 3$*, but the generalization is obvious). The next two figures illustrate how to modify the general rule in the remaining cases.*

7. *To conclude, we get rid of the extra objects introduced (strips and symbols* $+, -$*) and sum up all multiple colours.*

The number of vertices of Γ' *does not exceed* $2 + 8c_0 + 48c_1 + 8c_2$*, where* c_0 *is the number of isolated components of* Γ *with no crossing (plain circles),* c_1 *is the number of crossings of* Γ *and* c_2 *is the number of intersections with* ℓ*.*

Proof of III.1.1. The proof consists of a direct topological argument leading to a standard spine of the punctured manifold, and its step-by-step translation into the algorithmic procedure described.

For the sake of simplicity we assume that Γ has only one component: the generalization is straight-forward.

Let us start with the Bing house with two rooms B, shown in Fig. III.11, and let us identify the box in which Γ lies with the lower horizontal "face" of B, with ℓ corresponding to the singular segment contained in this "face" (we use quotes because an actual face is a component of the smooth part, whereas we are taking only a portion of it) —see also Fig. III.12. From now on we will concentrate on the portion B_0 of B which is shown in Fig. III.12, and stipulate that the rest is unchanged during our constructions.

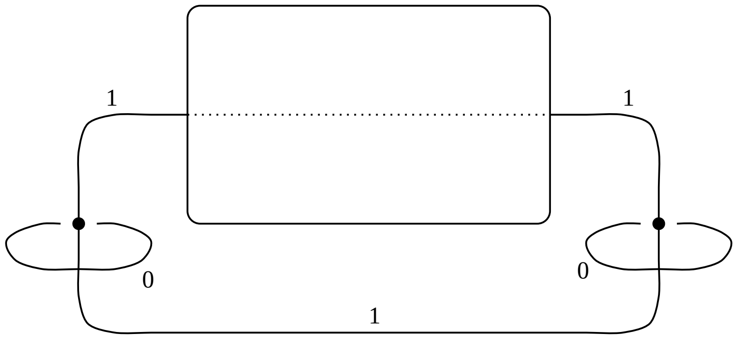

Figure III.1: How to operate outside the box

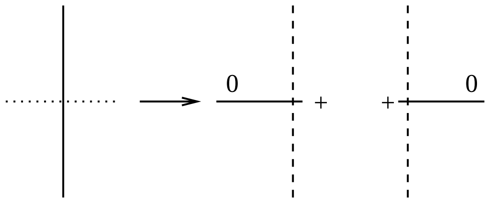

Figure III.2: How to operate at a plain intersection of ℓ and the link

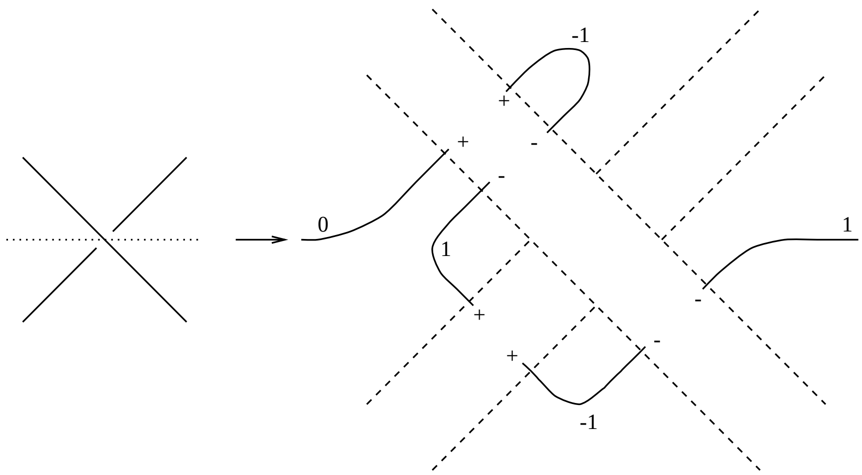

Figure III.3: How to operate at a crossing lying on ℓ: first case

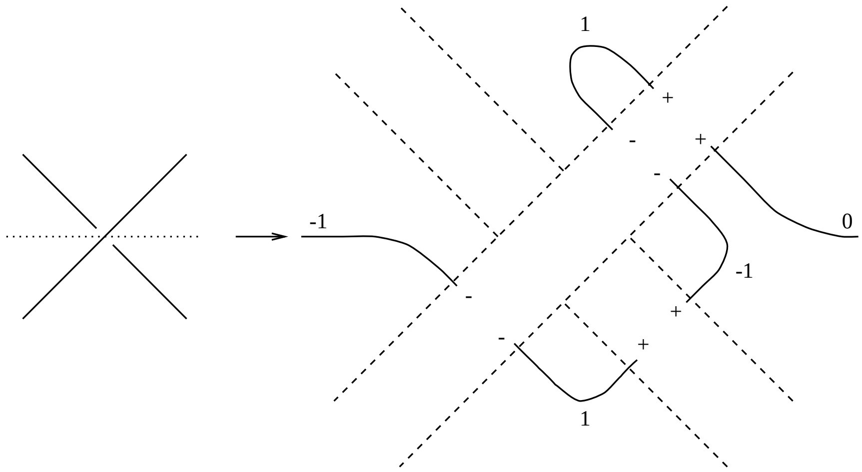

Figure III.4: How to operate at a crossing lying on ℓ: second case

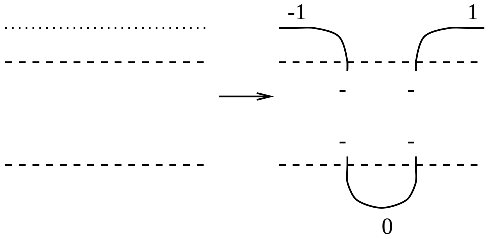

Figure III.5: What to do if there are less than three −-pairs

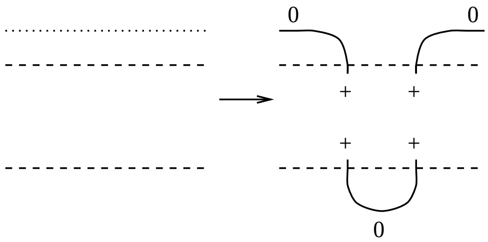

Figure III.6: What to do if there are less than three +-pairs

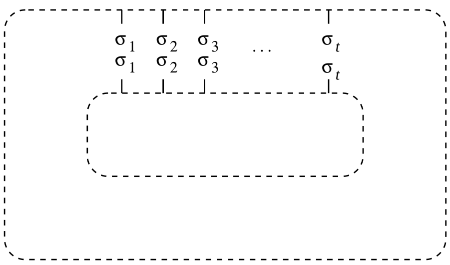

Figure III.7: A strip with its +-pairs and −-pairs

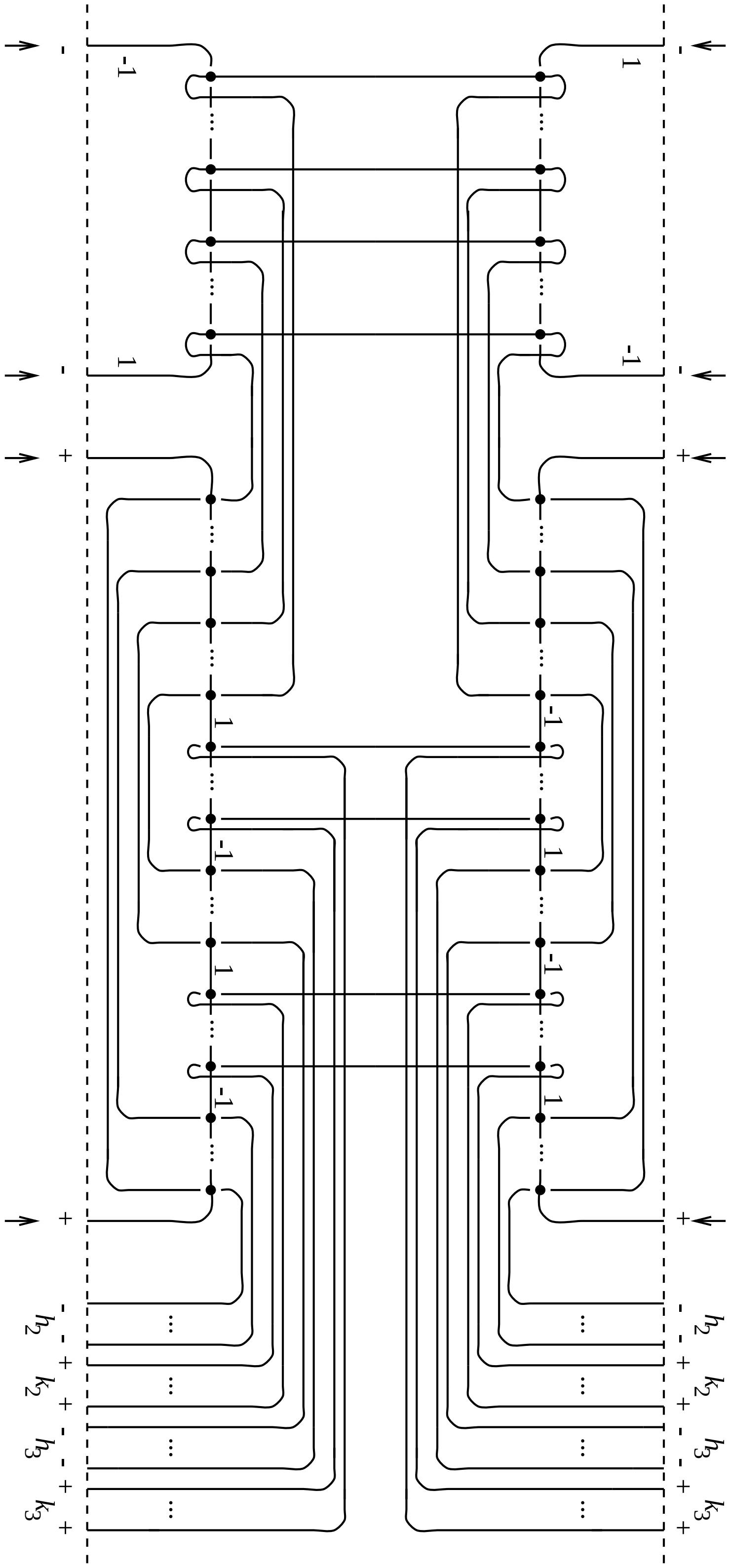

Figure III.8: How to operate within a strip: general rule (the reader is invited to turn the page to see the figure correctly)

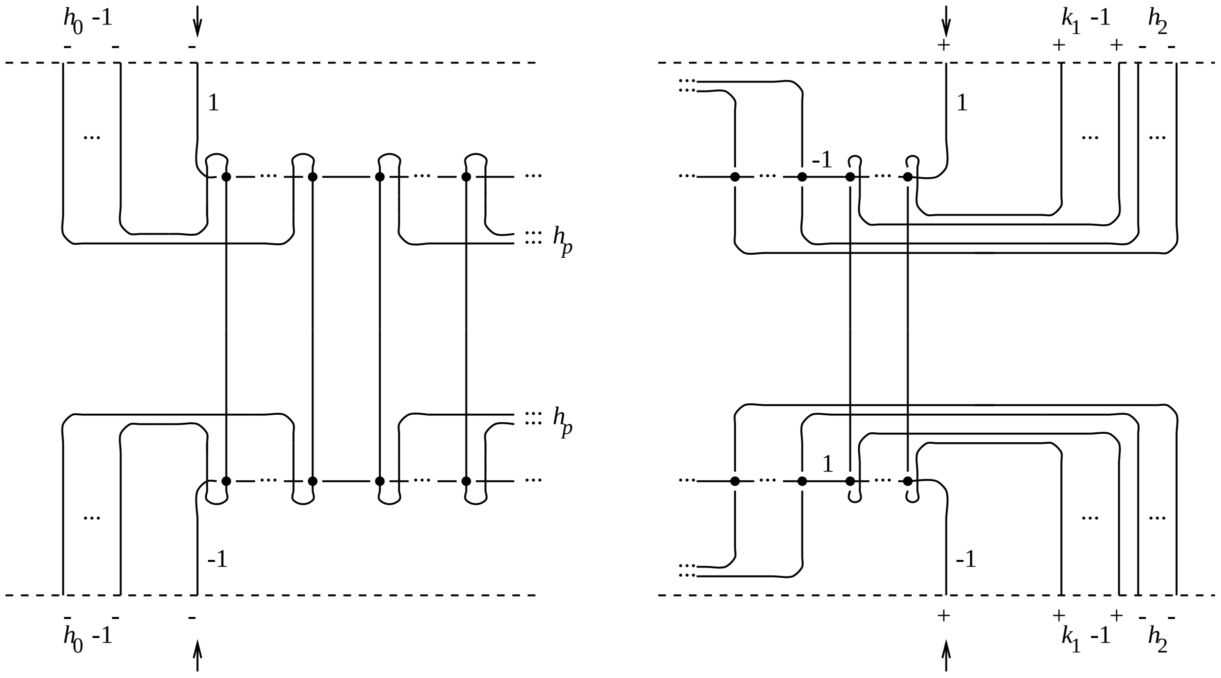

Figure III.9: How to operate within a strip: cases $h_0>1$ and $k_1>1$

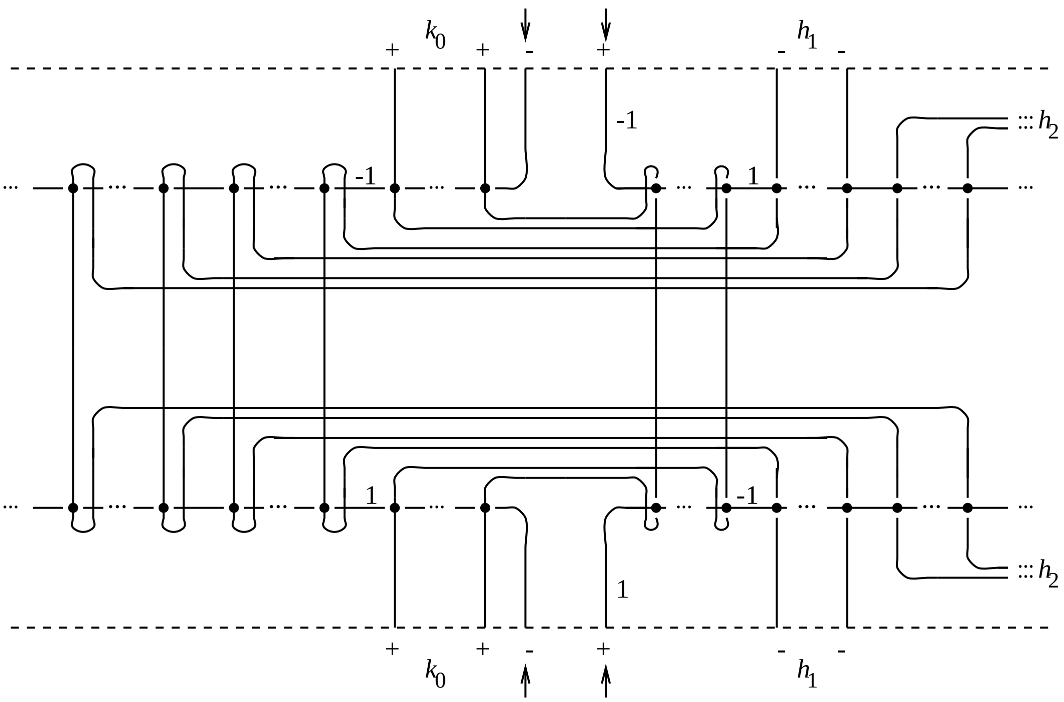

Figure III.10: How to operate within a strip: case $k_0>0$ and/or $h_1>0$

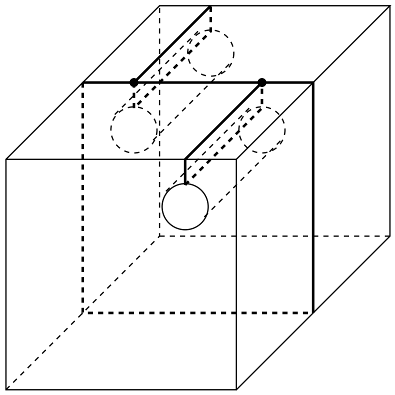

Figure III.11: The Bing house with two rooms

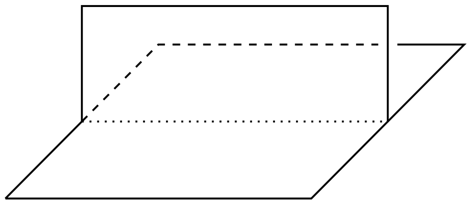

Figure III.12: The box is the lower "face" of B, and ℓ is the singular segment in it

The next step is to embed in B_0 the ribbon R defined by the framing. This is done in Figg. III.13 to III.15.

Now let T be a solid torus embedded in S^3 so that (see Fig. III.16):

- $T \cap B = R \cup S_1 \cup \ldots \cup S_k$, with S_j a "half-disc";
- $\partial T \cap R = \partial R$ (here ∂ has a relative meaning, in an obvious way);
- either component of ∂R is a longitude of T.

Let T_0 be the abstract solid torus $S^1 \times B^2$; give orientations to ∂T and ∂T_0 as boundaries and fix an orientation-preserving homeomorphism $f : \partial T \to \partial T_0$ such that $f(\partial R)$ consists of two meridians of T_0. By definition:

$$M = (S^3 \setminus \mathring{T}) \sqcup_f T_0.$$

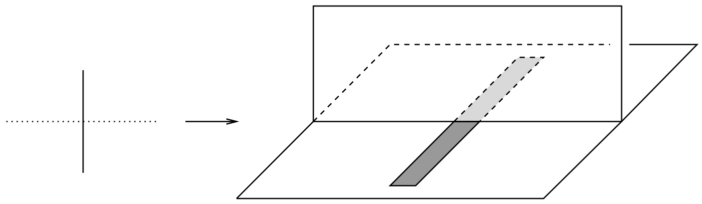

Figure III.13: Embedding R into B_0: first rule

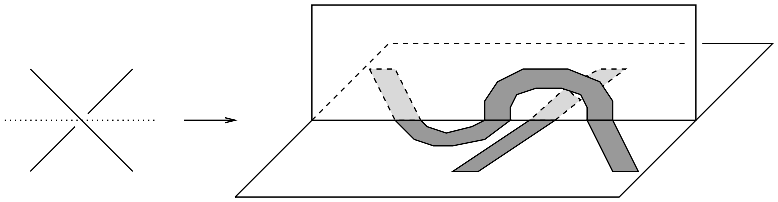

Figure III.14: Embedding R into B_0: second rule

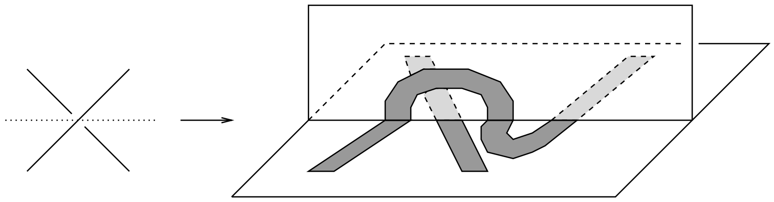

Figure III.15: Embedding R into B_0: third rule

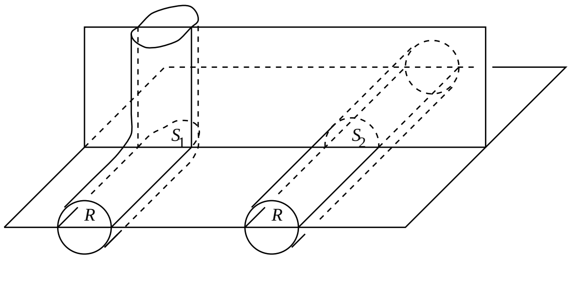

Figure III.16: How to embed the solid torus T along R

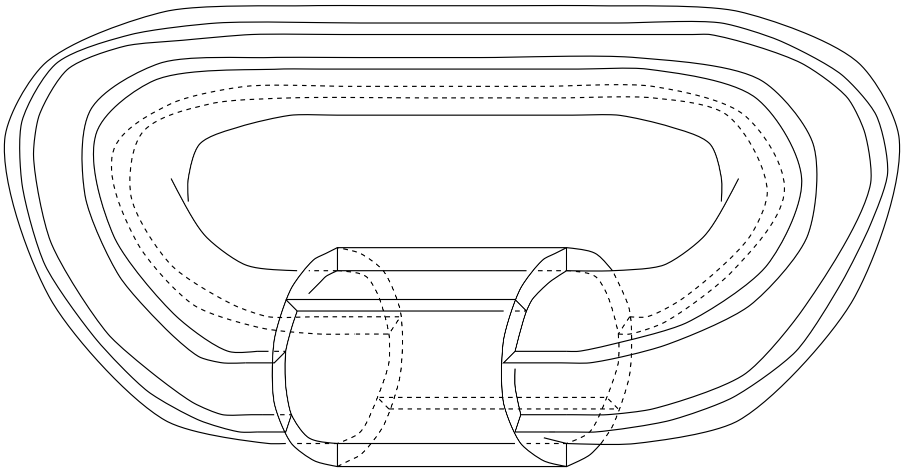

Figure III.17: A neighbourhood of T_0 in X

Moreover it is obvious that M with a puncture collapses onto

$$X = ((B \setminus \mathring{T}) \cup \partial T) \sqcup_f T_0.$$

Far from T_0 the set X is already a standard polyhedron. We will see now how to construct a standard polyhedron $Y \subset X$ such that X collapses onto Y and $X \setminus T_0 = Y \setminus T_0$.

So we examine what X looks like near T_0. This is shown in Fig. III.17. This figure consists of the following elements, for which we choose names for further reference: two meridinal annuli A_1 and A_2; the torus T_0 whose surface is divided into two cylinders C_+ and C_- by A_1 and A_2; some bridges joining A_1 and A_2 and based on C_+; some bridges joining A_1 and A_2 and based on C_-. Here are some remarks concerning this figure:

1. A_1 and A_2 result from extending R on B_0 outside T, and the bridges result from extending the half-discs S_j on B_0 outside T.

2. It has been possible to draw the bridges along parallel longitudes because no situation as in Fig. III.18 will ever arise, thanks to the very construction.

3. On C_+ and C_- there could actually be no bridges at all (this is the case for instance if Γ is a plain circle). But by adding some situations as in Figg. III.19 and/or III.20 we can assume that on both cylinders there are at least three bridges.

Now the construction of Y inside T_0 goes as follows:

1. We fix a positive direction for meridians of ∂T_0 and consistently follow A_1 and A_2 along this direction, meeting therefore $+$-bridges and $-$-bridges.

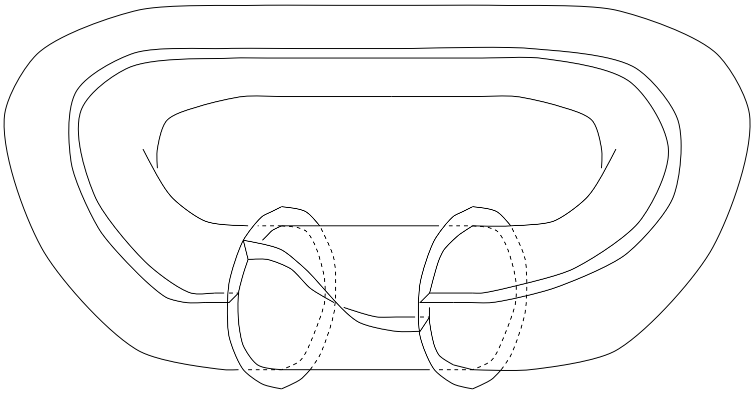

Figure III.18: Such a situation cannot arise

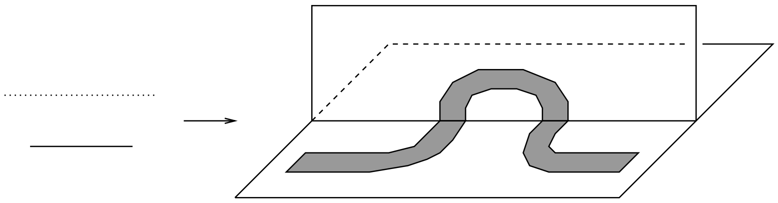

Figure III.19: This operation introduces two bridges on one of the cylinders

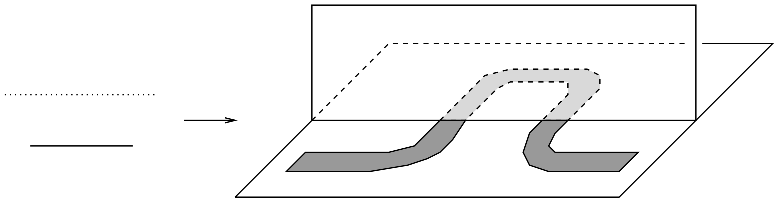

Figure III.20: This operation introduces two bridges on the other cylinder

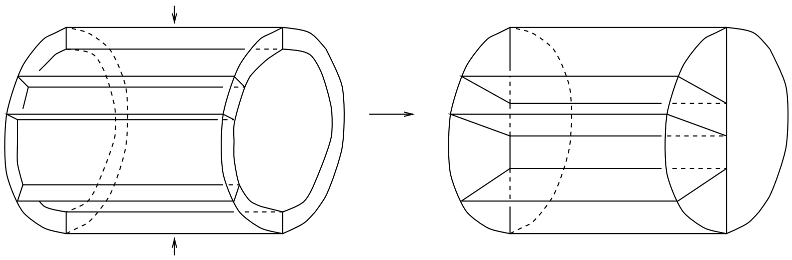

Figure III.21: How to cut one solid cylinder

We choose the starting point so that the sequence of signs met along the annuli appears as in the statement (of course it is possible). Now we choose two preferred bridges on C_+ and two on C_-, as suggested by the little arrows in the following formula:

$$(-)^{h_0-1}\underset{\uparrow}{-}(+)^{k_0}\underset{\uparrow}{-}\underset{\uparrow}{+}(-)^{h_1}\underset{\uparrow}{+}(+)^{k_1-1}(-)^{h_2}\cdots(+)^{k_p}.$$

2. We extend A_1 and A_2 to discs, so to cut T_0 into two solid cylinders.

3. First concentrating on one cylinder without worrying about the other one, we operate as in Fig. III.21, i.e. we extend the two preferred bridges until they meet to form a planar region, and then we extend the other bridges until they meet such a region, without any other intersection arising in the meantime.

4. We arrange things so that on both discs the situation is as in Fig. III.22

It is now easy to see that Y is a standard spine of the punctured M. For this aim it is important that there are at least 3 bridges: if the two preferred bridges are on the same component of the smooth part of $X\setminus T_0$ (which can be the case) then when we paste them together we form an annulus: but the singularities arising from the other bridges cut this annulus into discs. We are left to read back through the gluing function f how the original spine B has been modified, and compute the resulting o-graph. We use for this purpose figures which intermingle the o-graph notation with actual 3-dimensional objects.

The first step is shown in Fig. III.23: we use the o-graph of B which is easily computed.

The next step is to lay R down on the plane (with self-crossings, which we ignore), with A_1 and A_2 being actual horizontal annuli (also with self-crossings), and the bridges appearing as genuine bridges or tunnels, according to the cylinder they lie on. This is done in the two basic situations in Figg. III.24 and III.25, from which the relevant situations are deduced (Fig. III.13 translates into Fig. III.2, Fig. III.14 into Fig. III.3, Fig. III.15 into Fig. III.4, Fig. III.19 into Fig. III.5 and finally Fig. III.20 into Fig. III.6).

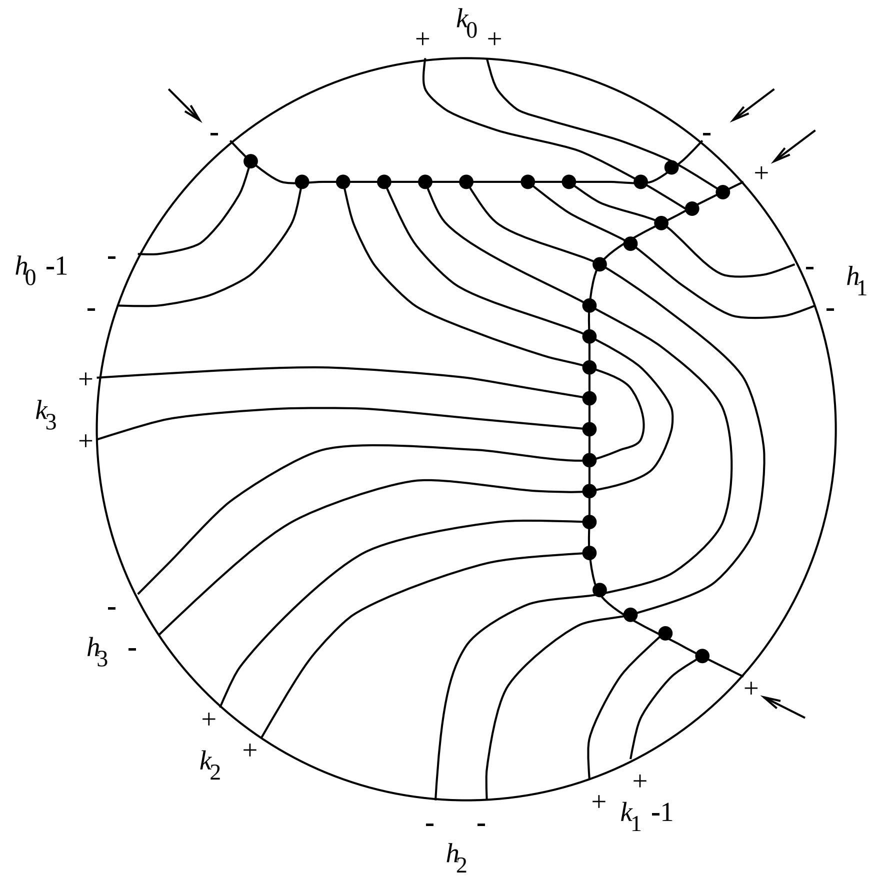

Figure III.22: On the discs which the solid cylinders share the construction goes as shown

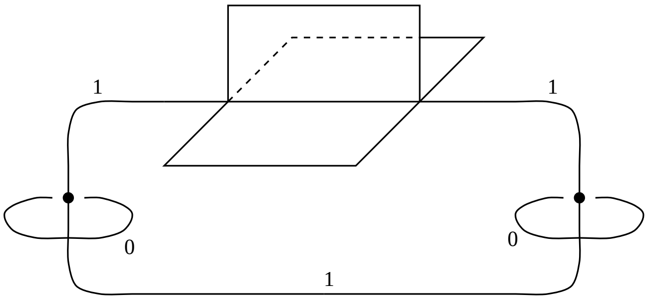

Figure III.23: Far from Γ we have the o-graph of the Bing house

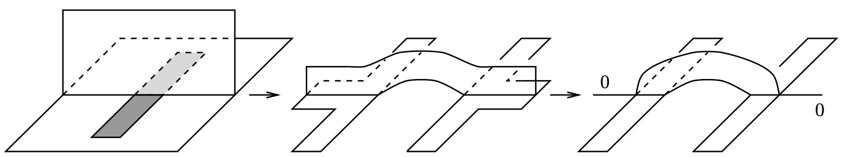

Figure III.24: First fundamental rule to lay R on the plane

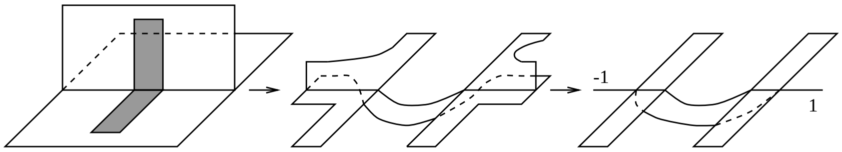

Figure III.25: Second fundamental rule to lay R on the plane

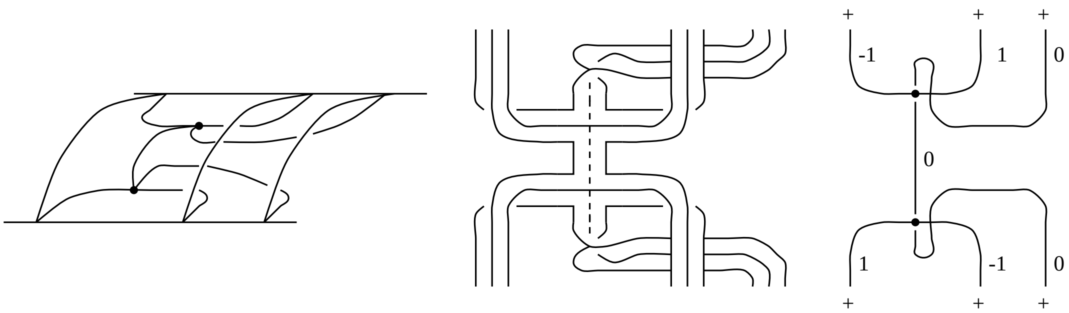

Figure III.26: Translation from the abstract torus to the real one: first case

Now we need to translate in terms of the actual torus the construction done inside the abstract torus (Figg. III.21 and III.22). We describe separately all the relevant situations in Figg. III.26 to III.30. It is not hard to put them together and deduce the rule given in Figg. III.8 to III.10.

Now the construction is complete and we are left to give an upper bound to the number of vertices of the resulting o-graph. Of course we have 2 "fixed" vertices (those of B) and 8 vertices on every isolated plain circle (see also the example below), so we need an estimate for the vertices coming from components with crossings.

If we look at Fig. III.22 we easily have that the vertices in it are at most 3 times the total number of signs on the boundary. So within the strips the vertices will be at most 6 times the total number $+$-pairs and $-$-pairs (i.e. the total number of bridges and tunnels). This is in turn bounded above by

$$4 \cdot \#(\text{crossings of the projection})$$

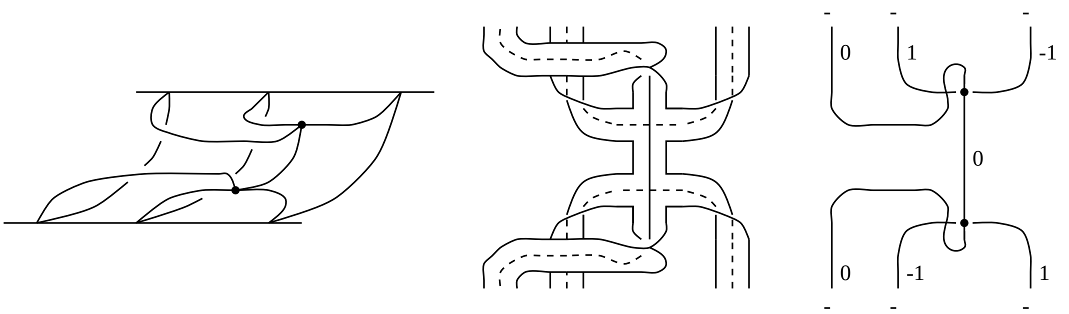

Figure III.27: Translation from the abstract torus to the real one: second case

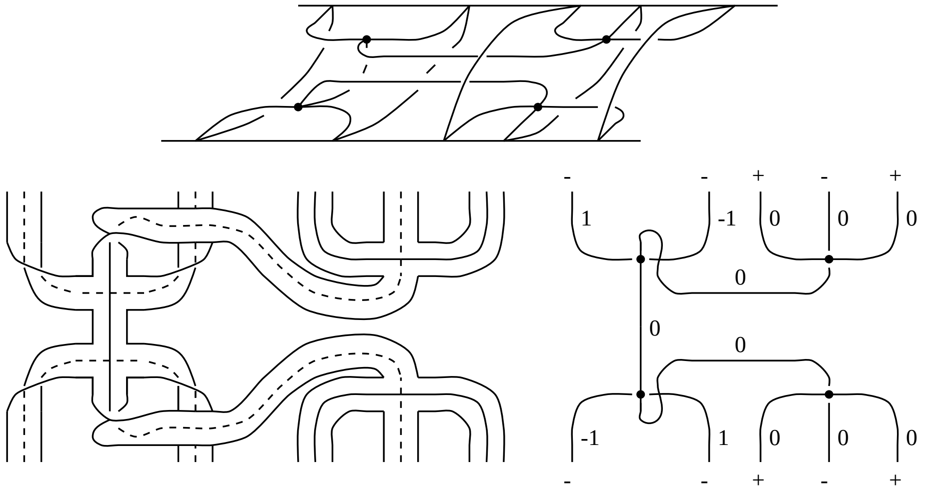

Figure III.28: Translation from the abstract torus to the real one: third case

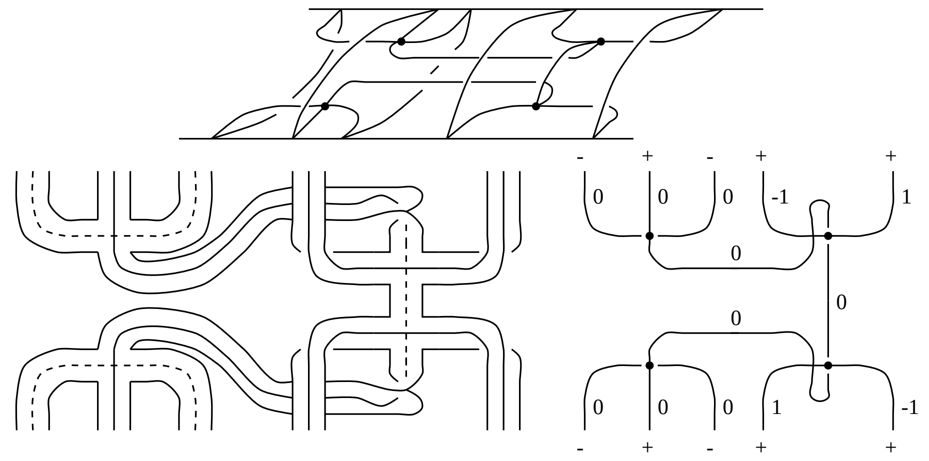

Figure III.29: Translation from the abstract torus to the real one: fourth case

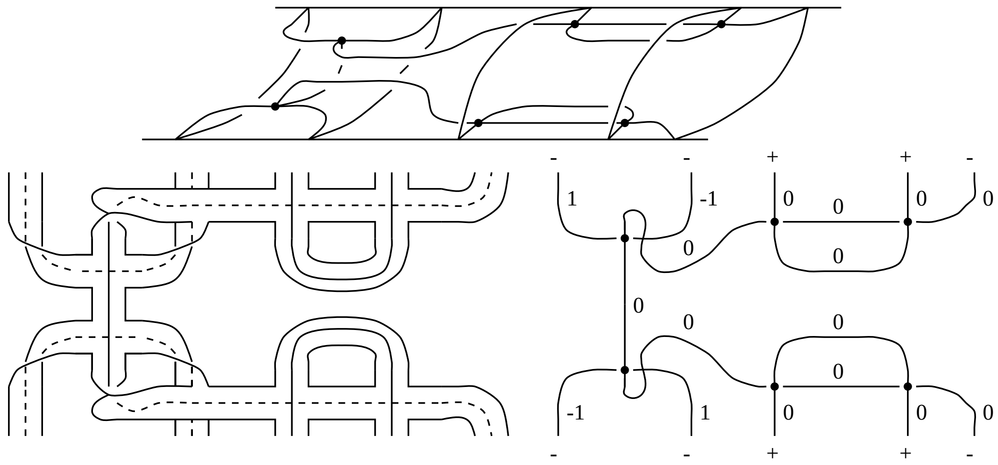

Figure III.30: Translation from the abstract torus to the real one: fifth case

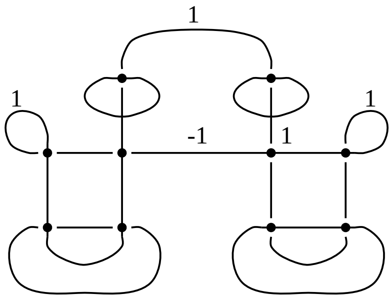

Figure III.31: An o-graph representing $S^2 \times S^1$ (colours 0 are omitted)

$$\begin{aligned} &+ \quad \#(\text{intersections with } \ell) \\ &+ \quad 4 \cdot \#(\text{components of the link}) \end{aligned}$$

(this is because each crossing contributes with 4 pairs, each intersection contributes with a pair and on every component we might need to add 2 +-pairs and 2 −-pairs). Now of course

$$\#(\text{components}) \leq \#(\text{crossings})$$

and the conclusion follows. $\boxed{\text{III.1.1}}$

Example III.1.2. *Figure III.31 illustrates the result of the application to the unknot of the algorithm described in Theorem III.1.1, and therefore provides an o-graph representation for a punctured* $S^2 \times S^1$.

Of course the number of unlinked unknotted components and the number of crossings can be taken as a natural measure of complexity of a link projection, whereas the number of intersections with a line which contains the vertices is not so natural. The following result implies that this extra number can be bounded linearly in terms of the natural complexity.

Proposition III.1.3. *Let* $\Gamma \subset \mathbb{R}^2 \subset S^2 \subset S^3$ *be a link projection with* n *crossings, and* $\ell \subset \mathbb{R}^2$ *be a line. Then an isotopy of* S^2 *carries* Γ *onto* Γ', *where all the crossings of* Γ' *are on* ℓ, *all intersections with* ℓ *are transverse and there are at most* $4(n-1)$ *intersections besides those given by crossings.*

Remark III.1.4. With the notation of Proposition III.1.3, of course Γ and Γ' are projections of isotopic links in S^3. But we have more: since the projection is changed by an isotopy of S^2, if the link projection represents a framed link via the diagrammatic convention, then the new framed link will be isotopic in S^3 to the old one.

Remark III.1.5. It will follow from the proof of Proposition III.1.3 that the transformation of Γ into Γ' is actually algorithmic in the combinatorial data.

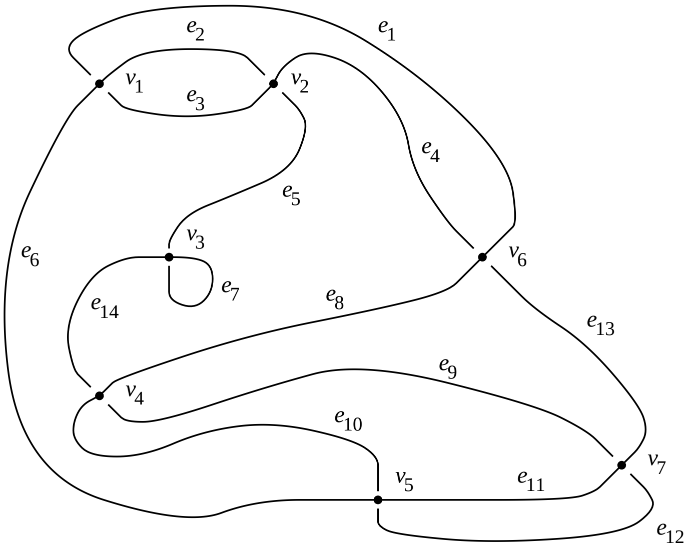

Figure III.32: A link projection

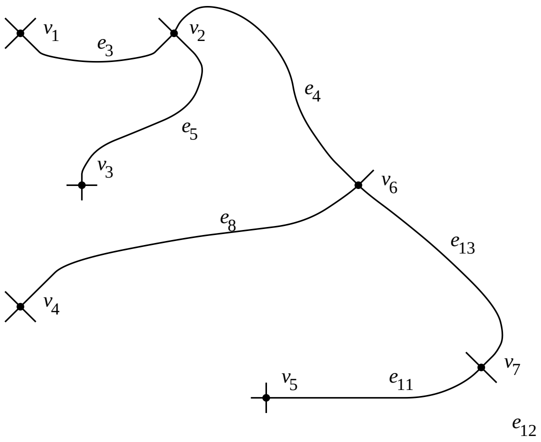

Figure III.33: A maximal tree

Remark III.1.6. The reader will easily see from the proof that the estimate $4(n-1)$ could be easily slightly improved, but the relevant fact from our point of view is that there is linear bound, so we do not worry about the best estimate.

Proof of III.1.3. Without loss of generality we can assume that Γ is connected. We describe the operations to be performed in a somewhat sketchy way, but we provide an example (Fig. III.32) which step-by-step clarifies the process. We will regard ℓ as the horizontal line in the plane and we will draw it as a dotted line in the figures.

We first forget of the under-over structure at vertices and we regard Γ just as quadrivalent graph in S^2. Let T be a maximal tree in Γ (Fig. III.33), let

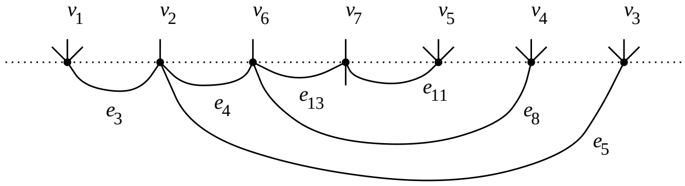

Figure III.34: An isotopic image of the tree

a be a terminal (non-separating) vertex in T and define a partial order on vertices of Γ where $b < c$ if there is a simple path in T from a to c which contains b.

Now we isotope Γ in S^2 so that the following properties are satisfied (Fig. III.34):

1. All the vertices lie on ℓ;

2. If $b < c$ are vertices joined by an edge in T then b lies on the left of c and this edge lies completely under ℓ.

It is not difficult to see that the position of T is essentially determined by these conditions, and can be constructed algorithmically starting from the combinatorics of T.

From now on we will leave T fixed and isotope the rest. The important facts needed below are the following:

1. $S^2 \setminus (\ell \cup T)$ is the union of the upper half-plane (a topological disc) together with a finite number of other discs;

2. Each of these discs has a portion of boundary which consists of a segment of ℓ (viewed as a circle in S^2);

3. Any point of each of these discs can be joined to a point of ℓ by a simple path which lies completely in the interior of the disc (this is a consequence of the previous point);

4. If a path starts and ends in the upper half-plane and misses T then up to an isotopy of S^2 which leaves T fixed we can assume that the path misses $T \cup \ell$ (this is a consequence of the first two points).

Now we need to draw the other edges of Γ which are not in T. Given such an edge we will have that the germs of its ends originate in one of the discs described above or in the upper half-plane. (Up to an isotopy which fixes T, we can also achieve uniqueness of the region in which a germ must be by prescribing that if the region is not a priori unique then the upper half-plane must be chosen: the reader will easily check that this is a consistent choice. See also Fig. III.34.) Using property 3 above we can now isotope and draw

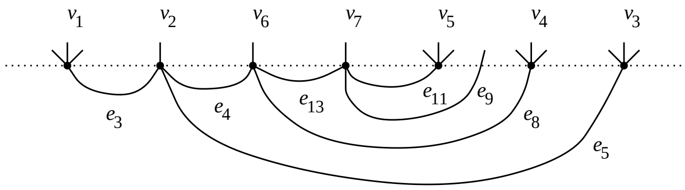

Figure III.35: The tree and the germs of edges

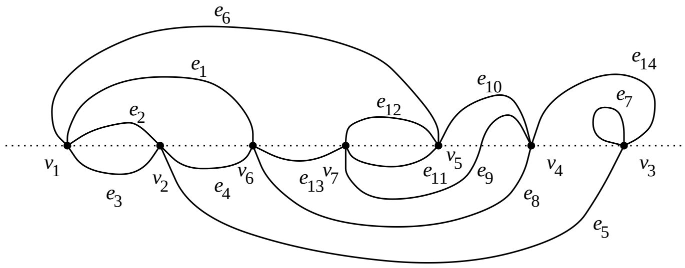

Figure III.36: An isotopic image of the projection without under-over structure

all the germs of edges long enough so that they end in the upper half-plane as in Fig. III.35 (this produces some intersections with ℓ which we will count soon). Now property 4 stated above also holds if we replace T by the union of T with the germs of edges thus drawn. Therefore we can assume that there are no other intersections after those just mentioned (Fig. III.36).

Let us remark that this process essentially means the following: once you have drawn T and the germs of edges as described above, the obvious way to match these germs in the upper half-plane corresponds to an isotopy on the initial graph.

Now, let us count the intersections introduced so far. There are $n+1$ edges which are not in T, which gives $2n+2$ germs of edges. On each germ of edge we need to put at most one intersection, but now we have that T must have at least two terminal vertices, and the 3 germs of edges originating from a terminal vertex already are in the upper half-plane. So we have here a bound $2n-4$ (an exception has to be made for $n=1$, but in this case the proposition is obvious).

The last step consists in restoring the under-over structure at vertices, which requires the introduction of at most 2 intersections with ℓ near each of the vertices, as shown in Fig. III.37 (actually, the "worst case" does not occur in the example, we show it in Fig. III.38). The proof is complete. $\boxed{\text{III.1.3}}$

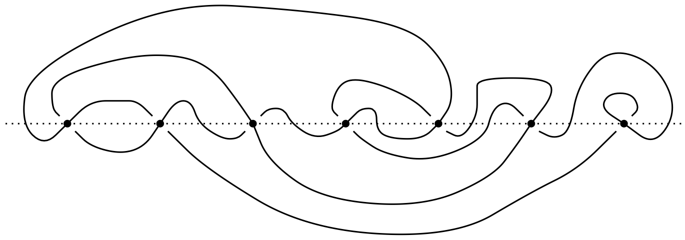

Figure III.37: Restoring the under-over structure

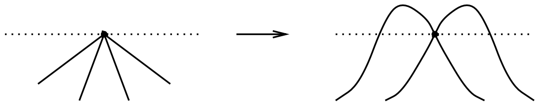

Figure III.38: Move preliminary to restoring the under-over structure in the worst case. After the move we only have to say which branch is over

III.2 From o-graphs to Heegaard splittings and diagrams

We show in this section that if an o-graph represents a once-punctured closed oriented manifold then we can obtain from the o-graph a Heegaard splitting of the manifold. This construction is algorithmic, but we make no attempt to control complexity.

We first recall the definition of Heegaard splitting (see [Rol], [Mi1] and [Mi2]) assuming the reader is familiar with the basic terminology of handle decompositions. Let H be a handlebody with boundary F of genus g (i.e. H is a closed 3-ball with g 1-handles attached); let X be a non-separating set of g simple loops on F and consider a tubular neighbourhood of X in F (a set of g strips); it can be shown that if we glue g 2-handles to H along the strips the resulting manifold has boundary S^2. Let M be the manifold obtained by capping off this sphere; then M is the union of two handlebodies (H and the complement of the interior of H) with common boundary F. Every such realization of a given closed oriented manifold is called a Heegaard splitting, while we call the pair (H, X) an *abstract* Heegaard diagram. In case H is embedded in $\mathbb{R}^3$ in the standard way (namely, in such a way that the complement in S^3 is a handlebody too), we will call the pair (H, X) a Heegaard diagram. We will represent Heegaard diagrams as shown in the example of Fig. III.39 (see [Rol]).

There is some ambiguity in the literature concerning what a Heegaard diagram is, and this is why we have given two definitions adding the adjective "abstract" for one of them. We just mention that it is also possible to define a Heegaard splitting using a surface F and two non-separating systems of simple loops X_0 and X_1 on F, where the manifold is obtained from $[0,1] \times F$

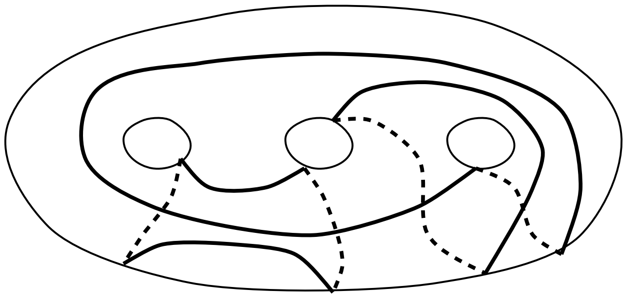

Figure III.39: An example of Heegaard diagram of genus 3

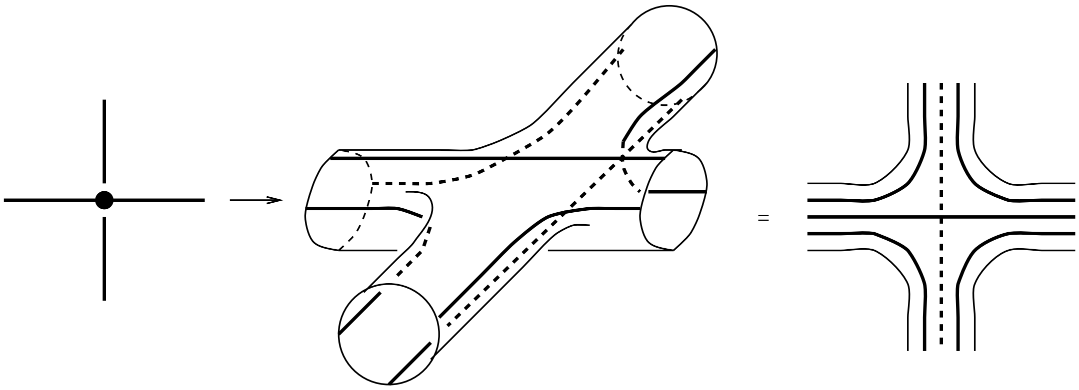

Figure III.40: Construction of the Heegaard splitting at vertices (3-dimensional and planar pictures)

by attaching 2-handles to tubular neighbourhoods of $X_i \subset \{i\} \times F$, and then capping off the two resulting spheres. In this context the name Heegaard diagram is sometimes used for the triple (F, X_0, X_1). We will not make use of this definition.

We show now how to get a Heegaard splitting from an o-graph. We refer the reader to Section II.3 for the description of how to recover the boundary from the o-graph and hence detect o-graphs which represent once-punctured closed manifolds.

Proposition III.2.1. *Let Γ be an o-graph which represents a once-punctured closed manifold M. Choose arbitrary simplifications in $\mathbb{R}^3$ for fake crossings, and define a submanifold with boundary H of $\mathbb{R}^3$, with a system of curves X embedded in the boundary, as shown in Figg. III.40 to III.42. Then (H, X) is an abstract Heegaard diagram for M.*

Proof of III.2.1. Since H is a regular neighbourhood of a graph embedded in $\mathbb{R}^3$ then H is of course a handlebody. If one goes back to the main construction described in Sections I.2 and I.3, one sees that the punctured version of M is obtained exactly by attaching 2-handles along tubular neighbourhoods in ∂H

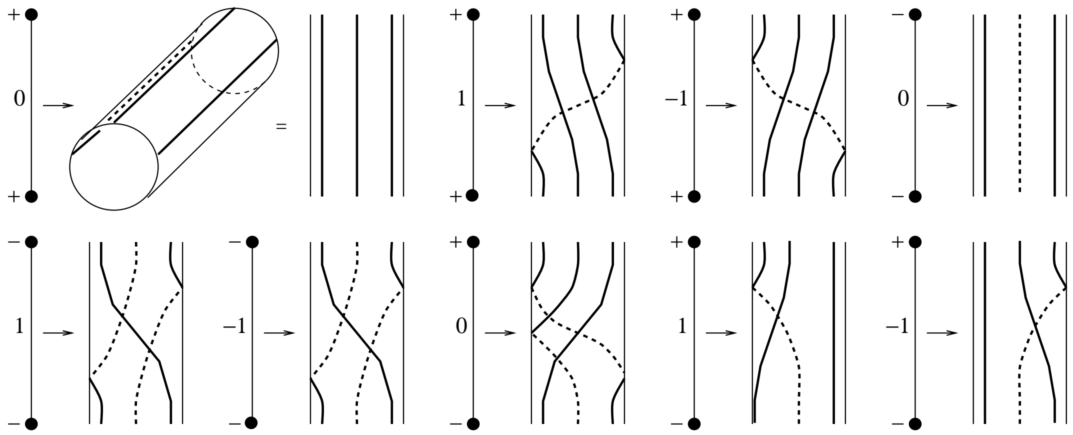

Figure III.41: Construction of the Heegaard splitting along edges: we show the 3-dimensional situation in the first case only, showing the planar picture in the other cases

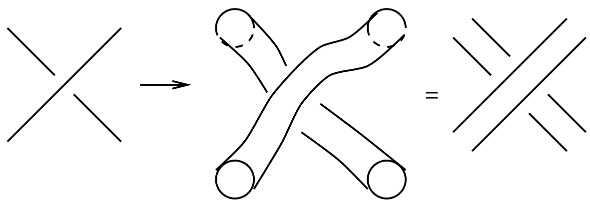

Figure III.42: Construction of the Heegaard splitting at fake crossings

of the components of X (compare Fig. III.41 with Fig. I.35). This implies that X is a non-separating system of as many simple loops as the genus of H, and hence that (H, X) is an abstract Heegaard diagram for M. $\boxed{\text{III.2.1}}$

If in Proposition III.2.1 we start with an o-graph which has no fake crossings then the handlebody we get is already embedded in $\mathbb{R}^3$ in the standard way, and it is not difficult to describe explicitly the Heegaard diagram resulting from the proof. However there are o-graphs which cannot be drawn without introducing fake vertices. Since (concrete) Heegaard diagrams are nicer objects than abstract ones, we will provide below a result which allows us to associate a Heegaard diagram to any o-graph. But we first devote a brief digression to the following question which naturally arises: *given an o-graph* Γ, *what is the minimum of the number of fake crossings over all o-graphs which are equivalent to* Γ *under isotopy and moves* R *and* C*?*

We still do not have a satisfactory answer to this question, we just prove some easy partial results toward it. Let us define $f(\Gamma)$ as the minimum of the number of fake crossings over all o-graphs equivalent to Γ (i.e. those which define the same oriented spine, see Proposition I.3.5).

Lemma III.2.2. $f(\Gamma)$ *depends only on the abstract graph* Γ_0 *supporting* Γ. *More precisely* $f(\Gamma) = \hat{f}(\Gamma_0)$, *where* $\hat{f}(G)$ *is defined for any abstract (maybe*

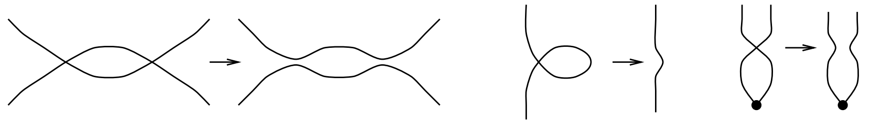

Figure III.43: Reducing the number of crossings

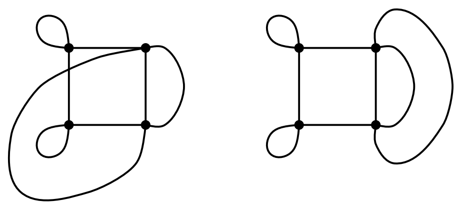

Figure III.44: Two pictures of the same graph

not quadrivalent) finite graph G as the minimum of the number of singularities over all transversal immersions of G in $\mathbb{R}^2$.

Proof of III.2.2. The freedom given by move C (Remark I.3.6) says that we can embed neighbourhoods of the vertices as we please; isotopy and moves R say that we can immerse the edges as we please. $\boxed{\text{III.2.2}}$

According to this result our question translates in a very general problem in graph theory. The number $\hat{f}(G)$ is called the *crossing number* of an asbtract graph G (recall however that graph-theorists do not accept loops and parallel edges, so our situation is slightly more general). The problem of deciding if a graph is planar (i.e. if it can be drawn without crossings) has been studied and completely solved [Tut1], [Tho], and also considerable attention has been devoted to determinig the crossing number of a graph [Gu], [Er-Gu], [Tut2] (see also [Gar-Jo] for the proof that the problem cannot be treated algorithmically and [Bi-De] for a recent contribution to a related problem). But apparently there is no result specific for the case of graphs with a fixed number of edges incident to each vertex.

Lemma III.2.3. *Let G be a finite graph. If a transversal immersion of G in $\mathbb{R}^2$ has $\hat{f}(G)$ singularities then the edges are simple and cross each other at most once, and edges originating from a common vertex do not cross each other. The converse is false (even for quadrivalent graphs).*

Proof of III.2.3. The proof of the two assertions is contained respectively in Figg. III.43 and III.44. $\boxed{\text{III.2.3}}$

We denote now by $N_v(n)$ the maximum over all connected v-valent graphs G with n vertices of $\hat{f}(G)$. We are interested in asymptotic estimates for N_v (in particular for $v = 4$).

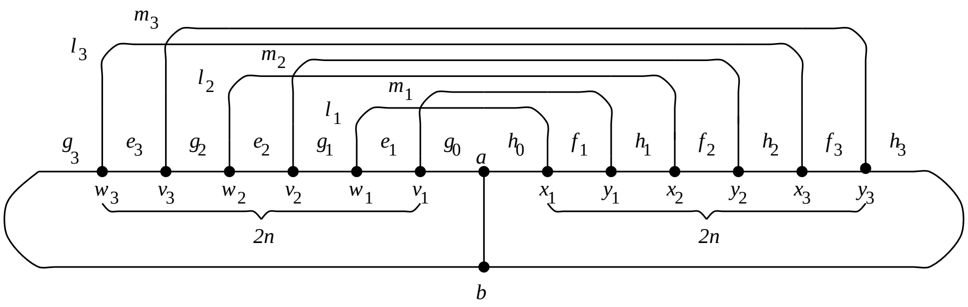

Figure III.45: The graph G_n

Proposition III.2.4. *For all $v \geq 3$ we have:*

$$\limsup_{n\to\infty} N_v(n)/n^2 \leq (v-2)^2/8,$$

$$\liminf_{n\to\infty} N_v(n)/n \geq 1/16$$

(where of course if v is odd we confine ourselves to even n's).

Proof of III.2.4. Fix a graph G with n vertices and a maximal tree T in G. Of course we can draw G so that the $n+1$ edges of T contain no singularity (first draw the maximal tree without self-crossings and then remark that the complement is connected). Now operating as in Fig. III.43 we can also assume that the other $vn/2-(n+1)$ edges cross each other at most once, so we have at most $(vn/2-(n+1))(vn/2-(n+1)-1)/2$ singularities and the first assertion is proved.

Since of course $N_v(n) \geq N_3(n)$ for all $v \geq 3$ and even n, it is sufficient to prove the second assertion when $v=3$. For this aim consider the graph G_n of Fig. III.45 which depends on an index n and has $4n+2$ vertices. We claim that for every immersion of G_n in $\mathbb{R}^2$, for $1 \leq i < n$ there must be some crossing on:

$$S_i = (e_i \cup m_i \cup f_i \cup l_i) \cup (h_i \cup g_i) \cup (e_{i+1} \cup m_{i+1} \cup f_{i+1} \cup l_{i+1}).$$

For odd $i < n$ the S_i's are at least $(n-1)/2$ pairwise disjoint subsets of G_n; observing that every crossing involves exactly two edges we obtain that every immersion of G_n in $\mathbb{R}^2$ contains at least $(n-1)/4$ crossings, and the conclusion easily follows.

We are left to prove the claim that S_i contains a crossing. Assume first that there is no crossing on $Q_i = e_i \cup m_i \cup f_i \cup l_i$; since in G_n it is always possible to join to each other avoiding Q_i any two elements of the set $\{h_i, h_{i-1}, g_i, g_{i-1}\}$, the situation must be as in Fig. III.46 (or a similar figure with all the germs of edges pointing outwards, but of course there is no essential difference). Now if we also assume that there is no crossing on $Q_{i+1} \cup (h_i \cup g_i)$ then S_i must be in one of the situations of Fig. III.47. But now in G_n we can join h_{i-1} to g_{i-1} avoiding S_i, and this gives a contradiction. $\boxed{\text{III.2.4}}$

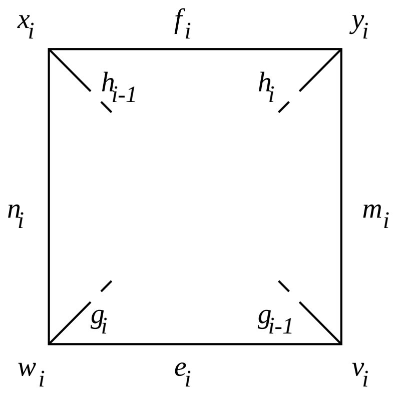

Figure III.46: A square without crossings

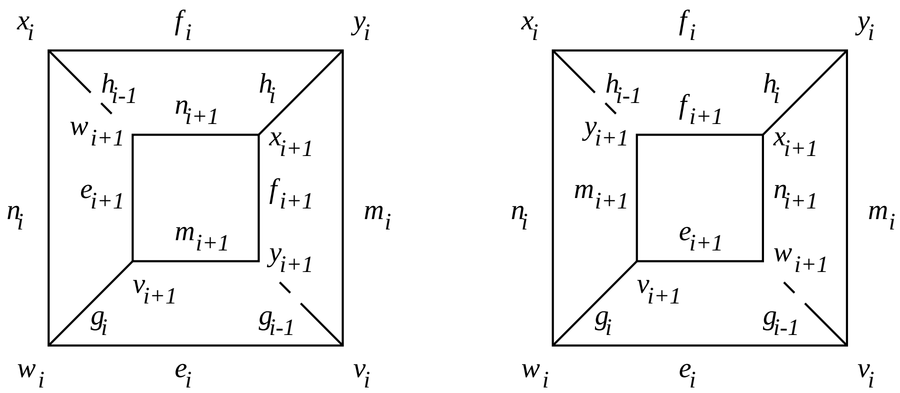

Figure III.47: Two “concentric” squares without crossings

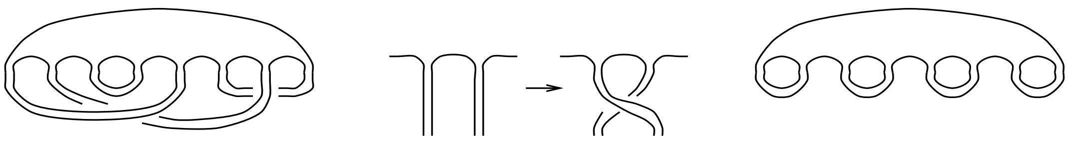

Figure III.48: An unknotted embedding of a handlebody and the move which relates it to the standard embedding

We quickly mention that in view of the above discussion a possible choice for the complexity of an o-graph Γ could be the pair (n_t, n_f), where n_t is the number of true vertices of Γ and n_f is the minimal number of fake vertices one is forced to introduce when he draws Γ in the plane. One interesting feature of this notion of complexity is that it still depends only on the spine associated to the o-graph, but it exploits the o-graph representation of spines in a more subtle way.

This concludes the digression.

We show now how to translate the abstract result of Proposition III.2.1 into an algorithm which produces a Heegaard diagram, in the general case where there are fake crossings.

Proposition III.2.5. *Let Γ be an o-graph which represents a once-punctured closed manifold M. Then the following steps lead to a Heegaard diagram of M:*

1. *Choose a maximal tree T in Γ and isotope so that T contains no fake crossing. Operating as in Fig. III.43 assume that edges are simple and meet each other at most once.*

2. *Choose a starting point and proceed counter-clockwise around T, simplifying fake crossings so that edges met earlier are over edges met later.*

3. *At vertices and along edges operate as shown in the planar pictures in Figg. III.40 to III.42.*

4. *Now the situation is as in the left-hand side of Fig. III.48 (where we have not shown the curves). Using the sliding move shown in the middle of the same figure we can reduce to the standard diagram shown on the right-hand side.*

5. *So we only need to describe the effect of the sliding move on the curves. This is done in Figg. III.49 to III.52 (here we are always assuming that there are two pieces of curves in the middle, but it is clear what to do with any number of curves).*

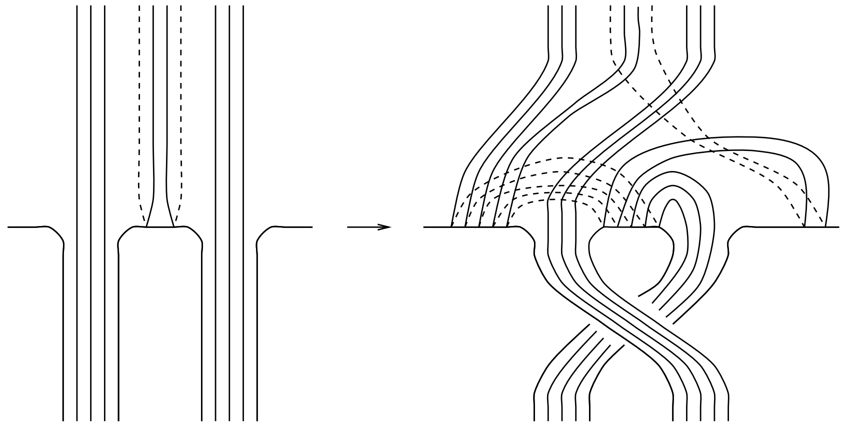

Figure III.49: Effect of the sliding on curves: first case

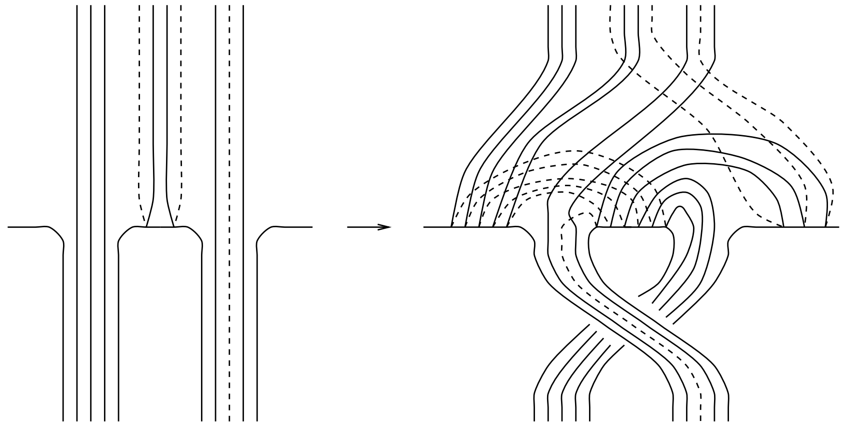

Figure III.50: Effect of the sliding on curves: second case

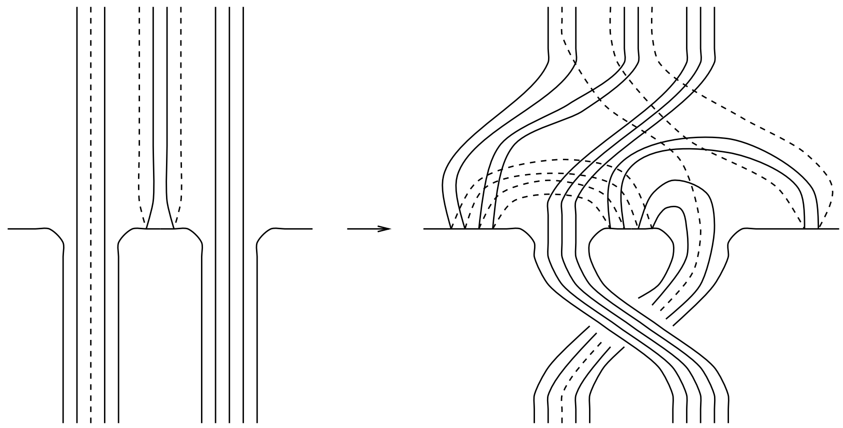

Figure III.51: Effect of the sliding on curves: third case

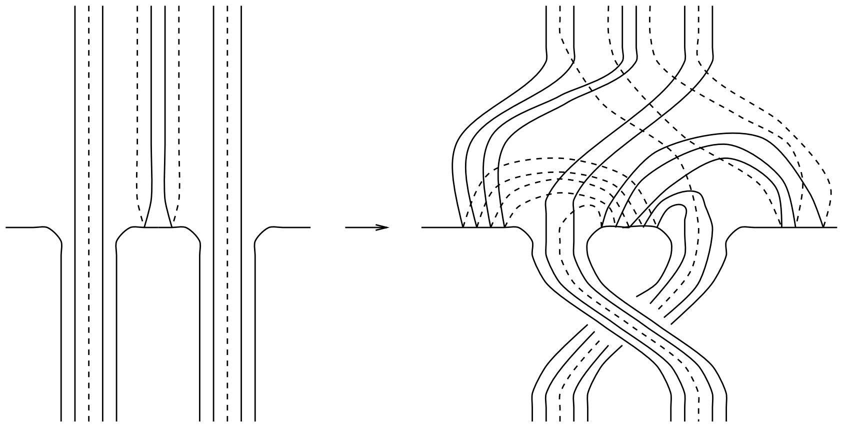

Figure III.52: Effect of the sliding on curves: fourth case

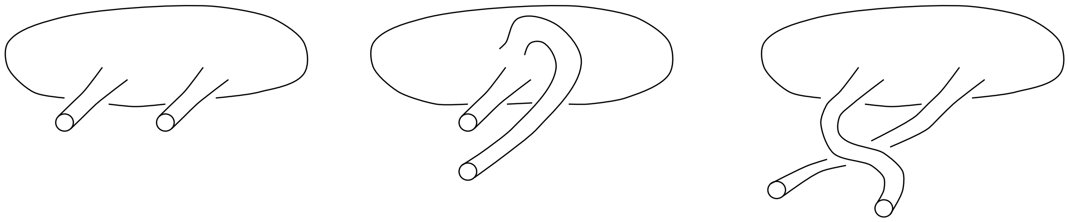

Figure III.53: 3-dimensional sliding move

Proof of III.2.5. Only step 5 needs comments: we prove that Figg. III.49 to III.52 describe the effect on curves of the 3-dimensional move shown in Fig. III.53, which gives rise to the move of Fig. III.48.

The proof is contained in Figg. III.54 to III.58, which are combined to give Figg. III.49 to III.52. $\boxed{\text{III.2.5}}$

We conclude this section by recalling that Rourke's [Rou] recursive construction of a surgery presentation from a Heegaard splitting is in principle algorithmic. Hence for closed oriented manifolds we have a circular scheme of

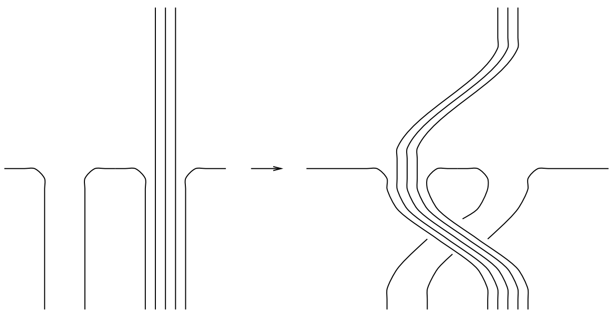

Figure III.54: Elementary effect of the sliding move on curves: first case

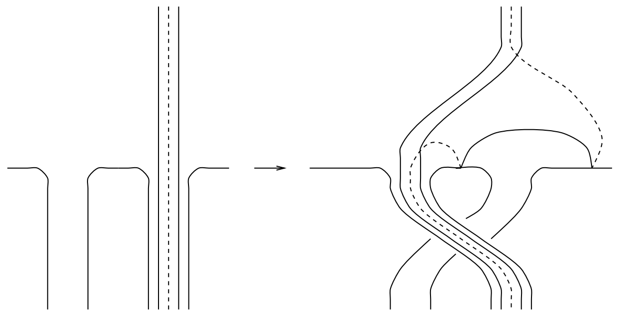

Figure III.55: Elementary effect of the sliding move on curves: second case

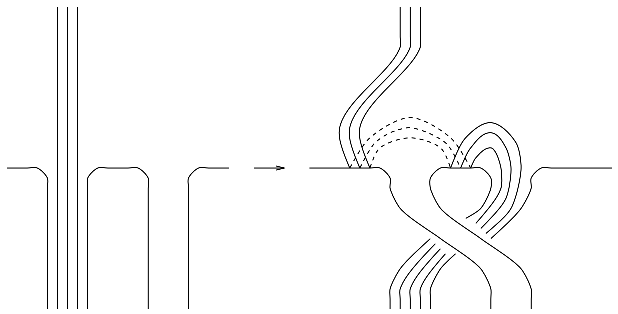

Figure III.56: Elementary effect of the sliding move on curves: third case

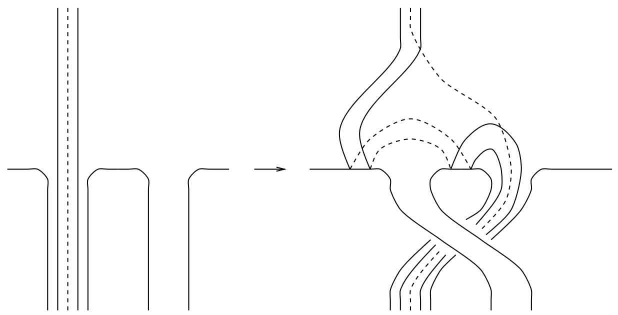

Figure III.57: Elementary effect of the sliding move on curves: fourth case

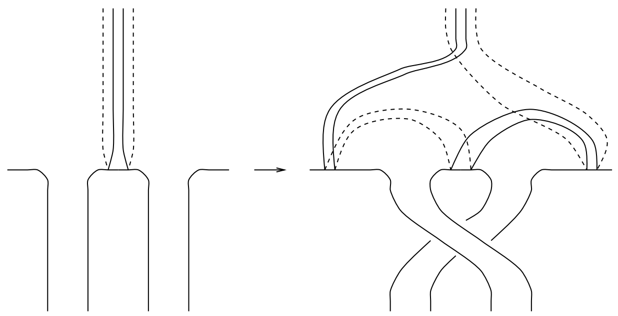

Figure III.58: Elementary effect of the sliding move on curves: fifth case transformations:

$$\begin{matrix}\text{framed}\\ \text{link}\end{matrix} \xrightarrow{1} \text{o-graph} \xrightarrow{2} \begin{matrix}\text{Heegaard}\\ \text{splitting}\end{matrix} \xrightarrow{3} \begin{matrix}\text{framed}\\ \text{link}\end{matrix}.$$

However in arrow 2 we have no control on complexity and in arrow 3 there are various aspects whose implementation is not perfectly straight-forward. To mention two of these aspects:

1. At a certain stage of the process one needs to complete a simple non-separating loop on a surface to a maximal set of loops with the same properties. Once the surface is explicitly given (e.g. combinatorially, by a triangulation) the isotopy classes of simple loops can be enumerated. Then one certainly can complete the system of loops, but it is not clear a priori the amount of time it will take.

2. The recursive process produces a ribbon R in the manifold M and another ribbon L in S^3 such that $\chi(M,R) = \chi(S^3,L)$. Then of course $M = \chi(S^3, L \cup R')$, but to find R' one needs to know explicitly the map which identifies $\chi(M,R)$ to $\chi(S^3,L)$, so the recursive process needs to keep track of explicit homeomorphisms.

III.3 O-graph of a link complement

In this section we provide an algorithmic construction which applies to a link diagram (a regular projection on the horizontal plane of a link in S^3) and gives an o-graph for the link complement. As we did when dealing with surgery presentations, we will proceed slightly informally.

Theorem III.3.1. *Let a link diagram be given and assume that no component is under at all its crossings, unless it is an isolated plain circle. Then the following steps 1-7 lead to an o-graph representing the complement in S^3 of the link.*

1. *Fix in the plane a box containing a line ℓ and isotope the link diagram in the plane so that:*
   (a) *the projection lies inside the box except for a single arc;*
   (b) *the projection meets ℓ transversely;*
   (c) *all the crossings are on ℓ;*
   (d) *isolated plain circles completely contained in the box intersect ℓ twice.*

   See Fig. III.59 for an illustration of these conditions.

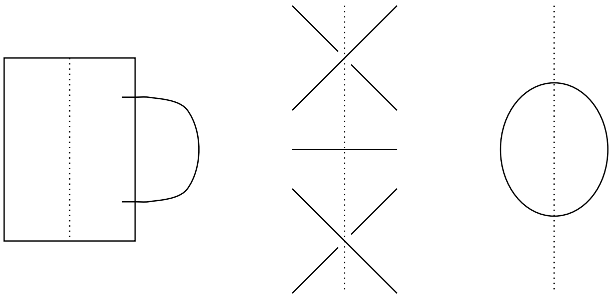

Figure III.59: Initial conditions on the projection

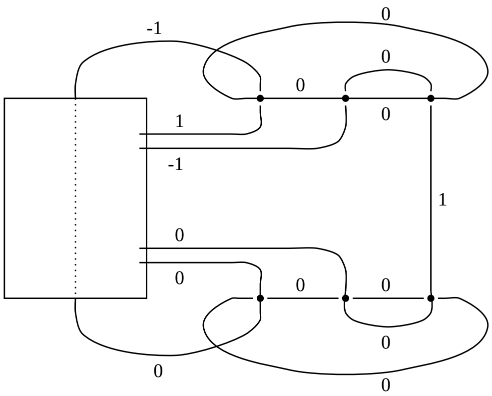

Figure III.60: How to operate outside the box

2. *Outside the box operate as in Fig. III.60.*
3. *Inside the box and far from ℓ take the double (diagrammatic parallel) of the projection.*
4. *At crossings operate as in Figg. III.61 and III.62.*
5. *At plain intersections with ℓ which are not part of a component without crossings, operate as in Fig. III.63.*
6. *Operate on isolated plain circles as in Fig. III.64.*
7. *To conclude sum up multiple colours.*

The number of vertices of the resulting o-graph does not exceed $6+6c_0+6c_1+2c_2$ *where* c_0 *is the number of components without crossings (isolated plain circles),* c_1 *is the number of crossings and* c_2 *is the number of intersections with* ℓ*.*

Remark III.3.2. To satisfy the preliminary condition we do *not* need to check if there are components which are unknots unlinked from the rest (this is in general difficult). What we mean is that if a component is *evidently* unknotted

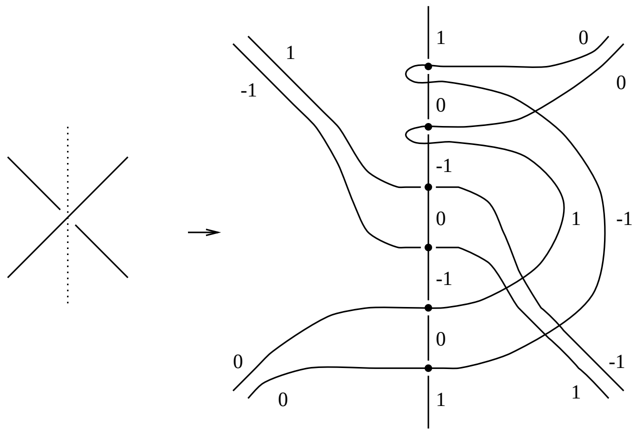

Figure III.61: How to operate at crossings: first case

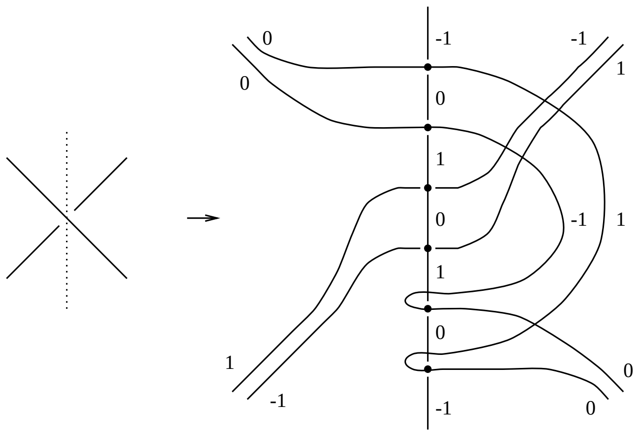

Figure III.62: How to operate at crossings: second case

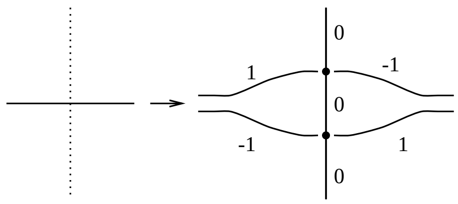

Figure III.63: How to operate at plain intersections

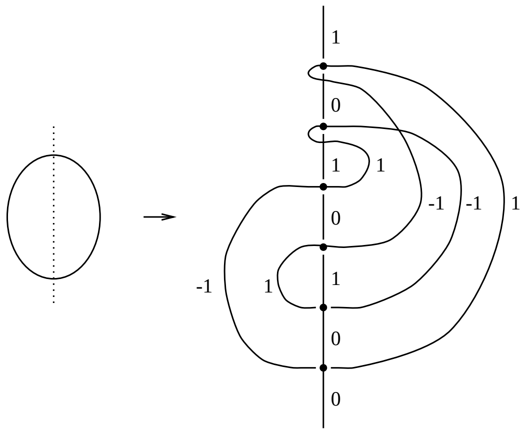

Figure III.64: How to operate on an unknot

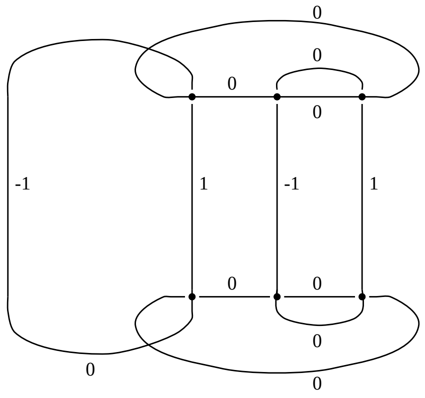

Figure III.65: An o-graph of the solid torus

because it is under at all crossings, we move it so that it appears as a genuine circle without crossings.

Remark III.3.3. As in the case of surgery the number of intersections with ℓ can be bounded by a linear function of the complexity of the projection, using Proposition III.1.3.

Corollary III.3.4. *By applying Theorem III.3.1 to the unknot we obtain the o-graph for the solid torus shown in Fig. III.65.*

Proof of III.3.1. The starting point is actually a direct proof of Corollary III.3.4. The sphere minus the unknot can be seen as the ball minus a cylinder (a thick diameter). Hence a standard spine of it is obtained by digging a tunnel across the Bing house, as shown in Fig. III.66. In this figure the singular edges are marked more heavily. Figure III.67 shows a neighbourhood of the singular set in Fig. III.66, which immediately implies Fig. III.65.

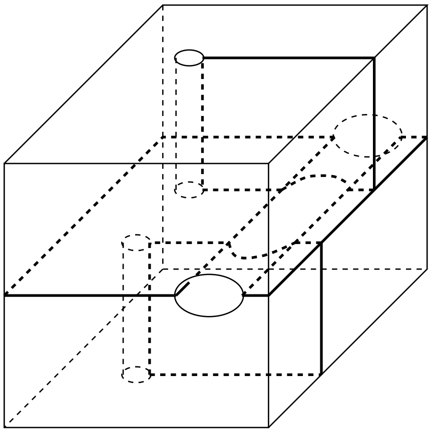

Figure III.66: A standard spine of the solid torus

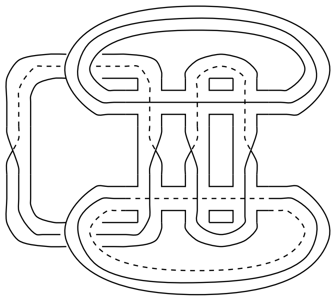

Figure III.67: A neighbourhood of the singular set

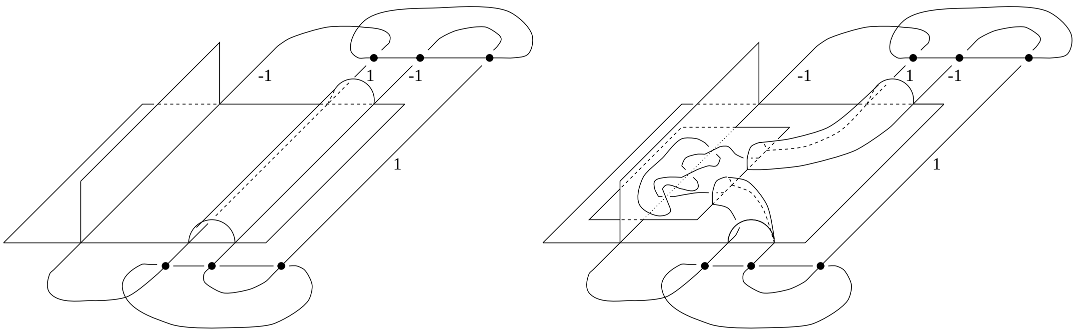

Figure III.68: Generalization of the situation

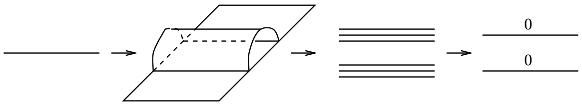

Figure III.69: Far from ℓ we double the link

For a more general link than the unknot we modify the above construction. We do this by identifying the box in which the projection lies with a subset of the spine previously constructed. This is illustrated in Fig. III.68; here we are using the mixed notation between o-graphs and actual pictures which we already used when dealing with surgery. The left-hand side refers to the case of the unknot, and the right-hand side to the general case.

The idea now is just to continue digging the tunnel following the link; for every new component we will need to start a new tunnel (which will be a torus rather than a cylinder). We describe how to do this and immediately translate the constructions in terms of o-graphs. To be precise, we show how to obtain a quasi-standard polyhedron onto which the link complement collapses; standardness of this polyhedron will be established in the end.

Figure III.69 shows that far from ℓ we only have to take the double of the link. At plain intersections of the link with ℓ Fig. III.70 shows what to do. We see crossings as shown in Fig. III.71; therefore the first type of crossing can be seen as a combination of a plain intersection and the phenomenon dealt with in Fig. III.72. We leave it to the reader to put things together and deal with the other type of crossing, obtaining the rules given in the statement. For a

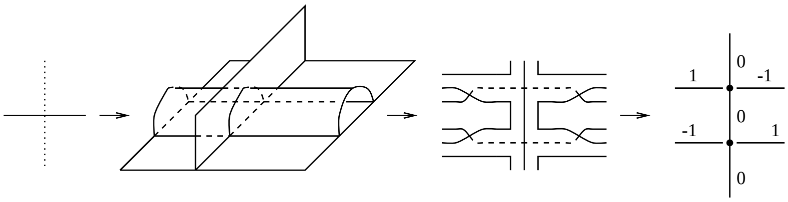

Figure III.70: Plain intersection

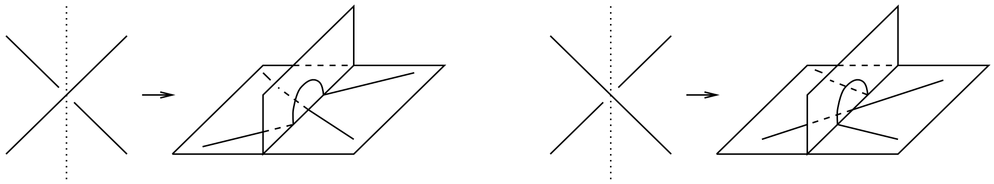

Figure III.71: At crossings the link still lives in the polyhdron

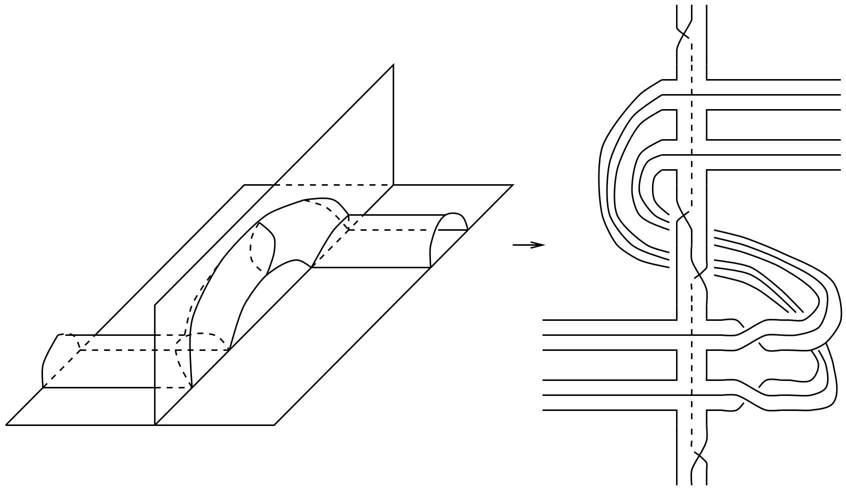

Figure III.72: This is one of the elements of a crossing

reason explained later unknots are seen as in Fig. III.73, which leads to the rule of the statement.

We are left to prove that the components of the smooth part of the quasi-standard polyhedron we have constructed are discs (of course there are vertices and the singular set is connected). We will refer to these components as regions.

We first remark that regions are either subsets of the border of some tunnel or subsets of the regions of the original Bing house, with exactly one exception. To see this recall that the Bing house has three regions; the two "small" ones are preserved by the construction (Figg. III.66 and III.68); the "big" one is cut

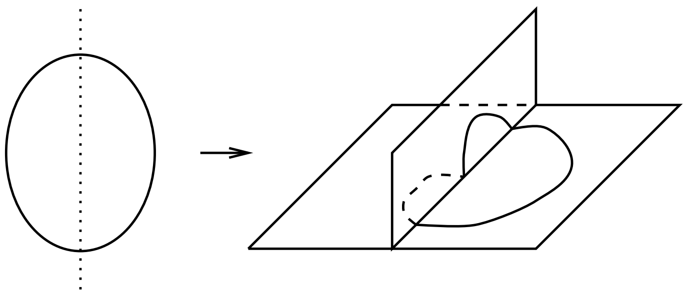

Figure III.73: How to see unknots

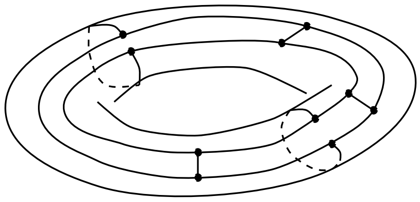

Figure III.74: Singular set on the border of a tunnel

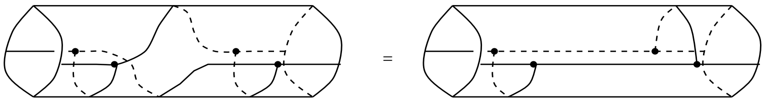

Figure III.75: Singular set on the border of a tunnel near an overcrossing

into several pieces, and some portions of cylinder (border of the first tunnel) are attached to one of these pieces (this gives the only exception).

During the construction the "big" region is cut into pieces by arcs with the endpoints on the boundary: this implies that regions which are subsets of the original regions of the Bing house are discs. This fact would of course be false without the assumption that the unknots inside the box are placed as in Fig. III.59.

Now we examine what is happening on the border of a toroidal tunnel. It is obvious that in some abstract version of the torus the singular set is either a pair of parallel longitudes or a "double" longitude, together with some semi-meridians, as shown in Fig. III.74. If we look at the local picture near a crossing where the component corresponding to the tunnel is over (Fig. III.72 or a similar picture for the other type of crossing) we see that things go as shown in Fig. III.75. This figure implies that if there is an overcrossing then in Fig. III.74 all the components are discs. The special rule given for unknots corresponds exactly to introducing artificially a situation as in Fig. III.72, so this case is also settled.

We are left with to deal with regions which are subsets of the border of the cylinder, and with the "special" region. We can do this at the same time, as shown in Fig. III.76. In this figure we show the cylinder and the way the "special" region (a subset of the original "big" region of the Bing house) is attached to the cylincre. If there is no overcrossing the longitudes of the cylinder in Fig. III.76 are connected "horizontally" in the obvious way, and maybe some semi-meridians are added: of course we are left with discs. If there is some overcrossing the longitudes way be twisted, but Fig. III.75 still implies that we have discs. This concludes the proof that the spine is standard.

The estimate on the number of vertices arising is left to the reader. $\boxed{\text{III.3.1}}$

As an appendix to this section we state two facts announced in the introduction to the chapter, which show that some natural operations on manifolds

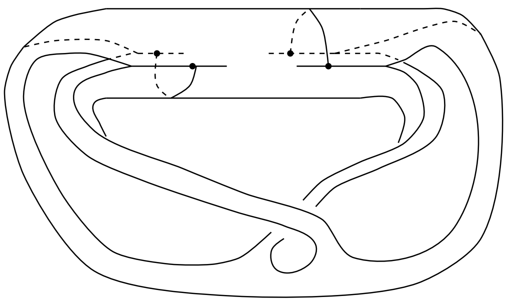

Figure III.76: Singular set on the cylinder and the special region

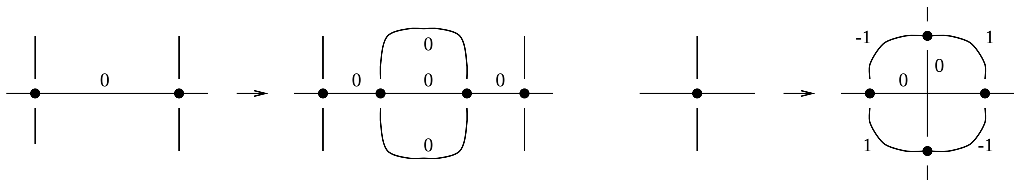

Figure III.77: Puncturing an o-graph

are very easily translated in terms of o-graphs. The proof of the first result is left to the reader.

Proposition III.3.5. *Let* Γ_1 *be an o-graph and let* Γ_2 *be obtained from it by one of the local moves shown in Fig. III.77. Then* $\mathcal{M}(\Gamma_2)$ *is* $\mathcal{M}(\Gamma_1)$ *with a puncture, i.e.* $\mathcal{M}(\Gamma_1)\#B^3$

Let us recall that in the set of compact oriented 3-manifolds (with boundary) connected sum is a well-defined binary operation.

Proposition III.3.6. *Consider two o-graphs* Γ_1, Γ_2 *with at least two vertices. Choose in* Γ_i *an edge with distinct endpoints and apply moves* C *so that this edge is over at both endpoints and has colour* 0*. Realize both graphs as disjoint subsets of the same plane as shown in Fig. III.78, and form a new o-graph* Γ *as described in the same figure. Then* $\mathcal{M}(\Gamma) = \mathcal{M}(\Gamma_1)\#\mathcal{M}(\Gamma_2)$.

Proof of III.3.6. Assume you have two standard spines of oriented manifolds and small portions of these spines embedded in $\mathbb{R}^3$ as shown in Fig. III.79 (at

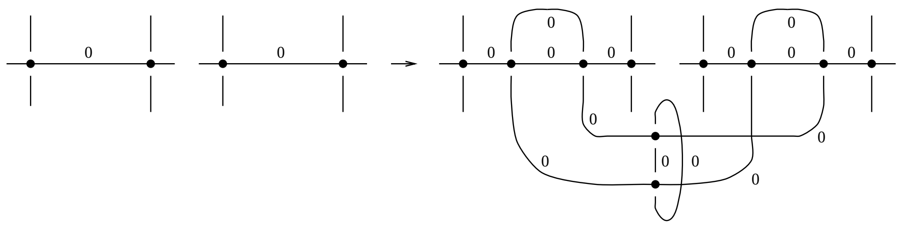

Figure III.78: Representation of connected sum on o-graphs

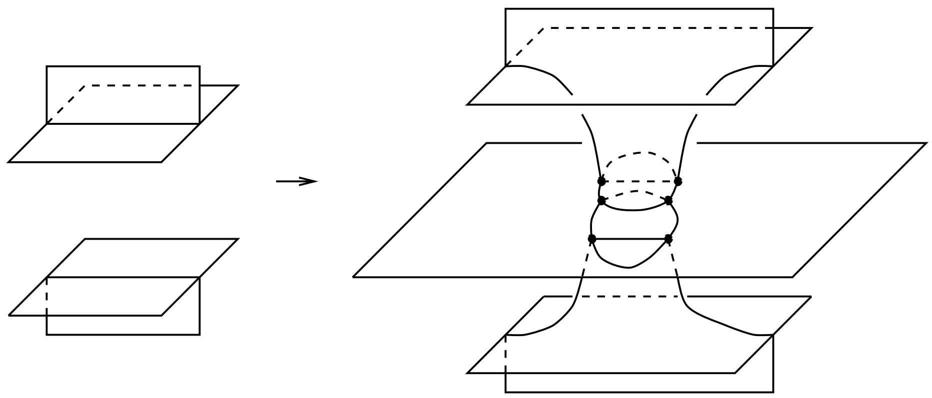

Figure III.79: Connected sum of spines

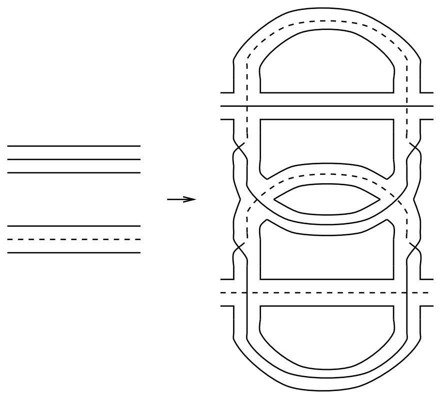

Figure III.80: The resulting singular set

different heights, to fix the ideas). Form a new standard polyhedron by taking a whole orizontal plane at intermediate height and modifying the two original spines only in the region which was embedded, as shown in the same Fig. III.79. (The unbounded region in the horizontal plane is a disc because it also contains ∞, of course.) It is not difficult to check that we have obtained a standard spine of the connected sum of the manifolds of which we had spines. Figure III.80 contains a top view (in the usual sense) of a neighbourhood of the singular set of the new spine. This translates in the rule shown in Fig. III.81, which must be understood as follows: $\Gamma_1 \# \Gamma_2 = \Gamma$ means that if Γ is constructed from Γ_1 and Γ_2 as explained by the picture then $\mathcal{M}(\Gamma) = \mathcal{M}(\Gamma_1) \# \mathcal{M}(\Gamma_2)$. Using the same convention and moves C the rule of Fig. III.81 can be reformulated as shown in Fig. III.82 and then as in Fig. III.83, from which the conclusion of the proof is deduced. We leave it to the reader to find the explicit moves C which translate the rules for # into each other. $\boxed{\text{III.3.6}}$

Remark III.3.7. As obvious from the very proof of Proposition III.3.6, there are other possible descriptions of the o-graph of a connected sum in terms of

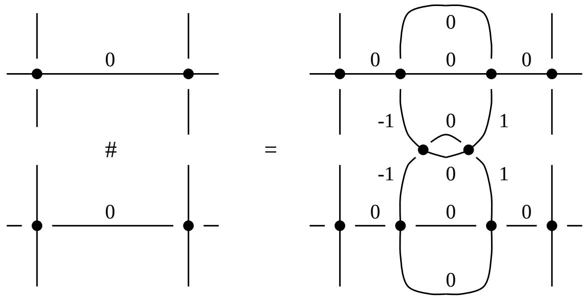

Figure III.81: First representation of connected sum on o-graphs

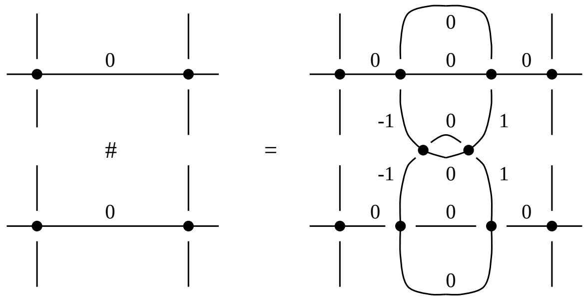

Figure III.82: Second representation of connected sum on o-graphs

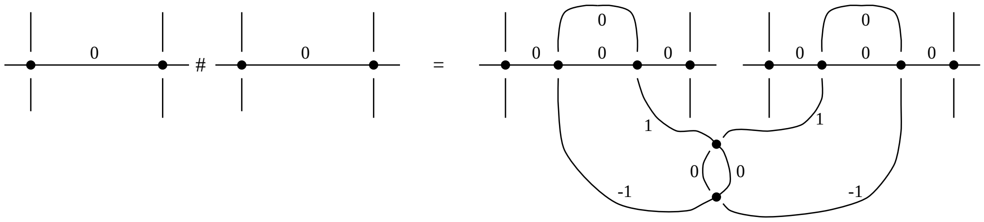

Figure III.83: Third representation of connected sum on o-graphs the o-graphs of the summands. The one of the statement is particularly nice because symmetry of # follows from isotopy and moves R only.

Remark III.3.8. To be completely formal the rule for connected sum of o-graphs stated in Proposition III.3.6 applies to pairs $(\Gamma, \vec{e})$, where $\vec{e}$ is a directed edge in Γ with colour 0 and positive endpoints. We will use the rule in this form in Section IV.6.

Chapter IV

Bracket invariants

In this chapter we exploit the presentation established in Chapter I and define "bracket-type" invariants of o-graphs (i.e. decorated spines), spines and 3-manifolds. The name is inspired by the Kauffman bracket for links in S^3 (see [Ka-Li], [Mort]) as our brackets share with the elementary prototype the property of being "state sums" which satisfy *linear skein relations.* Our definition in some sense already incorporates the idea of taking satellites (a very useful process in the study of links and manifolds, see e.g. [Mort]).

Bracket invariants are *computable* (in a precise sense we will explain in Section IV.3) and constitute an infinite family which can be filtered by a natural notion of complexity. The expectation is that as complexity increases they should become more and more precise in capturing the topology of spines and 3-manifolds. We already have experimental evidence that this is true for spines even at the lowest possible degree of complexity (Section IV.7). Non-triviality for 3-manifolds is here supported by showing that the Turaev-Viro [Tur-Vi] invariants are bracket invariants in our sense, and at a very low degree of complexity (Section IV.5). We will always consider the oriented case (see [Be-Pet2] for the sketch of an extension to the general case).

The structure of the chapter is as follows. We first introduce a very general definition of bracket of an o-graph (Sections IV.1 and IV.2) and then we define two different strategies to "normalize" the bracket so that it gives an invariant of manifolds (Sections IV.3 and IV.4). The second strategy is actually more restrictive than the first one, but it still includes the invariants of Turaev and Viro (Section IV.5). In Section IV.6 we show that basically all the invariants which we obtain are multiplicative under connected sum, and in the last section we provide spare material concerning some (essentially unsuccessful) numerical computations.

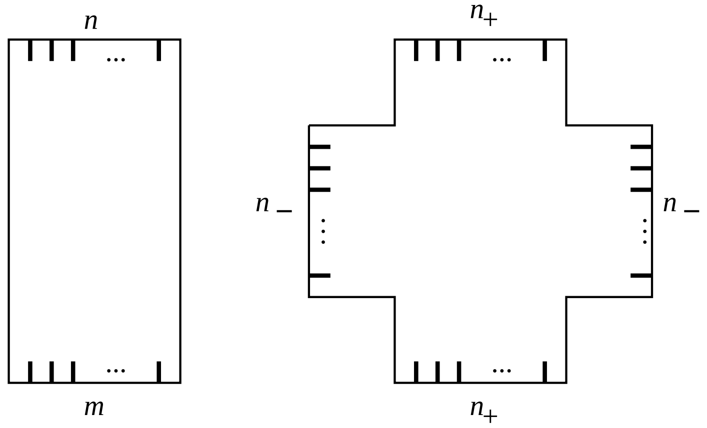

Figure IV.1: The rectangle is used to define $P^n_m(A)$ and the cross for $V^{n_+}_{n_-}(A)$

IV.1 The universal bracket for o-graphs

We start by introducing some notation. Let $\mathcal{O}$ be the set of o-graphs up to isotopy and moves R (this set has an intrinsic interpretation as the set of decorated oriented standard polyhedra —see Proposition I.3.4). Our first task is to define a very general bracket $[.]$ on $\mathcal{O}$. At the first stage it will take values which are formal power series in countably many variables, but in the next section we will define *reductions* to the case of polynomials in finitely many variables. This bracket will depend on a finite set A which we fix for the rest of the section. We also fix a commutative ring Z with unit (typically, $Z = \mathbb{Z}, \mathbb{Q}, \mathbb{C}$); since Z has unit there exists a natural ring homomorphism $\mathbb{Z} \to Z$; we warn the reader that all the coefficients of power series and polynomials which explicitly appear in this chapter will be integers, but we will view them as elements of Z through this homomorphism. We will not insist on this point later on.

Let $A^* = \cup_{p \geq 0} A^p$ denote the language with alphabet A and denote as usual by ϵ the word of length 0 in A^*. Let n, m be positive integers with even sum, and consider the rectangle shown in Fig. IV.1. Denote by $P^n_m(A)$ the set of all patterns resulting from completions of the rectangle, where:

1. A completion is obtained by connecting together in pairs the $n+m$ germs of strands;

2. Each of the arcs which gives the completion either has no colour or is divided into finitely many subarcs each having a colour in A. In other words if we direct the arc we have a well-defined word in A^* (the word ϵ corresponds to the case of no colour);

3. Two completions are regarded as identical if, starting from any germ of a strand, in both completions we meet the same colours and we end up

on the same germ of a strand.

If we number by $1, ..., n+m$ the germs of strands in the rectangle, we can formally define $P^n_m(A)$ as $(A^*)^{(n+m)/2} \times \mathfrak{S}_{n+m}/\sim$, where $\sim$ is the equivalence relation generated as follows: $(w_1, ..., w_{(n+m)/2}, \sigma) \sim (w'_1, ..., w'_{(n+m)/2}, \sigma')$ whenever for some $k \in 1, ..., (n+m)/2$ we have $w'_k = w_k^{-1}$ and $\sigma' = \sigma \cdot (2k-1, 2k)$, or for some $\tau \in \mathfrak{S}_{(n+m)/2}$ we have

$$\sigma'(2h-1) = \sigma(2\tau(h)-1),\ \sigma'(2h) = \sigma(2\tau(h)),\ w'_h = w_{\tau(h)}\ \forall h = 1, ..., (n+m)/2.$$

Here $[w_1, ..., w_{(n+m)/2}, \sigma]$ defines the completion in which for $k = 1, ..., (n+m)/2$ an arc goes from the $\sigma(2k-1)$-th germ to the $\sigma(2k)$-th germ with colours $w_k = a^k_1 \cdots a^k_{l_k}$. We prefer to deal with patterns as concrete diagrams, so we avoid this formal definition.

The rectangle in Fig. IV.1 must be viewed as having a fixed position in the plane. In particular if $m = n$ the rotation through angle π defines an involution $\phi_n(A) : P^n_n(A) \to P^n_n(A)$ which is the identity only if $n = \#A = 1$. Similarly we can define $\phi^n_m(A) : P^n_m(A) \to P^m_n(A)$ for $n \neq m$.

Consider now two positive integers n_+, n_- with even sum. (The reason why we change notation is that we will apply the definition of $P^n_m(A)$ just given for $(n, m) = (n_+, n_+), (n_+, n_-), (n_-, n_-), (n_-, n_+)$.)

Now we define $V^{n_+}_{n_-}(A)$ as the set of patterns resulting from completion of the cross shown in Fig. IV.1, where the definition of completion is the natural extension of that given for the rectangle. Also the cross must be considered fixed in the plane; in particular we define an involution $\psi^{n_+}_{n_-}(A) : V^{n_+}_{n_-}(A) \to V^{n_+}_{n_-}(A)$ through the rotation of angle π.

As in other parts of the work we will symbolize the fact that the endpoint of an edge of an o-graph is over (respectively under) by attaching to it a sign $+$ (respectively $-$).

We define a (n_+, n_-, A)-*strand-decoration of an edge* e of an o-graph to be the choice of a direction of e and an element of $P^{n_{\sigma_1}}_{n_{\sigma_2}}(A)$, where σ_2 is the sign of the first endpoint of e and and σ_1 is the sign of the second endpoint. We define a (n_+, n_-, A)-*strand-decoration of a vertex* of Γ to be the choice of an element of $V^{n_+}_{n_-}(A)$ plus a direction for the over-arc.

We denote by $\tilde{\mathcal{O}}^{n_+}_{n_-,A}$ the set of all partially (n_+, n_-, A)-strand-decorated o-graphs (i.e. o-graphs where some of the edges and vertices are decorated). From now on the term 'decoration' will mean strand-decoration. Let us introduce the variables:

$$\begin{array}{cl} K^{\sigma_1, n_{\sigma_1}}_{\sigma_2, n_{\sigma_2}}(p, \alpha) & \sigma_1, \sigma_2 \in \{+, -\},\ p \in P^{n_{\sigma_1}}_{n_{\sigma_2}}(A), \alpha \in \mathbb{Z}_3, \\ H^{n_+}_{n_-}(s) & s \in V^{n_+}_{n_-}(A), \\ X_w & w \in A^*, \end{array}$$

subject to the symmetry relations:

$$K^{\sigma_1, n_{\sigma_1}}_{\sigma_2, n_{\sigma_2}}(p, \alpha) = K^{\sigma_2, n_{\sigma_2}}_{\sigma_1, n_{\sigma_1}}(\phi^{n_{\sigma_1}}_{n_{\sigma_2}}(A)(p), \alpha),$$

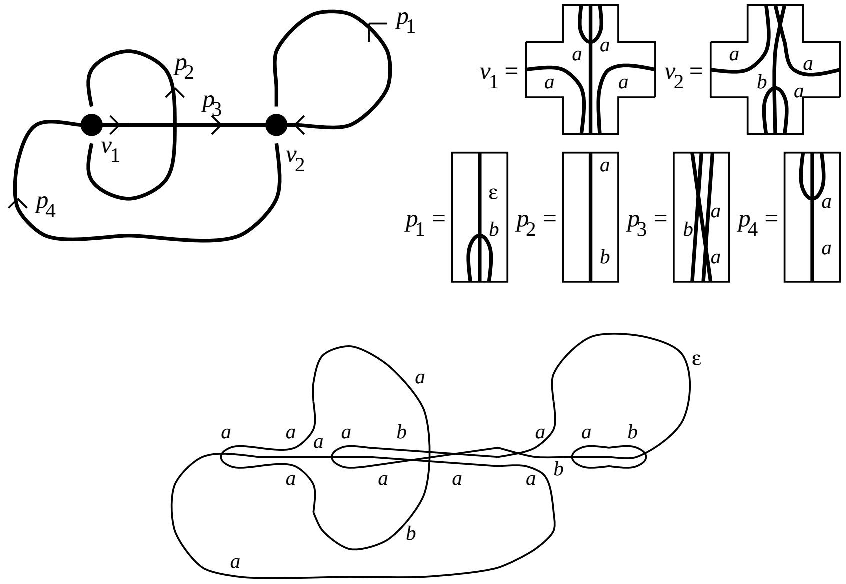

Figure IV.2: An example of how to compute the value of a totally strand-decorated o-graph. We have here $n_+ = 3, n_- = 1$ and the bracket is $X_{a^4b}X_{ab}X_{a^4}X_{aba^2b}$

$$\begin{aligned} &H^{n_+}_{n_-}(s) = H^{n_+}_{n_-}(\psi^{n_+}_{n_-}(A)(s)), \\ &X_{a_1\cdots a_t} = X_{a_2\cdots a_t\, a_1} = X_{a_t\cdots a_2\, a_1}. \end{aligned}$$

We define now a function $[.]^{n_+}_{n_-,A,Z}$ from $\tilde{\mathcal{O}}^{n_+}_{n_-,A}$ to the space of formal power series with coefficients in Z in the above variables, which will always be assumed to commute. To give this definition we need to decide in what order the monomials will appear in the series, i.e. we fix a bijection from $\mathbb{N}$ to the set of monomials in the variables K, H, X. The definition of the bracket is obtained by setting the value of totally decorated o-graphs and giving two linear relations which express the value of a partially decorated o-graph by means of the value of o-graphs which are more decorated.

Bracket of a totally decorated o-graph Γ. We fatten the o-graph and put four cuts around every vertex so that we have a union of crosses and rectangles (we do not worry about unmarked vertices of the graph: we know that they "do not really exist"). Then we trace the decoration of an edge or vertex inside the corresponding rectangle or cross, with the convention that the direction should point upwards in the abstract version of the rectangle and cross (instead of formalizing this process we give the example of Fig. IV.2). Thanks to the conventions stated above, the result is now a union of finitely many circuits which meet each other in fake crossings. Each circuit is divided into subarcs, and each subarc has a colour in A or no colour. We define the value of a circuit as X_w if $w = a_1 \cdots a_t$ are the colours met around the circuit (no matter starting from where and in what direction, thanks to the symmetries of X). We finally define $[\Gamma]^{n_+}_{n_-,A,Z}$ as the product of the values of all the circuits. Remark that this is always a monomial.

Edge skein relations. Let e be a non-decorated edge of an o-graph Γ, let $\alpha \in \mathbb{Z}_3$ be its colour, let e_1 and e_2 be the two germs of edges at its endpoints and let σ_i be the sign of e_i. Choose for e the direction from e_2 to e_1 and for $p \in P^{n_{\sigma_1}}_{n_{\sigma_2}}(A)$ denote by Γ_p the graph obtained by decorating e with the fixed direction and p. Then we define:

$$[\Gamma]^{n+}_{n-,A,Z} = \sum_{p \in P^{n_{\sigma_1}}_{n_{\sigma_2}}(A)} K^{\sigma_1, n_{\sigma_1}}_{\sigma_2, n_{\sigma_2}}(p, \alpha)[\Gamma_p]^{n+}_{n-,A,Z}.$$

To be completely precise, we must specify what we mean by this formula. The coefficient in $[\Gamma]^{n+}_{n-,A,Z}$ of a monomial M is the (finite) sum of the coefficient in $[\Gamma_p]^{n+}_{n-,A,Z}$ of $M/K^{\sigma_1, n_{\sigma_1}}_{\sigma_2, n_{\sigma_2}}(p, \alpha)$, where the sum extends over all $p \in P^{n_{\sigma_1}}_{n_{\sigma_2}}(A)$ such that $K^{\sigma_1, n_{\sigma_1}}_{\sigma_2, n_{\sigma_2}}(p, \alpha)$ divides M . All infinite sums which appear in the sequel must be interpreted like this. The symmetry of $K^{\sigma_1, n_{\sigma_1}}_{\sigma_2, n_{\sigma_2}}$ implies that this definition is independent of the direction initially fixed when $\sigma_1 = \sigma_2$ (for $\sigma_1 \neq \sigma_2$ there is no possible ambiguity).

Vertex skein relations Let v be a non-decorated vertex of Γ. We fix an arbitrary direction for the over-arc, and for $s \in V^{n+}_{n-}(A)$ we denote by Γ_s the graph obtained by decorating v with the fixed direction and s. Then we define:

$$[\Gamma]^{n+}_{n-,A,Z} = \sum_{s \in V^{n+}_{n-}(A)} H^{n+}_{n-}(s)[\Gamma_s]^{n+}_{n-,A,Z}.$$

Again the symmetry of H^{n+}_{n-} implies that the choice of the direction does not affect the result.

We summarize the definition of the bracket in the following very natural symbolic way:

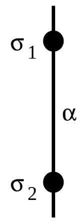

$$= \sum_{p \in P^{n_{\sigma_1}}_{n_{\sigma_2}}(A)} K^{\sigma_1, n_{\sigma_1}}_{\sigma_2, n_{\sigma_2}}(p, \alpha)$$
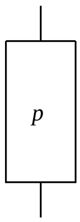

,

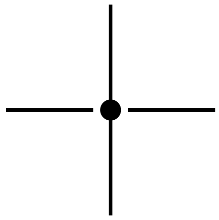
$$= \sum_{v \in V^{n+}_{n-}(A)} H^{n+}_{n-}(v)$$
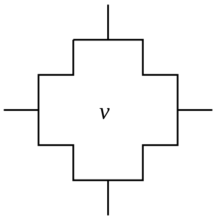

,

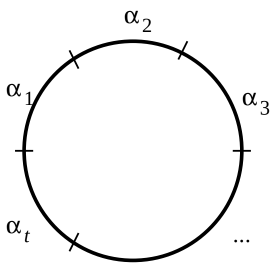

$= X_{\alpha_1 \cdots \alpha_t}$.

To see that $[.]^{n+}_{n_-,A,Z}$ is actually well-defined we must check that the order in which the skein relations are applied is not relevant. This is basically obvious as the skein relations apply to a single edge or vertex and neither affect nor are affected by the surrounding graph. Another way to see this is the following: to every total decoration of a graph Γ we can associate a monomial in the variables K, H, X which encodes the patterns used for the decoration and the value of the resulting totally decorated graph: then $[\Gamma]^{n+}_{n_-,A,Z}$ is the sum over all total decorations of Γ of the monomial associated to the decoration. Along this line we can also regard a total decoration as a state of the graph, and hence see the bracket as the *sum over all states* of the value of the state.

Having defined $[.]^{n+}_{n_-,A,Z}$ we simply set now:

$$[\Gamma]_{A,Z} = \sum_{n_+,n_-\geq 1,\ n_++n_-\ \text{even}} [\Gamma]^{n+}_{n_-,A,Z}.$$

Since of course each variable K and H appears finitely many times, each monomial has a well-defined coefficient in this sum.

The function $[.]_{A,Z}$ takes values which are formal power series with coefficients in Z in infinitely many variables.

Remark IV.1.1. It is readily checked that the definition of $[.]_{A,Z}$ is actually invariant under isotopy and moves R.

IV.2 Finite reductions

Let all the notations of the previous section be fixed. We define a *finite reduction* of the variables X to be a map f defined on the set of these variables (taking into account the symmetries) with values in some commutative ring, with the property that the equivalence classes of the relation:

$$w_1 \sim_f w_2 \text{ if } f(X_{w_1 \cdot w}) = f(X_{w_2 \cdot w})\ \forall w \in A^*$$

are finitely many. Given a finite reduction f, whenever there is no risk of misunderstanding, we will write X_w instead of $f(X_w)$, i.e. we consider f as introducing more relations in the set of variables X.

Let a finite reduction f be given, and consider two integers n_+, n_- with even sum. We define $P^{n_+}_{n_+}(A,f)$ in the same way as $P^{n_+}_{n_+}(A)$, with the difference that we consider two patterns as identical if starting from any germ of a strand we end up on the same germ, and along the arc we meet words which are equivalent under $\sim_f$. We define $P^{n_-}_{n_-}(A,f)$, $P^{n_+}_{n_-}(A,f)$, $P^{n_-}_{n_+}(A,f)$ and $V^{n_+}_{n_-}(A,f)$ in a similar way. Remark that these are now finite sets. We define $\tilde{\mathcal{O}}^{n_+}_{n_-,f,A}$ as the set of partially (n_+,n_-,f,A)-strand-decorated o-graphs (in an obvious sense). Then the same procedure as in the previous section allows us to define $[.]^{n_+}_{n_-,f,A,Z}$ on $\tilde{\mathcal{O}}^{n_+}_{n_-,f,A}$ by considering patterns and variables X reduced modulo f. We just need to remark that, by the very definition of $\sim_f$, if we choose any representative in each class and use it instead of the class, the result does not depend on the representative chosen.

We have introduced $\tilde{\mathcal{O}}^{n_+}_{n_-,f,A}$ in order to have internal skein relations, but of course we are only interested in the restriction of $[.]^{n_+}_{n_-,f,A,Z}$ to $\mathcal{O}$. Now, fix an integer $N \geq 1$. Then for $\Gamma \in \mathcal{O}$ we set:

$$[\Gamma]_{N,f,A,Z} = \sum_{1\leq n_+,n_-\leq N,\ n_++n_-\ \text{even}} [\Gamma]^{n_+}_{n_-,f,A,Z}$$

where the right-hand side belongs the Z-algebra $\mathcal{R}_{N,f,A,Z}$ of polynomials with coefficients in Z and variables:

$$\begin{array}{ll} K^{\sigma_1,n_{\sigma_1}}_{\sigma_2,n_{\sigma_2}}(p,\alpha) & \sigma_1,\sigma_2\in\{+,-\},\ 1\leq n_+,n_-\leq N,\ n_++n_-\ \text{even}, \\ & \qquad p\in P^{n_{\sigma_1}}_{n_{\sigma_2}}(A,f),\ \alpha\in\mathbb{Z}_3, \\ H^{n_+}_{n_-}(v) & 1\leq n_+,n_-\leq N,\ n_++n_-\ \text{even},\ v\in V^{n_+}_{n_-}(A,f), \\ f(X_w) & w\in A^*/_{\sim_f} \end{array}$$

(with the same symmetries as above). Here we are using the terminology with some abuse because the $f(X_w)$'s already live in a commutative ring, so there could be relations between them, and therefore $\mathcal{R}_{N,f,A,Z}$ is not strictly speaking a polynomial ring. However the finite reductions which one devises are such that $f(X_w)\in Z$ for many w's, and all other $f(X_w)$ are independent from each other. In particular this is the case for the reduction which leads to the Turaev-Viro invariants, and therefore we will always refer to the elements of $\mathcal{R}_{N,f,A,Z}$ as polynomials.

In the introduction we have referred to a filtration of our sequence of brackets through a natural notion of complexity: we can define for instance the complexity of $[.]_{N,f,A,Z}$ as

$$N + \#A + \#(A^*/_{\sim_f}).$$

We consider now a special case of the bracket and give in this case a few examples of finite reductions. We do this to show that even in a very simple case there is still a considerable freedom of choice, and because these special brackets are those which arise in the most natural way. Other types of reductions and specializations will be considered in Section IV.5 below.

Let the set of colours A be $\mathbb{Z}_3$, and let us consider only $(1,1,A)$-strand decorations. For $p \in P^1_1(A)$ let $K^{\sigma_1;1}_{\sigma_2,1}(p,\alpha)$ be 1 in case p is a segment without subdivisions and colour α, 0 otherwise (in other words every edge is seen as already strand-decorated by itself). Define also $H^1_1(s)$ to be 0 unless all the segments in s have no subdivision and no colour (i.e. colour ϵ): there remain exactly 3 variables. We denote the bracket under these specializations by $[\![.]\!]$ and call it *basic bracket.*

If we choose names R, L, S for the surviving variables H we have that $[\![.]\!]$ is defined by the following single skein relation (plus the values on circuits defined as usual)

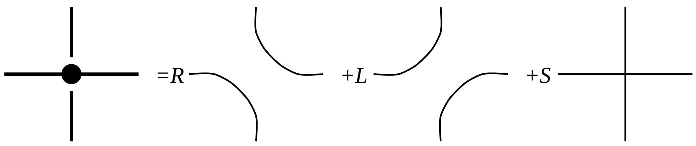

from which one also understands the names chosen for the variables.

We consider now finite reductions for the variables X_w, $w \in \mathbb{Z}_3^*$ which appear in the basic bracket $[\![.]\!]$. Let $r = (r_\alpha)_{0\leq\alpha\leq 2}$ and $t = (t_{\alpha,\beta})_{0\leq\alpha\leq\beta\leq 2}$, where the r_α's and $t_{\alpha,\beta}$'s are positive integers. Consider the symbols $Y^b_{a,\delta_1,\delta_2}$ with:

- $a = (a_\alpha)_{0\leq\alpha\leq 2}$ and $0 \leq a_\alpha \leq r_\alpha - 1$;
- $b = (b_{\alpha,\beta})_{0\leq\alpha\leq\beta\leq 2}$ and $0 \leq b_{\alpha,\beta} \leq t_{\alpha,\beta} - 1$;
- $\delta_1, \delta_2 \in \mathbb{Z}_3$.

We define a finite reduction f^t_r by $f^t_r(X_{\gamma_1,\ldots,\gamma_k}) = Y^b_{a,\alpha_1,\alpha_2}$ where:

1. a_α is the number of j's such that $\gamma_j = \alpha$, reduced modulo r_α;
2. $b_{\alpha,\beta}$ is the number of pairs $j, j+1$ (with $j+1 = 1$ if $j = k$) such that $\{\gamma_j, \gamma_{j+1}\} = \{\alpha, \beta\}$, reduced modulo $t_{\alpha,\beta}$;
3. δ_α is the sum (in $\mathbb{Z}_3$) of all $\gamma_j = \alpha$.

Remark IV.2.1. If $Y^b_{a,\delta_1,\delta_2}$ is the image of some $X_{\gamma_1,\ldots,\gamma_k}$ and r_α is a multiple of 3 for $\alpha \in \{1,2\}$ then δ_α is the class of a_α in $\mathbb{Z}_3$. So in this case not all the symbols Y are actually relevant, but this is the only case where this happens. In other words if we we consider only $Y^b_{a,\delta_1,\delta_2}$ with δ_α the class of a_α when $3|r_\alpha$, then all the Y's appear.

One can easily devise further finite reductions obtained from these f_r^t. A particularly simple one is to take the $t_{\alpha,\beta}$ all equal to 0 and the r_α all equal to r_0, and to map $Y^0_{(a_0,a_1,a_2),\delta_1,\delta_2}$ to a new variable $Z_{c,\delta}$ where $a_0+a_1+a_2 \equiv c \bmod r_0$ and $\delta = \delta_1 + \delta_2 \in \mathbb{Z}_3$. The result is a finite reduction f_{r_0} whose range consists of $3(r_0+1)$ variables.

If we rename by x_α the variable $Z_{0,\alpha}$ then $[\![.]\!]$ under the specialization f_1 is a function $\langle . \rangle : \mathcal{O} \to \mathbb{Z}[R, L, S, x_0, x_1, x_2]$ which is in a sense the prototype of all our brackets. Despite being a very radical reduction of the most general bracket it still has some interesting features (on spines only, while it is trivial on 3-manifolds —see Section IV.7).

IV.3 Bracket invariants of spines and 3-manifolds

Before turning to how the bracket can be used to define invariants, we briefly explain what is the underlying idea. We know that 3-manifolds up to homeomorphism "are" elements of $\mathcal{O}$ up to two well-understood moves (Theorem I.0.1). Assume for a moment that $[.]_{N,f,A,Z} : \mathcal{O} \to \mathcal{R}_{N,f,A,Z}$ is injective for some choice of N, A, f, Z . Then the problem of deciding whether two 3-manifolds are homeomorphic would be faithfully translated in $\mathcal{R}_{N,f,A,Z}$, which has the advantage of having a very rich algebraic structure. In fact, instead of considering in $\mathcal{R}_{N,f,A,Z}$ the equivalence relation from the set-theoretic viewpoint we can consider it from the Z-module viewpoint (i.e. we can take the Z-submodule generated by differences of elements which must be equivalent) and from the (potentially "blinder") ring viewpoint (i.e. we can take the ideal generated by differences of elements which must be equivalent). This leads to equivalence classes which group together some of the original classes (i.e. invariants): the hope is that they do not group up too many. If the assumption that for some choice the bracket is injective is false (which is probably the case), this scheme works as well, but already at the first stage we lose some information about the manifold.

Let us remark that even if $[.]_{N,f,A,Z} : \mathcal{O} \to \mathcal{R}_{N,f,A,Z}$ is probably never injective, we conjecture that if $\Gamma_1, \Gamma_2 \in \mathcal{O}$ are different then there exists some choice such that $[\Gamma_1]_{N,f,A,Z} \neq [\Gamma_2]_{N,f,A,Z}$ (maybe one can also fix $Z = \mathbb{Z}$, n_+, n_- and A a priori, provided $\#A \geq 2$, and find f such that $[.]^{n_+}_{n_-,f,A,Z}$ does the job).

One important feature of the next result we will establish (Theorem IV.3.1) is that by combining the ideas of taking the Z-submodule and the ideal, we are able to obtain sequences of invariants which are *computable* in the following precise sense: we exhibit fixed elements $p_1, ..., p_s$, $q_1, ..., q_t$ of $\mathcal{R}_{N,f,A,Z}$ with integer coefficients, and the manifolds corresponding to o-graphs Γ_1 and Γ_2 have the same invariant if and only if there exist $\lambda_1, ..., \lambda_s \in Z$ such that $[\Gamma_1] - [\Gamma_2] - \sum \lambda_i p_i$ belongs to the ideal generated by $q_1, ..., q_t$. It is well known

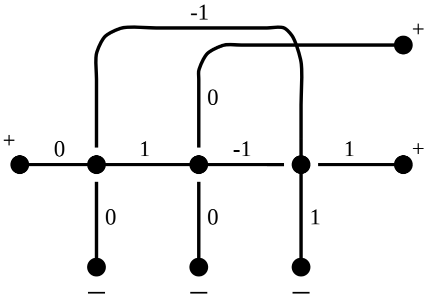

Figure IV.3: An example of o-graphs with truncations

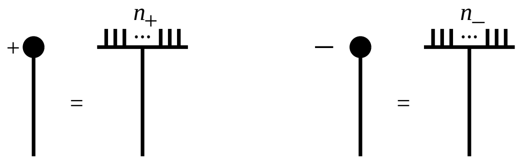

Figure IV.4: Conventions for the meaning of the solid dots

that this problem is decidable under mild hypotheses on Z. Moreover this kind of *membership problem* is one of the central themes in recent powerful developments of *computer algebra*, which are making it more and more *practicable*, and not only theoretically possible, to find actual solutions.

Taking the Z-submodule "up to a certain level" and then the ideal, we obtain sequences of invariants which in some sense give better and better approximations to the invariant obtained by taking the Z-submodule only. This last invariant is hopefully not so far from the purely set-theoretic one, but it is not computable.

For the purpose of stating our main result, we need to slightly extend the class of objects to which we apply the bracket. We define an o-graph with truncations as a connected graph which looks as an o-graph apart from the fact that edges are allowed to terminate in single solid dots which bear a sign $+$ or $-$. Instead of giving a formal definition we give an example in Fig. IV.3. Fix for a moment integers $n_+, n_- \geq 1$ with even sum, and let us view the dot with symbol $+$ (respectively, $-$) as the source of n_+ (respectively, n_-) germs of strands, as shown in Fig. IV.4. Given an o-graph with truncations with p symbols $+$ and q symbols $-$, we can see the graph as having $n_+p + n_-q$ open germs of strands; we define a (n_+, n_-, A)-completion of it as a way to connect in pairs these n_+p+n_-q strands by A^*-coloured segments (one easily sees that $p+q$ must be even, so $n_+p + n_-q$ is even). See Fig. IV.5 for an example of completion of an o-graph with truncations.

If a finite reduction f is under consideration we regard as identical arcs which are coloured by words equivalent under $\sim_f$, and we get a finite set of completions which we denote by $\mathcal{C}^{n_+}_{n_-}(A, f)(\Gamma)$. Of course for $c(\Gamma) \in \mathcal{C}^{n_+}_{n_-}(A, f)(\Gamma)$

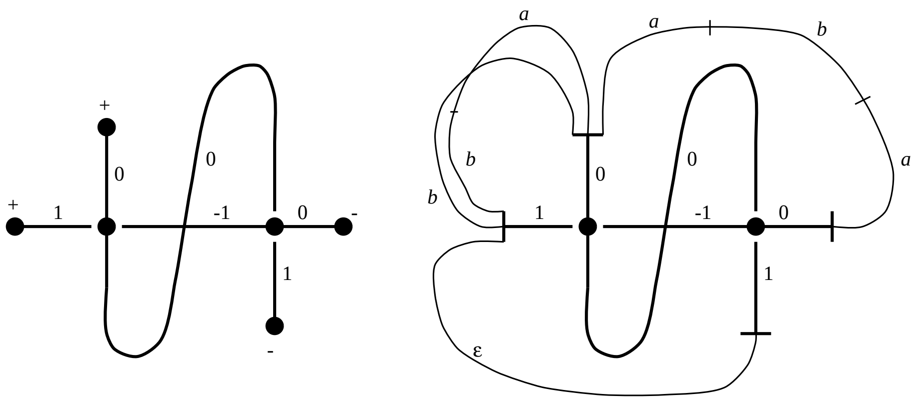

Figure IV.5: An example of completion of an o-graph with truncations

the value of $[c(\Gamma)]^{n_+}_{n_-,f,A,Z}$ is naturally defined (if we decorate edges and vertices with patterns we have a union of A^*-coloured circuits).

Now, for an integer $N \geq 1$, we define $\mathcal{C}(A,f)(\Gamma)$ as the cartesian product

$$\mathcal{C}(A,f)(\Gamma) = \prod_{1\leq n_+,n_-\leq N,\ n_++n_- \ \text{even}} \mathcal{C}^{n_+}_{n_-}(A,f)(\Gamma).$$

If $c(\Gamma) \in \mathcal{C}(A,f)(\Gamma)$ with $c = (c^{n_+}_{n_-})$ we finally set:

$$[c(\Gamma)]_{N,f,A,Z} = \sum_{1\leq n_+,n_-\leq N,\ n_++n_- \ \text{even}} [c^{n_+}_{n_-}(\Gamma)]^{n_+}_{n_-,f,A,Z}.$$

If ν is an integer or ∞ let us denote by $\mathcal{O}_{\leq\nu}$ (respectively, $\hat{\mathcal{O}}_{\leq\nu}$) the set of all o-graphs (respectively, o-graphs with truncations) having at most ν vertices. We also define $\mathcal{O}_\nu$ and $\hat{\mathcal{O}}_\nu$ by requiring that the vertices are exactly ν. If $\nu < \infty$ all these sets are finite (and easily enumerable). We also denote by $\mathcal{O}_{\geq 2}$ the set of o-graphs with at least two vertices (this is the set by which we present manifolds).

We can define on $\hat{\mathcal{O}} = \hat{\mathcal{O}}_\infty$ the moves C and MP in an obvious way, by the requirement that they apply to regions where the graph looks like a veritable o-graph. If $\Gamma \in \hat{\mathcal{O}}$ and Γ' is obtained by move C or MP from Γ, then there is a natural bijective correspondence

$$\eta_{\Gamma,\Gamma'} : \mathcal{C}(A,f)(\Gamma) \to \mathcal{C}(A,f)(\Gamma')$$

which is deduced from the fact that Γ and Γ' have "the same" open strands.

We are finally ready to prove the main result of this chapter.

Theorem IV.3.1. *Let $N \geq 1$ be an integer, let A be a finite set, let Z be a commutative ring whith unit and let f be a finite reduction of the variables X. Consider the map $[.] = [.]_{N,f,A,Z}$ which (constructively) assigns to every completion of an element of $\hat{\mathcal{O}}$ an element of $\mathcal{R}_{N,f,A,Z}$. Let $\nu \geq 0$ and $\mu \geq 1$ be integers and define in $\mathcal{R}_{N,f,A,Z}$:*

1. *$\mathcal{S}_\nu$ as the Z-submodule generated by $[c(\Gamma)] - [\eta_{\Gamma,\Gamma'}(c)(\Gamma')]$ as Γ varies in $\mathcal{O}_{\leq\nu}$, Γ' varies in the graphs obtained from Γ via* C *and c varies in $\mathcal{C}(A,f)(\Gamma)$.*

2. *$\mathcal{I}_\nu$ as the ideal generated by $[c(\Gamma)] - [\eta_{\Gamma,\Gamma'}(c)(\Gamma')]$ as Γ varies in $\hat{\mathcal{O}}_{\nu+1}$ and Γ', c are as in 1.*

3. *$\mathcal{S}^\mu$ as the Z-submodule generated by $[c(\Gamma)] - [\eta_{\Gamma,\Gamma'}(c)(\Gamma')]$ as Γ varies in $\mathcal{O}_{\leq\mu}$, Γ' varies in the graphs obtained from Γ via* MP *and c varies in $\mathcal{C}(A,f)(\Gamma)$.*

4. *$\mathcal{I}^\mu$ as the ideal generated by $[c(\Gamma)] - [\eta_{\Gamma,\Gamma'}(c)(\Gamma')]$ as Γ varies in $\hat{\mathcal{O}}_{\mu+1}$ and Γ', c are as in 3.*

Then the following holds:

1. *The generators listed in these definitions are finitely many and have integer coefficients in all four cases.*

2. *If π_ν is the natural projection*

$$\pi_\nu : \mathcal{R}_{N,f,A,Z} \to \frac{\mathcal{R}_{N,f,A,Z}}{\mathcal{S}_\nu + \mathcal{I}_\nu}$$

   then $\pi_\nu \circ [.]$ restricted to $\mathcal{O}$ is invariant under C, *and therefore defines an invariant of oriented standard polyhedra.*

3. *If π_ν^μ is the natural projection*

$$\pi_\nu^\mu : \mathcal{R}_{N,f,A,Z} \to \frac{\mathcal{R}_{N,f,A,Z}}{(\mathcal{S}_\nu + \mathcal{S}^\mu) + (\mathcal{I}_\nu + \mathcal{I}^\mu)}$$

   then $\pi_\nu^\mu \circ [.]$ restricted to $\mathcal{O}_{\geq 2}$ is invariant under C *and* MP, *and therefore defines an invariant of compact oriented* 3*-manifolds with non-empty boundary.*

Proof of IV.3.1. The first assertion is obvious.

We prove the second assertion for $[.]^{n_+}_{n_-,f,A,Z}$ rather than for $[.]_{N,f,A,Z}$, the general case being obtained just by considering summations over n_+, n_- and using the definitions. So, assume $\Gamma \in \mathcal{O}$ and Γ' is obtained from Γ via a combination of moves C. We want to show that:

$$[\Gamma] - [\Gamma'] \in \mathcal{S}_\nu + \mathcal{I}_\nu.$$

Since $\mathcal{S}_\nu + \mathcal{I}_\nu$ is a Z-submodule one easily checks that it is sufficient to refer to the case where Γ' is obtained from Γ via only one move C.

If $\Gamma \in \mathcal{O}_{\leq\nu}$ then $[\Gamma]-[\Gamma']$ is one of the generators of $\mathcal{S}_\nu$. Assume Γ has more than ν vertices. Choose a set L of $\nu+1$ vertices in Γ, including the vertex where C is applied, in such a way that any two elements of L can be joined without touching vertices not in L. Consider the corresponding set of vertices L' in Γ'. Let E be the set of edges in Γ which do not touch L and let V be the set of vertices of Γ which do not belong to L. If E' and V' are defined in a similar way in Γ' there are natural bijections $E \leftrightarrow E'$ and $V \leftrightarrow V'$, and the correspondence $E \leftrightarrow E'$ preserves the properties of the edge (endpoints under or over and colour).

Let us remove from Γ all the elements of $E \cup V$. If the endpoint of some edge in the resulting graph is not a vertex, we assign to it the symbol $+$ if the corresponding endpoint was originally above, $-$ otherwise. Then we obtain an element $\hat{\Gamma}$ of $\hat{\mathcal{O}}_{\nu+1}$. If we do the same in Γ' we get $\hat{\Gamma}' \in \hat{\mathcal{O}}_{\nu+1}$ and of course $\hat{\Gamma}'$ is obtained from $\hat{\Gamma}$ via C.

Now, recall the bijections $E \leftrightarrow E'$ and $V \leftrightarrow V'$, and apply the skein relations to the elements of $E \cup V$ in Γ and $E' \cup V'$ in Γ'. We obtain:

$$[\Gamma] = \sum k_i[\Gamma_i] \qquad [\Gamma'] = \sum k_i[\Gamma'_i]$$

where the monomials k_i (products of K's and H's) are the same in the two sums, and Γ_i, Γ'_i are partially decorated "in the same way", with obvious meaning. In Γ_i let us trace the decoration on the graph; if we remove all closed circuits which arise and consider their value as a multiplication factor, we obtain:

$$[\Gamma_i] = x_i[c_i(\hat{\Gamma})],$$

where x_i is a product of X's and $c_i \in \mathcal{C}^{n_+}_{n_-}(f,A)(\hat{\Gamma})$. If we do the same in Γ'_i we obtain:

$$[\Gamma'_i] = x_i[\eta_{\hat{\Gamma},\hat{\Gamma}'}(c_i)(\hat{\Gamma}')]$$

which implies the conclusion.

The third assertion is proved virtually in the same way. $\boxed{\text{IV.3.1}}$

Remark IV.3.2. Since patterns are affected by the two operations on edges and vertices which translate the change of orientation (*cf.* Theorem I.0.1(3)), the invariants produced by Theorem IV.3.1 are in principle sensitive to the orientation.

We close this section with a remark which has no relation with the notion of bracket of an o-graph: it answers a natural question which arises when trying to construct invariants via standard spines.

Remark IV.3.3. The reader may wonder if the singular set of the spine of a manifold, i.e. the abstract graph supporting an o-graph of the manifold, can be used to produce non-trivial invariants. The answer is no, and the reason is that from the point of view of the abstract graph the Matveev-Piergallini move is the following: if an edge e has endpoints v_0, v_1 and the other edges incident to v_i are a_i^1, a_i^2, a_i^3, we can delete e, add a triangle with vertices w_1, w_2, w_3 and join a_i^j to w_j. This does no harm, but when we come to the inverse of this move we see that we cannot distinguish a_1^j from a_2^j. So one way to apply the inverse move leads to a graph which differs from the original one only in that a_1^1 is now incident to v_2, and a_2^1 to v_1. It is not difficult to check that under this move all quadrivalent graphs with a given number of vertices are equivalent to each other.

IV.4 Hyperlocal invariants

The aim of Theorem IV.3.1 was to provide the most general framework in which brackets can be used to produce invariants of spines and manifolds. On the contrary here we restrict the generality (in other words we take quotients by bigger ideals) and show that even this restricted version of our bracket invariants contains the very important invariants of Turaev and Viro [Tur-Vi].

Let us recall that the essential idea of Theorem IV.3.1 to achieve invariance under the moves is to control "by hand" all cases up to a certain level of complexity and then take an ideal which ensures invariance for higher complexity: as we choose higher and higher levels of complexity, we obtain invariants which are a priori more and more sensitive. In this section we have the opposite goal in mind: instead of seeking the broadest generality we try to keep the complexity of the ideal as small as possible.

For the sake of simplicity in this section we will confine ourselves to brackets defined via patterns with a fixed number of strands (one fixed number for overarcs and one for underarcs). We leave to the reader the extension to the case of brackets defined as the sum of all brackets satisfying a certain bound on the number of strands.

Fix integers n_+, n_- with even sum, a finite set A, a finite reduction f on A and a commutative ring with unit Z. Denote (for the whole section):

$$[.] = [.]^{n_+}_{n_-,f,A,Z},$$

denote by $\mathcal{R}$ the Z-algebra where $[.]$ takes values: namely $\mathcal{R}$ is the ring of "polynomials" with coefficients in Z in the variables:

$$\begin{array}{ll} K^{\sigma_1,n_{\sigma_1}}_{\sigma_2,n_{\sigma_2}}(p,\alpha) & \sigma_1,\sigma_2 \in \{+,-\},\ p \in P^{n_{\sigma_1}}_{n_{\sigma_2}}(A,f),\ \alpha \in \mathbb{Z}_3, \\ H^{n_+}_{n_-}(v) & v \in V^{n_+}_{n_-}(A,f), \\ f(X_w) & w \in A^*/_{\sim_f} \end{array}$$

subject to the symmetry relations stated in the previous section. We will always replace n_+ and $(+, n_+)$ by $+$ only, and similarly with $-$. We will also

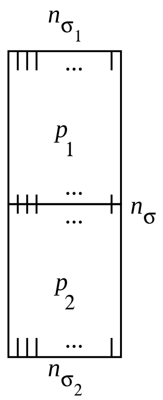

Figure IV.6: Definition of the product of two patterns

omit to mention explicitly f and A, so that for instance the skein relation for edges can be re-written for the bracket [.] in question in the formally simpler form:

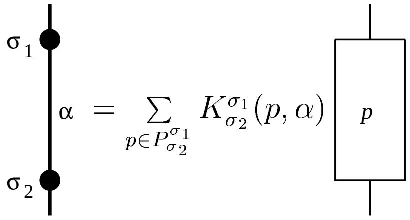

(in this section the symbols $\sigma_1, \sigma_2, \sigma$ will always denote arbitrary elements of $\{+,-\}$). We describe now an ideal $\mathcal{J}$ of $\mathcal{R}$ such that modulo $\mathcal{J}$ the bracket [.] is an invariant of 3-manifolds. The ideal has 3 lists of generators.

Edge-associativity generators. Denote by $\mathcal{A}_{\sigma_2}^{\sigma_1}$ the $\mathcal{R}$-module freely generated by $P_{\sigma_2}^{\sigma_1}$. We can define a "product"

$$\mathcal{A}_{\sigma}^{\sigma_1} \times \mathcal{A}_{\sigma_2}^{\sigma} \to \mathcal{A}_{\sigma_2}^{\sigma_1}$$

by extending by bilinearity the product thus defined on the generators: given $p_1 \in P_{\sigma}^{\sigma_1}$ and $p_2 \in P_{\sigma_2}^{\sigma}$ we form an element of $\mathcal{A}_{\sigma_2}^{\sigma_1}$ by positioning p_1 above p_2 as shown in Fig. IV.6 and replacing each circuit which appears by the appropriate factor X_w. The result is therefore of the form xp with $x \in \mathcal{R}$ and $p \in P_{\sigma_2}^{\sigma_1}$, and we denote it by $p_1 \cdot p_2$.

We define $\mathcal{J}_0$ as the ideal of $\mathcal{R}$ generated by the expressions

$$K_{\sigma_2}^{\sigma_1}(p, \alpha_1 + \alpha_2) - \sum_{p_1 \in P_{\sigma}^{\sigma_1},\ p_2 \in P_{\sigma_2}^{\sigma},\ p_1 \cdot p_2 = xp} x K_{\sigma}^{\sigma_1}(p_1, \alpha_1) K_{\sigma_2}^{\sigma}(p_2, \alpha_2)$$

as $\sigma, \sigma_1, \sigma_2$ vary in $\{+,-\}$, p varies in $P_{\sigma_2}^{\sigma}$ and α_1, α_2 vary in $\mathbb{Z}_3$.

C-invariance generators. Let us consider the object shown on the left in Fig. IV.7. If we apply the skein relations to the four edges and to the vertex,

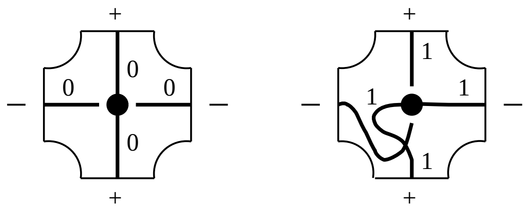

Figure IV.7: Patterns to be expanded via skein relations

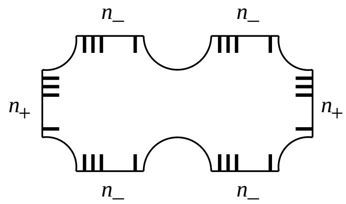

Figure IV.8: $\mathcal{U}$ consist of completions of this diagram

and we replace each circuit by the appropriate multiplying factor, we get a formal combination of elements of V_-^+ with coefficients in $\mathcal{R}$:

$$\sum_{v\in V_-^+} c_1(v)\cdot v.$$

If we do the same for the object shown on the right in Fig. IV.7 we obtain another combination

$$\sum_{v\in V_-^+} c_2(v)\cdot v.$$

and we define $\mathcal{J}_1$ as the ideal generated by all the differences $c_2(v)-c_1(v)$.

MP-invariance generators. Define $\mathcal{U}$ as the set af all (f,A)-completions of the object shown in Fig. IV.8 (this definition is analogous to that of V_-^+: only the "border" of the box has a different shape, see Fig. IV.1). Using the skein relations as we did before the two objects shown in Fig. IV.9 are expressed as linear combinations

$$\sum_{u\in\mathcal{U}} m_i(u)\cdot u, \qquad i=1,2$$

and we define $\mathcal{J}_2$ as the ideal generated by all the differences $m_2(u)-m_1(u)$.

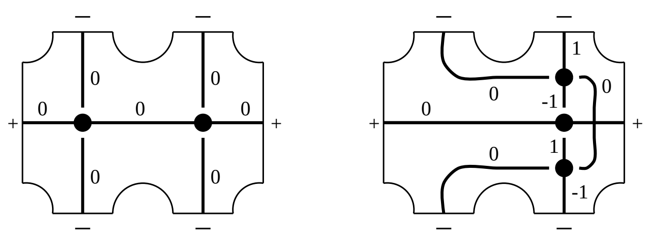

Figure IV.9: More patterns to be expanded via skein relations

Theorem IV.4.1. *Define* $\mathcal{J}$ *as* $\mathcal{J}_0 + \mathcal{J}_1 + \mathcal{J}_2$. *Then with the notation of Theorem IV.3.1 we have* $\mathcal{J} \supset \mathcal{I}_0 + \mathcal{I}^1$. *In particular* $[\Gamma] + \mathcal{J}$ *is an invariant of the manifold represented by* Γ.

Proof of IV.4.1. We check that all the generators of $\mathcal{I}_0$ and $\mathcal{I}^1$ are zero modulo $\mathcal{J}$. We leave to the reader the case of $\mathcal{I}_0$ (i.e. move C) and give a complete proof for the more complicated case of $\mathcal{I}_1$.

So let Γ be an o-graph with truncations having two vertices and an edge e_0 with colour 0 which is above at both vertices. Let Γ' be obtained from Γ by move MP at the edge e_0. Let $\hat{\Gamma}$ be a completion of Γ and $\hat{\Gamma}'$ be the corresponding completion of Γ'. We must check that

$$[\hat{\Gamma}'] - [\hat{\Gamma}] \in \mathcal{J}.$$

Let us denote by Γ_0 and Γ'_0 the o-graphs with truncations used to define $\mathcal{J}_2$. If $\Gamma = \Gamma_0$ then we have with obvious meaning

$$[\hat{\Gamma}] = \sum_{u \in \mathcal{U}} m_1(u)[\hat{u}], \qquad [\hat{\Gamma}'] = \sum_{u \in \mathcal{U}} m_2(u)[\hat{u}]$$

and therefore these quantities are equal modulo $\mathcal{J}$.

Now it is false in general that $\Gamma = \Gamma_0$, because two phenomena can occur:

- there could be in Γ some non-truncated edge other than e_0;
- some truncated germ may have colour different than 0.

We show how to reduce to the case $\Gamma = \Gamma_0$ on two examples where these two phenomena occur separately and only once: the reader will easily complete the proof. The key point is that modulo $\mathcal{J}$ the bracket does not change if we make a replacement as follows:

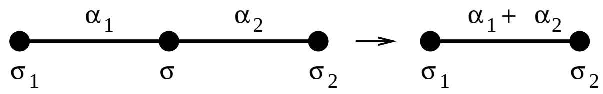

Here is how to treat a case where there is another closed edge (equalities hold modulo $\mathcal{J}$)

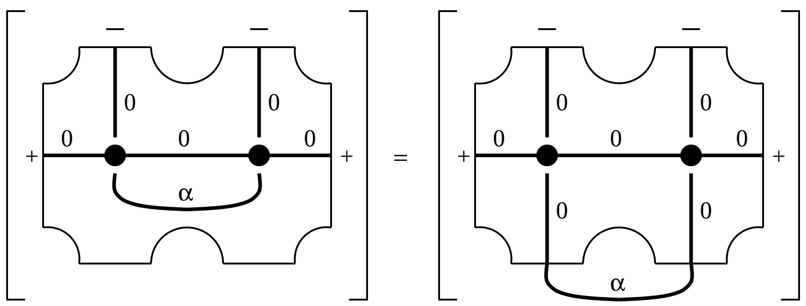

$= \sum_{p\in P_-^-} K_-^-(p,\alpha)\cdot$ 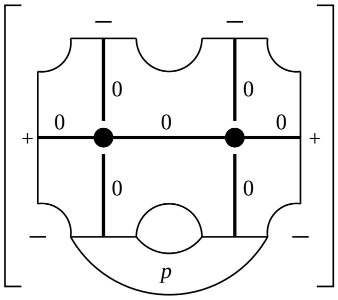

$= \sum_{p\in P_-^-} K_-^-(p,\alpha)\cdot$ 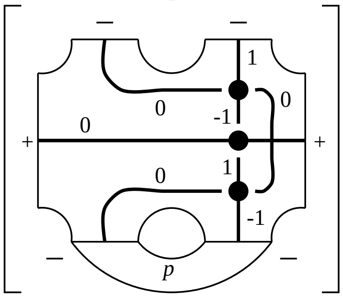

$=$ 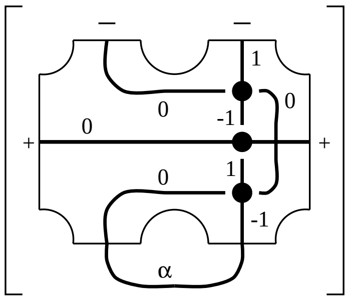

$=$ 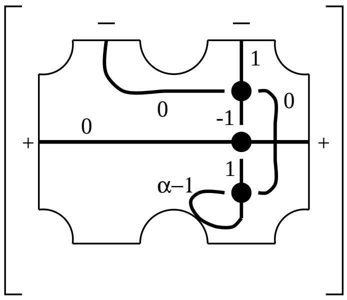

and in a similar way with less details for the case of a germ with non-zero colour

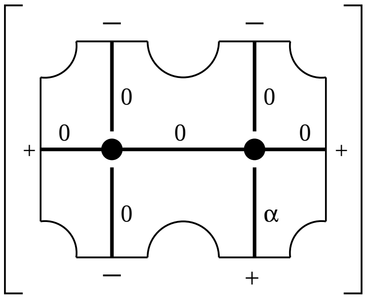

$= \sum_{p\in P_+^-} K_+^-(p,\alpha)\cdot$ 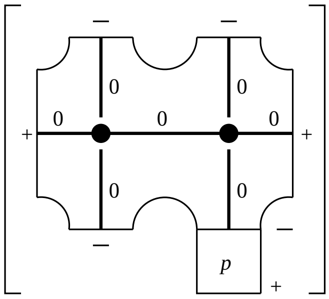

$= \sum_{p\in P_+^-} K_+^-(p,\alpha)\cdot$ 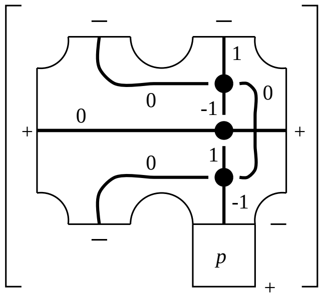

$=$ 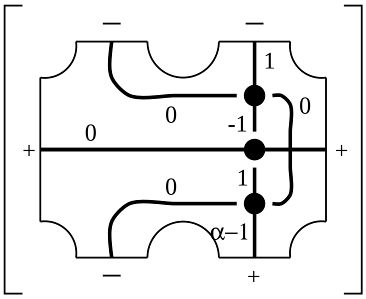

.

This concludes the proof. $\boxed{\text{IV.4.1}}$

As a final comment we mention the reason why we have chosen the name "hyperlocal" for the class of invariants given by Theorem IV.4.1. What the relators $\mathcal{J}$ ask is that inside a box around the move nothing actually changes with the move. The approach of the previous section (ideals $\mathcal{I}_0$ and $\mathcal{I}^1$) can be summarized as follows: inside a box around the move things change in such a way that, whatever we put outside, the whole thing (inside+outside) is actually unchanged. We also remark that the relators $\mathcal{J}_0$ allow a "canonical" choice of the box to put around the move. A hyperlocal approach to invariance without the relators $\mathcal{J}_0$ is possible, but we do not think it is very promising so we do not get into the details. The idea of introducing the relators $\mathcal{J}_0$ (which is natural but somewhat arbitrary, as we just said) goes in the direction of choosing finite reductions which have some special properties but still leave room for further choices.

IV.5 Turaev-Viro invariants as hyperlocal bracket invariants

We prove in this section that the invariants of Turaev and Viro [Tur-Vi] appear in the framework of Theorem IV.4.1 (and hence in particular in that of Theorem IV.3.1). It is particularly remarkable that our bracket depends on many parameters, and these invariants appear virtually all for the same choice of the parameters, at a low degree of complexity.

We first roughly recall how Turaev and Viro produce their invariants. They start with a finite set of colours A and a notion of what is an admissible triple of colours (i.e. they take a subset of $A^3/\mathfrak{S}_3$). They derive the notion of what is an admissible 6-tuple in the following way: given $(a_1, ..., a_6)$ they colour the edges of a tetrahedron so that (a_1, a_2, a_3) are the colours on a face and a_{i+3} is opposite to a_i, and they ask all the faces of the tetrahedron to be admissibly coloured. In some commutative ring Z they fix an invertible element z, an invertible element z_a for each $a \in A$ and an element $|T|$ for each admissibly coloured tetrahedron T. Then they assume that some complicated relations between these elements are satisfied (what is remarkable, of course, is that there are non-trivial models).

Given a triangulation of a closed manifold where the edges are admissibly coloured (in an obvious sense) they consider the number:

$$z^{-2\#\text{vertices}} \prod_{e \text{ edge}} z^2_{\text{colour of } e} \prod_{T \text{ tetrahedron}} |T|.$$

Then their result is that the sum over all admissible colorations of this number is an invariant of the manifold, i.e. it is independent of the triangulation.

For compact manifolds with non-empty boundary there is a definition of invariants "relative to a certain coloration of the boundary" which we do not want to get into. We just remark that for manifolds with boundary the same scheme as above works for ideal triangulations (*cf.* the end of Section I.1) and gives an invariant. Remark in particular that since there are no vertices z does not appear.

The method of Turaev and Viro to compute their invariants (and show that they are invariant indeed) is to use a more general version of Lemma I.1.10: nameley they associate to a triangulation the 2-skeleton of the dual cellularization (a quasi-standard polyhedron) and they deal with the moves which relate two such polyhedra arising from different triangulations. In the next result we show that the invariant of an ideally triangulated manifold with boundary is a hyperlocal bracket invariant as defined in Theorem IV.4.1. We emphasize that the next result applies only to the Turaev-Viro invariants defined through ideal decompositions. In particular we do not need to include z in the initial data of the invariant. Below we will provide a version which applies to closed manifolds.

Proposition IV.5.1. *Fix the data $Z, A, \{z_a\}, \{|T|\}$ of one of the invariants of Turaev and Viro, as described above. Then there exists a finite reduction $f : \{X_w\} \to Z$ and a point L of the variety of zeroes of the ideal $\mathcal{J} \subset \mathcal{R}^3_{3,f,A,Z}$ defined in Theorem IV.4.1 such that $[\Gamma]^3_{3,f,A,Z}(L)$ is the Turaev-Viro invariant in question of the manifold represented by Γ.*

Proof of IV.5.1. Let f be defined as follows:

$$f(X_{a_1\cdots a_t}) = \begin{cases} z_a^2 & \text{if } t > 0,\ a_1 = \ldots = a_t = a, \\ 0 & \text{otherwise,} \end{cases}$$

so that the equivalence classes of $\sim_f$ are naturally represented by A itself.

Now the ring where $[.]^3_{3,f,A,Z}$ takes values is $Z[K^{\sigma_1,3}_{\sigma_2,3}(p,\alpha), H^3_3(v)]$ with the usual notation and symmetries. Let L be the point defined by:

$$K^{\sigma_1,3}_{\sigma_2,3}(p,\alpha) = \begin{cases} 1 & \text{if } \sigma_1,\sigma_2,\alpha,p \text{ are as in Fig. IV.10,} \\ 0 & \text{otherwise,} \end{cases}$$

$$H^3_3(v) = \begin{cases} \begin{vmatrix} a_1 & a_2 & a_3 \\ a_4 & a_5 & a_6 \end{vmatrix} & \text{if } v \text{ is as in Fig. IV.11 and } (a_1,\ldots,a_6) \text{ is admissible,} \\ 0 & \text{otherwise.} \end{cases}$$

We first check that $[.]^3_{3,f,A,Z}$ is the Turaev-Viro invariant under consideration and later we will show that $\mathcal{J}(L) = 0$. We refer to Lemma I.1.10 which establishes the correspondence between standard spines and ideal triangulations. Figure I.17 implies that the edges of the ideal decomposition correspond to discs in the standard spine, so it is the discs that we must colour with the elements of A.

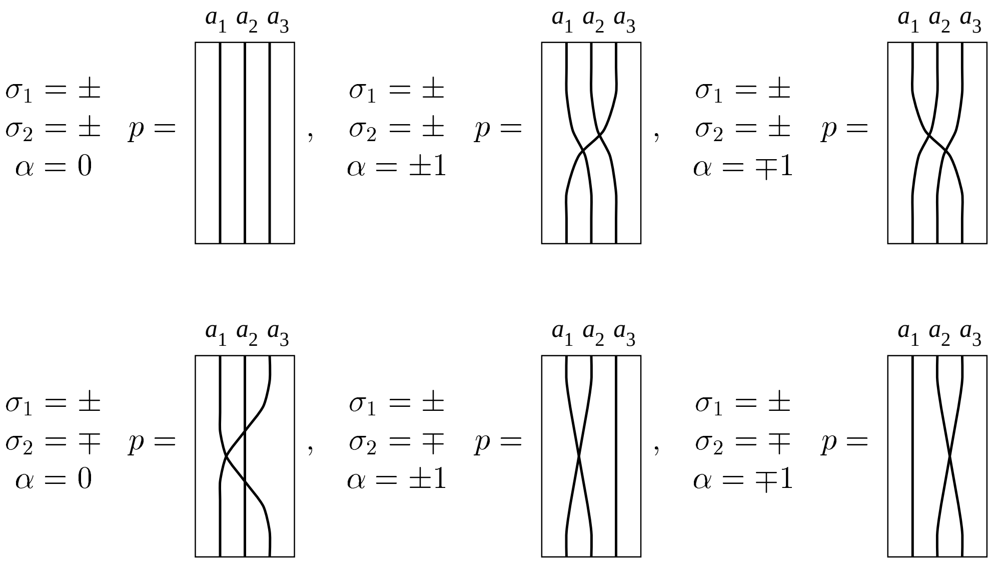

Figure IV.10: Cases where $K^{\sigma_1,3}_{\sigma_2,3}(p,\alpha)$ is 1

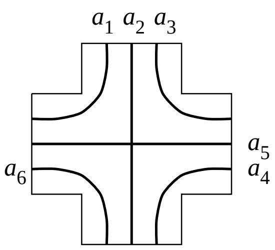

Figure IV.11: $H(v)$ is non-zero only if v is like this with $(a_1,\ldots,a_6)$ is admissible

Let us remark the following: if we use the skein relations to compute $[\Gamma]^3_{3,f,A,Z}$ we obtain $\sum l_i[\Gamma_i]$, where l_i is a product of K's and H's. If we evaluate this expression at the point L and we restrict the sum to non-zero l_i's all the totally decorated graphs Γ_i are geometrically identical (i.e. they differ only for the coloration). If one goes back to the construction of Section I.2 it is quite easy to see that the geometric circuits in these decorations correspond exactly to the discs of the spine.

Assume now $[\Gamma_i] \neq 0$; then on every circuit all the colours are the same, i.e. we have a coloration of every edge of the ideal tetrahedra decomposition. Moreover since $l_i \neq 0$ the coloration is admissible, and by definition $l_i[\Gamma_i]$ is the value of the coloration according to Turaev and Viro. Since we have the sum over all possible ways to colour the various bits, the result is the sum over all admissible colorations.

Now let $\mathcal{J}$ be the ideal of $Z[K^{\sigma_1,3}_{\sigma_2,3}(p,\alpha), H^3_3(v)]$ defined in Theorem IV.4.1. To show that $\mathcal{J}(L) = 0$ we show that all the generators of $\mathcal{J}$, evaluated at L, are 0.

For edge-associativity relators the proof essentially follows from the fact shown in Section I.2 that the geometric pattern defined by a colour $\alpha+\beta \in \mathbb{Z}_3$ is the geometric product of the patterns defined by α and β (see Fig. I.41). We leave to the reader to deal with A-colours and formally prove that $r(L) = 0$ when r is an edge-associativity relator.

We also leave to the reader the case of C-invariance relators, and we deal with the more complicated case of MP-invariance relators. The diagram before the move is expanded as follows:

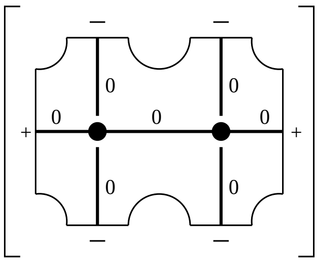

$$= \sum \begin{vmatrix} a_1 & a_2 & a_3 \\ a_4 & a_5 & a_6 \end{vmatrix} \begin{vmatrix} a_1 & a_2 & a_3 \\ a_7 & a_8 & a_9 \end{vmatrix} \cdot$$

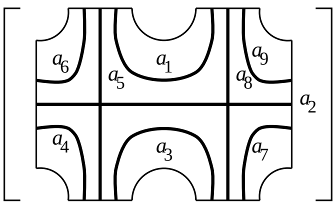

where all the brackets are evaluated at L and the sum extends over all indices $a_1, ..., a_9 \in A$ such that the tetrahedra symbols $|\,.\,|$ make sense (i.e. the tetrahedra are admissibly coloured). In a similar way after the move:

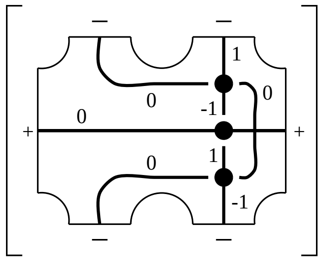

$$= \sum \begin{vmatrix} a_1 & a_5 & a_6 \\ a & a_9 & a_8 \end{vmatrix} \begin{vmatrix} a_2 & a_4 & a_6 \\ a & a_9 & a_7 \end{vmatrix} \begin{vmatrix} a_3 & a_7 & a_4 \\ a & a_5 & a_8 \end{vmatrix} \cdot$$

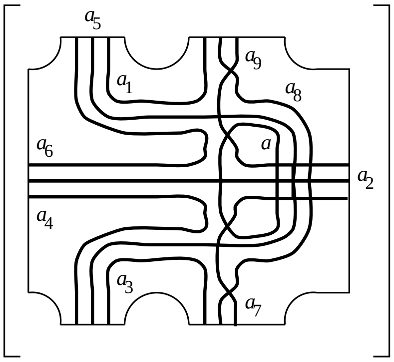

$$= \sum z_a^2 \begin{vmatrix} a_1 & a_5 & a_6 \\ a & a_9 & a_8 \end{vmatrix} \begin{vmatrix} a_2 & a_4 & a_6 \\ a & a_9 & a_7 \end{vmatrix} \begin{vmatrix} a_3 & a_7 & a_4 \\ a & a_5 & a_8 \end{vmatrix} \cdot$$

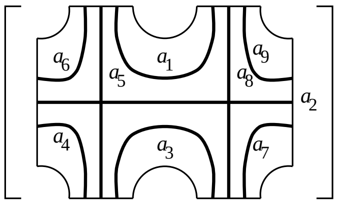

where again brackets are evaluated at L and the sum extends over indices $a_1, ..., a_9, a \in A$ such that all the tetrahedra symbols $|\,.\,|$ make sense.

The conclusion now follows from the fundamental Biedenharn-Elliot (pentagon) formula [Tur-Vi], [Ka-Li]. $\boxed{\text{IV.5.1}}$

Remark IV.5.2. Let us apply Proposition IV.5.1 to $A = \{a\}$, where (a, a, a) is acceptable, z is any invertible element, $z_a = z$ and $|(a, ..., a)| = z^{-2}$. Then the resulting invariant is z raised to twice the Euler chracteristic, i.e. the Euler characteristic of the boundary. This can be seen very easily using the above proof, from which it is evident that the bracket gives z raised to twice the number of discs of the spine minus twice the number of vertices. Since the edges are twice as many as the vertices this difference is just twice the Euler characteristic of the spine, i.e. of the manifold.

Proposition IV.5.3. *Let $A, Z, z, \{z_a\}, \{|T|\}$ be the initial data of a Turaev-Viro invariant. Then there exists a finite reduction $f : \{X_w\} \to Z$ and a point L of the variety of zeroes of the ideal $\mathcal{J} \subset \mathcal{R}^3_{3,f,A,Z}$ defined in Theorem IV.4.1 such that $[\Gamma]^3_{3,f,A,Z}(L)$ is the Turaev-Viro invariant in question of the closed manifold M whenever the o-graph Γ represents M with an arbitrary number of punctures.*

Proof of IV.5.3. This is essentially a combination of Proposition IV.5.1 and Remark IV.5.2, so we confine ourselves to a sketch. Let N be obtained by puncturing M, and consider an ideal decomposition of N. Since the boundary of N consists of spheres, if we add a vertex for each boundary component we have a cellular decompositon of M (in particular also genuine triangulations of M can be obtained in this way). The value of an admissible coloration of this triangulation of M is z to minus twice the number of boundary components times the value of the corresponding ideal triangulation of N.

Hence if we define the reduction as:

$$f(X_{a_1\cdots a_t}) = \begin{cases} z^{-2}z_a^2 & \text{if } t>0,\ a_1=...=a_t=a, \\ 0 & \text{otherwise} \end{cases}$$

and the point L by:

$$K^{\sigma_1,3}_{\sigma_2,3}(p,\alpha) = \begin{cases} 1 & \text{if } \sigma_1,\sigma_2,\alpha,p \text{ are as in Fig. IV.10,} \\ 0 & \text{otherwise,} \end{cases}$$

$$H_3^3(v) = \begin{cases} z^2 \begin{vmatrix} a_1 & a_2 & a_3 \\ a_4 & a_5 & a_6 \end{vmatrix} & \text{for } v \text{ as in Fig. IV.11 and } (a_1,...,a_6) \text{ admissible,} \\ 0 & \text{otherwise,} \end{cases}$$

we have that $[.]^3_{3,f,A,Z}(L)$ is the Turaev-Viro invariant, and the proof that $\mathcal{J}(L)=0$ is unchanged. $\boxed{\text{IV.5.3}}$

We conclude this section with the remark that the Turaev-Viro invariants can be found also at higher levels, not only at the $(3,3)$-one. One way to understand this is to see the Turaev-Viro invariants as colorations of the Euler characteristic (*cf.* Remark IV.5.2 and the proof of Proposition IV.5.1). Now we can produce many patterns which give integer multiples of the Euler characteristic, and an easy argument allows us to colour these patterns to obtain the Turaev-Viro invariants (remark however that we must be able to take roots of the elements of Z, which is always the case for concrete examples as $Z=\mathbb{C}$).

We know that the key point in computing the Euler characteristic is to be able to count the discs of the spine. We give examples of how to do this in the next result whose statement and proof are sketchy (details are left to the reader).

Proposition IV.5.4. *The rules of Fig. IV.12 and those of Fig. IV.13 lead to twice as many circles as the discs of the spine. The rules of Fig. IV.14 and those of Fig. IV.15 lead to three times as many circles as the discs of the spine.*

Proof of IV.5.4. For Figg. IV.12 and IV.14 this is obvious. From Section II.3 one sees that in Fig. IV.13 we are counting the discs on the boundary, and the conclusion follows. Figure IV.15 is a picture of the trivial 3-points-bundles

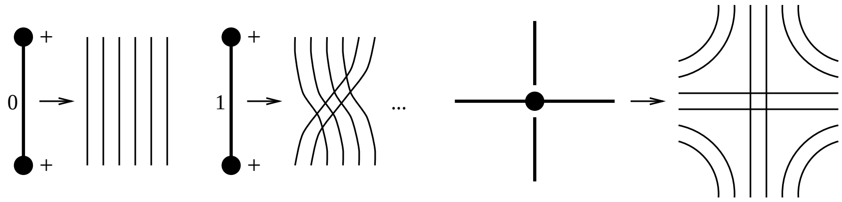

Figure IV.12: These rules allow us to compute twice χ

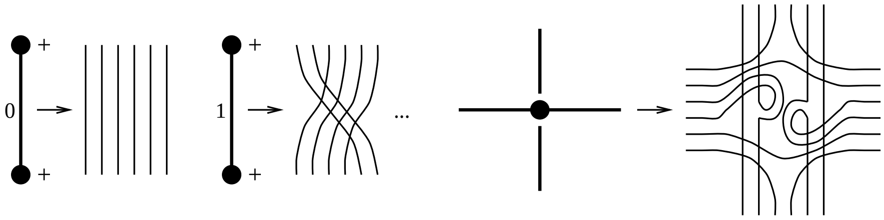

Figure IV.13: Also these rules allow us to compute twice χ

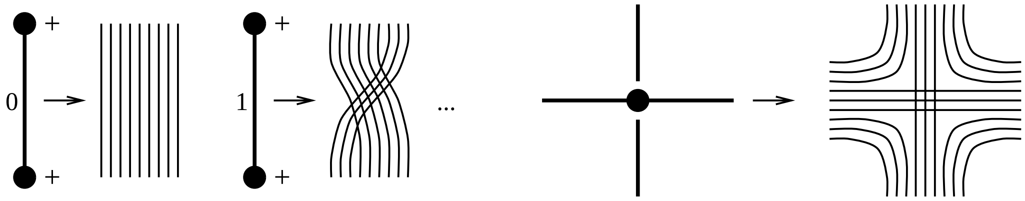

Figure IV.14: These rules allow us to compute three times χ

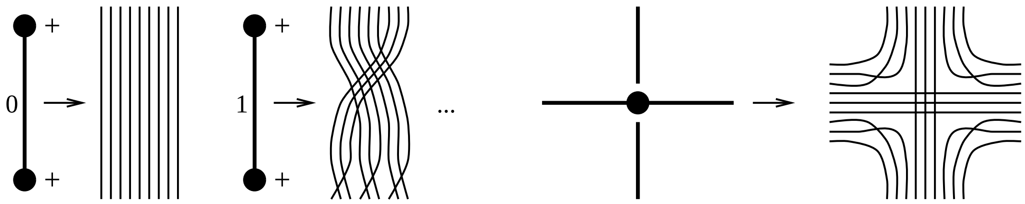

Figure IV.15: Also these rules allow us to compute three times χ

over the boundary of the discs of the spine, and again the conclusion easily follows. $\boxed{\text{IV.5.4}}$

One interesting feature of Proposition IV.5.4 is that, given the data of a Turaev-Viro invariant, at both the $(6,6)$-level and the $(9,9)$-level we find two points which enjoy the following properties:

1. They are "very far" from each other (nemely they are supported by essentially different geometric patterns);

2. They belong to the variety of zeroes of the ideal $\mathcal{J}$ defined in Theorem IV.4.1 (and therefore the same is true for the ideal $\mathcal{I}_0 + \mathcal{I}^1$ defined in Theorem IV.3.1);

3. The bracket evaluated at them gives the Turaev-Viro invariant.

These facts suggest that it could be an interesting problem to study the variety mentioned in point 2 and check whether the bracket is constant on it.

IV.6 Multiplicativity under connected sum

We show in this section that under a natural condition a numerical invariant obtained in the framework of Theorem IV.3.1 is, up to a normalization, multiplicative under connected sum. What we prove is actually more general (it applies to invariants whose values are not necessarily in a field), but it easily implies the more expressive fact just stated. This applies in particular to the invariants obtained by Theorem IV.4.1.

Fix integers $n_+, n_- \in \mathbb{N}$ with $n_+ + n_-$ even, a finite set A, a commutative ring with unit Z and a finite reduction f from the symbols $\{X_w\}_{w\in A^*}$ to some other commutative ring. Let $[.] = [.]^{n_+}_{n_-,f,A,Z} : \mathcal{O} \to \mathcal{R}$ be the associated bracket, where $\mathcal{R}$ is the ring of polynomials with coefficients in Z having some "free" indeterminates (the symbols K and H) and some variables which live in a ring (the $f(X_w)$'s).

Let $\mathcal{I} \subset \mathcal{R}$ be the ideal generated by $[\Gamma] - [\Gamma']$ where either:

- Γ is an (f, A)-completion of a graph with truncations having one vertex, and Γ' is obtained from Γ by move C at the vertex, or:

- Γ is an (f, A)-completion of a graph with truncations having two vertices, and Γ' is obtained from Γ by a move MP (when applicable).

In the language of Theorem IV.3.1 this is $\mathcal{I}_0 + \mathcal{I}^1$.

Let $\varphi : \mathcal{R} \to \mathcal{R}'$ be a homomorphism of commutative rings with unit such that $\mathrm{Ker}(\varphi) \supset \mathcal{I}$, whence $[.]' = \varphi\circ[.]$ defines an invariant of compact oriented 3-manifolds with boundary, which we denote by I. Remark that $[.]'$ is itself computed using skein relations, where the coefficients must be viewed under

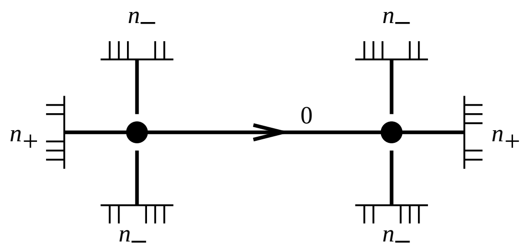

Figure IV.16: V is generated by completions of this diagram. We put the direction on the edge to emphasize that the diagram has a fixed position in the plane, so rotation through angle π is not the identity

φ (it is important for this aim that φ be a ring homomorphism and not only a homomorphism of additive groups).

Let V be the free $\mathcal{R}'$-module generated by (f, A)-completions of the diagram shown in Fig. IV.16

Given $\Gamma \in \mathcal{O}$ and a directed edge $\vec{e}$ of Γ which has colour 0 and positive distinct endpoints, we define $\pi_{\vec{e}}(\Gamma)$ as follows: apply the skein relations of $[.]'$ to all edges but e and to all vertices but the endpoints of e, and replace every closed circuit which appears by the appropiate coefficient. The result is in a natural way a linear combination with coefficients in $\mathcal{R}'$ of completions of the diagram of Fig. IV.16. Denote by W the $\mathcal{R}'$-submodule of V generated by all possible $\pi_{\vec{e}}(\Gamma)$'s.

The bracket $[.]'$ is of course well-defined on the generators of V, hence we can extend it by $\mathcal{R}'$-linearity to V, and consider its restriction to W, which we denote by $[.]'_W$.

Theorem IV.6.1. *Under the above assumptions, suppose also that:*

1. *There exists some manifold M whose invariant $I(M)$ is an invertible element of $\mathcal{R}'$.*
2. $\mathrm{Ker}([.]'_W)$ *is generated as an $\mathcal{R}'$-module by elements of the form*

$$\pi_{\vec{e}_1}(\Gamma_1) - \pi_{\vec{e}_2}(\Gamma_2)$$

where Γ_1 and Γ_2 are graphs representing the same manifold and $\vec{e}_1$ and $\vec{e}_2$ are such that the formula makes sense.

Then there exists a universal constant $c \in \mathcal{R}'$ such that

$$I(M_1 \# M_2) = c \cdot I(M_1) \cdot I(M_2).$$

In particular $I(.)/c$ is a multiplicative invariant.

Remark IV.6.2. Of course all the elements $\pi_{\vec{e}_1}(\Gamma_1) - \pi_{\vec{e}_2}(\Gamma_2)$ taken into consideration in assumption 2 belong to $\mathrm{Ker}([.]'_W)$.

Remark IV.6.3. The case one actually has in mind is that $\mathcal{R}'$ is a field, so that $\mathrm{Ker}([.]'_W)$ is a hyperplane of the finite-dimensional vector space W. So in this case the tools of linear algebra allow us to find easy sufficient conditions for property (2) to hold.

Proof of IV.6.1. Recall that in Proposition III.3.6 we have defined

$$(\Gamma_1, \vec{e}_1)\#(\Gamma_2, \vec{e}_2)$$

whenever $\vec{e}_i$ is a directed edge in Γ_i with colour 0 and positive distinct endpoints, and we have shown that this operation corresponds to taking the connected sum of the associated manifolds. Then $[.\ \#\ .]'$ is naturally defined as a bilinear symmetric function on $V \times V$, so in particular on $W \times W$. We claim that for all $w_1 \in \mathrm{Ker}([.]'_W)$ and $w_2 \in W$ we have:

$$[w_1 \# w_2]' = 0.$$

Using bilinearity, assumption 2 and the definition of W we can suppose that $w_1 = \pi_{\vec{e}_1}(\Gamma_1) - \pi_{\vec{e}_2}(\Gamma_2)$ where Γ_1 and Γ_2 are graphs representing the same manifold, and $w_2 = \pi_{\vec{e}}(\Gamma)$ where Γ is some o-graph.

Therefore we have to check that:

$$[\pi_{\vec{e}_1}(\Gamma_1)\#\pi_{\vec{e}}(\Gamma)]' = [\pi_{\vec{e}_2}(\Gamma_2)\#\pi_{\vec{e}}(\Gamma)]'.$$

It follows from the definition of $\#$ on graphs that

$$[\pi_{\vec{e}_1}(\Gamma_1)\#\pi_{\vec{e}}(\Gamma)]' = [(\Gamma_1, \vec{e}_1)\#(\Gamma, \vec{e})]'$$

Similarly

$$[\pi_{\vec{e}_2}(\Gamma_2)\#\pi_{\vec{e}}(\Gamma)]' = [(\Gamma_2, \vec{e}_2)\#(\Gamma, \vec{e})]'.$$

On the right-hand side of the previous two formulae we have brackets of graphs which represent the same manifold, and our claim is proved.

Now let M be a manifold such that $I(M)$ is invertible, and let Γ be any o-graph with at least two vertices representing M. Of course we can assume that Γ has an edge e with colour 0 and positive distinct endpoints, and give a direction to e. Then if we set $w = \pi_{\vec{e}}(\Gamma)$ we have $[w]'_W = I(M)$; we denote this fixed invertible element of $\mathcal{R}'$ by u.

Given any $w_1, w_2 \in W$ we have

$$w_1 - u^{-1} \cdot [w_1]'_W \cdot w \in \mathrm{Ker}[.]'_W$$

and then

$$\left[(w_1 - u^{-1} \cdot [w_1]'_W \cdot w)\#w_2\right]'_W = 0$$

that is

$$[w_1\#w_2]'_W = (u^{-1}\cdot[w\#w_2]'_W)\cdot[w_1]'_W.$$

So there exists a function $c: W\to\mathcal{R}'$ such that

$$[w_1\#w_2]'_W = c(w_2)\cdot[w_1]'_W.$$

Using w again and the symmetry we get

$$c(w_2) = (u^{-1}\cdot c(w))\cdot[w_2]'_W$$

and we deduce that for the universal constant $c = u^{-1}\cdot c(w)$ we have

$$[w_1\#w_2]'_W = c\cdot[w_1]'_W\cdot[w_2]'_W$$

for all $w_1, w_2\in W$.

Given two manifolds M_1 and M_2 represented by graphs Γ_1 and Γ_2 with edges $\vec{e}_1$ and $\vec{e}_2$ suitable for application of $\#$, we now have that:

$$\begin{aligned} I(M_1\#M_2) &= [(\Gamma_1,\vec{e}_1)\#(\Gamma_2,\vec{e}_2)]' = [\pi_{\vec{e}_1}(\Gamma_1)\#\pi_{\vec{e}_2}(\Gamma_2)]'_W \\ &= c\cdot[\pi_{\vec{e}_1}(\Gamma_1)]'_W\cdot[\pi_{\vec{e}_2}(\Gamma_2)]'_W = c\cdot[\Gamma_1]'\cdot[\Gamma_2]' = c\cdot I(M_1)\cdot I(M_2). \end{aligned}$$

The theorem is proved. $\boxed{\text{IV.6.1}}$

We have now a simple result of algebra which tells us that condition (1) is not very restrictive for non-trivial invariants.

Proposition IV.6.4. *Either* $[\Gamma]\in\sqrt{\mathcal{I}}$ *for all o-graphs* Γ *or there exists a homomorphism* $\varphi:\mathcal{R}\to\mathcal{R}'$ *of commutative rings with unit such that* $\mathrm{Ker}\varphi\supset\mathcal{I}$ *and* $\varphi\circ[.]$ *attains invertible values.*

Proof of IV.6.4. We give just a sketch. By first taking the quotient $\mathcal{R}/\mathcal{I}$ we can restrict to $\mathcal{I}=0$. Assume $x\notin\sqrt{0}$. We consider the ideal

$$S=\{y:\ yx^n=0 \text{ for some } n\ge 0\}$$

and by taking the quotient $\mathcal{R}/S$ we see that we can assume that no power of x is a divisor of 0. We set

$$\mathcal{R}'=\{y/x^n:\ y\in\mathcal{R}, n\ge 0\}$$

with $y/x^n\sim z/x^m$ if $yx^m=zx^n$. Then $\varphi(y)=y/x^0$ is a homomorphism and $\varphi(x)=1$.

Of course if $\varphi:\mathcal{R}\to\mathcal{R}'$ and $\varphi(x)$ is invertible then $x\notin\sqrt{I}$. $\boxed{\text{IV.6.4}}$

We conclude with some remarks concerning the case where condition (2) of Theorem IV.6.1 fails to be true.

Let W_0 be the space generated by differences $\pi_{\vec{e}_1}(\Gamma_1) - \pi_{\vec{e}_2}(\Gamma_2)$, as Γ_1 and Γ_2 represent the same manifold. Then the composition of $[.]'$ with the natural projection of W onto the quotient W/W_0 defines an invariant J of 3-manifolds which takes values in the $\mathcal{R}'$-module $X = W/W_0$. If $[.]'$ takes an invertible value and $W_0 = \mathrm{Ker}[.]'_W$ then J coincides with I and Theorem IV.6.1 applies.

If W_0 is a proper subset of $\mathrm{Ker}[.]'_W$ then J is a more general type of invariant (to fix the ideas, if $\mathcal{R}'$ is a field then X is an $\mathcal{R}'$-vector space which has dimension more than 1). Using the definition of # on graphs it is not difficult to check that there exists a fixed bilinear symmetric function $S : X \times X \to X$ such that

$$J(M_1 \# M_2) = S(J(M_1), J(M_2)).$$

This fact can be seen as a multiplicativity property for invariants whose values are not scalars.

IV.7 Experimental results

We mention in this section some computer experiments which we have carried out with the help of Francesco Amoroso, Carlo Traverso, Patrizia Gianni and Barry Trager. We warmly thank them all.

As announced, these computations have led to no new invariant of manifolds, but nonetheless we think that they might have some interest. In this section we systematically omit proofs. Our experiments all deal with the case where the colour set is $\mathbb{Z}_3$ itself and the skein relation for edges is the tautological one. The value on circuits is given as follows:

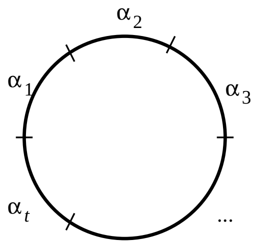

$= x_{\sum_{i=1}^t \alpha_i}$

(where the sum is taken in $\mathbb{Z}_3$), whereas the skein relation for vertices is:

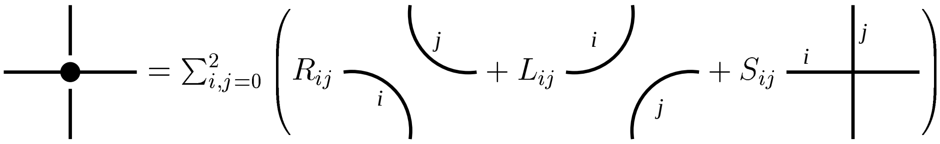

with the symmetry relations $R_{ij} = R_{ji}$ and $L_{ij} = L_{ji}$. This defines a bracket $[.]$ on $\mathcal{O}$ whose values are polynomials with integer coefficients in the 24 variables $x_i, R_{ij}, L_{ij}, S_{ij}$.

Basic bracket. Under the further specialization $R_{ij} = R\delta_i^0\delta_j^0$, $L_{ij} = L\delta_i^0\delta_j^0$,

$S_{ij} = S\delta_i^0\delta_j^0$ the resulting function $\langle . \rangle$ has been called basic bracket. We provide some evidence here of the fact that $\langle . \rangle$ defines non-trivial invariants of oriented spines. We recall that in Theorem IV.3.1 we have defined $\mathcal{I}_0$ as the ideal generated by all differences $\langle \Gamma' \rangle - \langle \Gamma \rangle$ where Γ is the completion of an o-graph with truncations and one vertex and Γ' is the corresponding completion of an o-graph obtained via move C from Γ. We know that $\langle . \rangle + \mathcal{I}_0$ is an invariant of oriented spines so in particular $\langle . \rangle(p)$ is an invariant when p is a solution of the system $\mathcal{I}_0(p) = 0$.

Proposition IV.7.1. *The solutions of the system $\mathcal{I}_0(p) = 0$ are exactly those which factor through the following:*

1. $x_0 = x_1 = x_2 = 1$;
2. $x_0 = x_1 = x_2$, $R = L = S$;
3. $x_0 = -4$, $x_1 = x_2 = 2$, $R = L = S$.
4. $x_\alpha = x_0 t^\alpha$, $R = tS$, $L = t^2 S$ *with* $1 \neq t$ *a cubic root of* 1;
5. $x_\alpha = t^\alpha$, $R + L + S = 0$ *with* t *as above;*
6. $x_\alpha = -2t^\alpha$, $R + tL + t^2 S = 0$ *with* t *as above;*
7. $x_0 = 2$, $x_1 = -t$, $x_2 = -t^2$, $R = tS$, $L = t^2 S$ *with* t *as above.*

Some of these solutions of course give trivial invariants, and several properties can be observed for the other solutions. We confine ourselves to mentioning a few interesting facts.

Proposition IV.7.2. *There are exactly* 6 *oriented standard spines with one vertex, and the invariant given by solution 7 tells them apart from each other.*

Remark IV.7.3. For the invariants associated to solutions 4 and 6 the following holds: if $\Gamma \in \mathcal{O}$, the sum of the colours in Γ is α and Γ_0 is obtained from Γ by setting all the colours to 0 then the value of Γ is t^α times the value of Γ_0. Solution 4 gives as bracket S raised to the number of vertices times a polynomial in $x = x_0$ which we denote by $\langle . \rangle_t$.

In the sequel the uncoloured version Γ_0 of an o-graph Γ will be called the "geometric form" of Γ. In the next two results we show how $\langle . \rangle_t$ can be used to partially classify o-graphs with 2 and 3 vertices. This can be useful when trying to construct examples.

Proposition IV.7.4. *Every o-graph with two vertices, using moves* C, *can be transformed in one and only one of the geometric forms shown in Fig. IV.17, and the value of $\langle . \rangle_t$ allows us to say which one.*

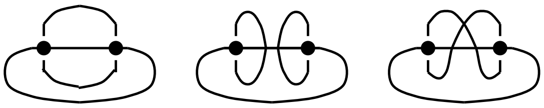

Figure IV.17: Geometric forms for o-graphs with two vertices

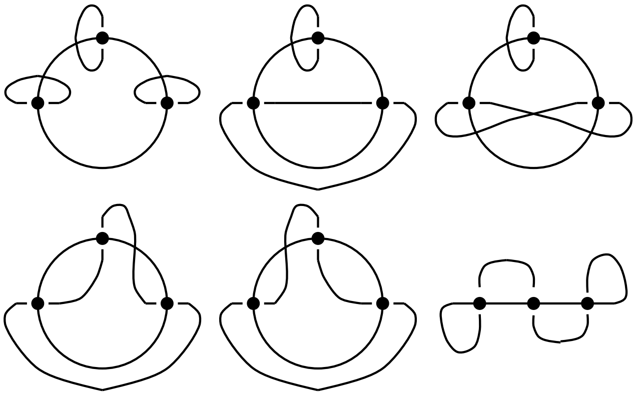

Figure IV.18: Geometric forms for o-graphs with three vertices

Proposition IV.7.5. *Every o-graph with three vertices, using moves* C*, can be transformed in one and only one of the geometric forms shown in Fig. IV.18. If the o-graph contains no triangle the corresponding form is the last one, otherwise the value of* $\langle . \rangle_t$ *tells which of the first five forms is appropriate.*

The next result implies that $\langle . \rangle$ is not useful for studying manifolds. We recall that in Theorem IV.3.1 we have defined $\mathcal{I}^1$ as the ideal generated by all differences $\langle \Gamma' \rangle - \langle \Gamma \rangle$ where Γ is the completion of an o-graph with truncations and two vertex and Γ' is the corresponding completion of an o-graph obtained via move MP from Γ. We know that $\langle . \rangle + \mathcal{I}_0 + \mathcal{I}^1$ is an invariant of manifolds.

Theorem IV.7.6. *If* p *is a solution of the systems* $\mathcal{I}_0(p) = 0$ *and* $\mathcal{I}^1(p) = 0$ *then* $\langle . \rangle(p)$ *is constant.*

Other brackets. We go back now to the bracket $[.]$ defined at the beginning of the section and mention the three explicit computations which we have carried out. In the first two experiments we have taken respectively:

1. $R_{ij} = R\delta_i^0\delta_j^0 + L\delta_i^1\delta_j^1 + S\delta_i^{-1}\delta_j^{-1}$,
   $L_{ij} = L\delta_i^0\delta_j^0 + S\delta_i^1\delta_j^1 + R\delta_i^{-1}\delta_j^{-1}$,
   $S_{ij} = S\delta_i^0\delta_j^0 + R\delta_i^1\delta_j^1 + L\delta_i^{-1}\delta_j^{-1}$.
2. $R_{ij} = R\delta_i^{-1}\delta_j^{-1}$, $L_{ij} = L\delta_i^1\delta_j^1$, $S_{ij} = S\delta_i^0\delta_j^0$.

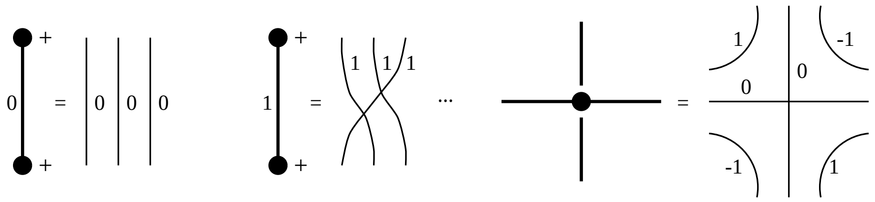

Figure IV.19: How to colour the Euler characteristic patterns getting null total colours

The motivation for (1) is that this choice corresponds to summing the basic bracket over all C-conjugates of an o-graph, so that in particular the bracket under (1) is automatically invariant under C. The motivation for (2) is that if one wants to colour the patterns which give the Euler characteristic in such a way that the total colour of each circuit is automatically 0, the recipe is as shown in Fig. IV.19 (compare with Proposition IV.5.4: actually Fig. IV.19 is a translation of Fig. IV.15). The "naturality" of the specialization (2) reflects in a certain flexibility which remains after having imposed the C-invariance relations.

Under both specializations (1) and (2) the bracket takes values in the ring $\mathbb{Z}[x_0, x_1, x_2, R, L, S]$. After considering the C-invariance ideal $\mathcal{I}_0$ (which is 0 in case (1) and rather harmless in case (2)) we need to take the MP invariance ideal $\mathcal{I}^1$. This has a priori $15 \times 27 = 405$ generators, but with some care it is not diffucult to reduce to 111 only. The quotient $\mathbb{Z}[x_0, x_1, x_2, R, L, S]/(\mathcal{I}_0 + \mathcal{I}^1)$ is of course non-zero (for instance for $x_0 = x_1 = x_2 = 1$ and $R + L + S = 1$ we get the constant invariant $1 \neq 0$). However by computer we have checked that:

Proposition IV.7.7. *Under (1) and under (2) the function $\Gamma \mapsto [\Gamma] + \mathcal{I}_0 + \mathcal{I}^1$ is constant on o-graphs with two vertices.*

Now it is not difficult to deduce from this that:

Proposition IV.7.8. *Under (1) and under (2) the function $\Gamma \mapsto [\Gamma] + \mathcal{I}_0 + \mathcal{I}^1$ is constant on the set of o-graph.*

Now for the most general bracket [.] the approach to invariants via Theorem IV.3.1 has an excessive complexity (the bracket of an o-graph with 3 vertices is a polynomial which is the sum of a priori as many as $27^3 = 19683$ monomials, and we have 111 generators of $\mathcal{I}^1$ which involve such big polynomials. So for the general bracket we have confined ourselves to the hyperlocal approach of Theorem IV.4.1. Actually one easily sees that a "mixed" local and hyperlocal approach always works, i.e. $[.] + \mathcal{J}_0 + \mathcal{I}_0 + \mathcal{J}_2$ is an invariant of 3-manifolds. Moreover for [.] the skein relation for edges is automatically associative, i.e. $\mathcal{J}_0 = 0$. Unfortunately what the computer said is:

Proposition IV.7.9. $\mathcal{I}_0 + \mathcal{J}_2 = \mathbb{Z}[x_0, x_1, x_2, R, L, S]$.

As a final comment we mention the fact that in all our experiments the computer has been able to find in a reasonable time the Gröbner basis of the ideal, which has made it rather fast to check the triviality properties stated for the invariants.

Bibliography

[Ad-Hi-We] C. C. Adams – M. Hildebrand – J. Weeks, *Hyperbolic invariants of knots and links.* Trans. Amer. Math. Soc. **326** (1991), 1-56.

[Be-Pet1] R. Benedetti – C. Petronio, Lectures on Hyperbolic Geometry. Universitext, Springer-Verlag, Berlin-Heidelberg-New York, 1992.

[Be-Pet2] R. Benedetti – C. Petronio, *A finite graphic calculus for 3-manifolds and related bracket invariants.* Preprint, 1994.

[Be-Pet3] R. Benedetti – C. Petronio, *On Roberts' proof of the Turaev-Walker theorem.* Preprint, 1994.

[Bi-De] D. Bienstock – N. Dean, *New results on rectilinear crossing number and plane embeddings.* J. Graph. Theory **16** (1992), 389-398.

[Ca] B. G. Casler, *An imbedding theorem for connected* 3*-manifolds with boundary.* Proc. Amer. Math. Soc. **16** (1965), 559-566.

[Ep-Pen] D. B. A. Epstein – R. Penner, *Euclidean decomposition of non-compact hyperbolic manifolds.* J. Diff. Geom. **27** (1988), 67-80.

[Ep-Pet] D. B. A. Epstein – C. Petronio, *An exposition of Poincaré's polyhedron theorem.* Enseign. Math. **40** (1994), 113-170.

[Er-Gu] P. Erdös – R. K. Guy, *Crossing number problems.* Amer. Math. Monthly **80** (1973), 52-58.

[Fen-Rou] R. A. Fenn – C. P. Rourke. *On Kirby's calculus on links.* Topology **18** (1979), 1-15.

[Fer-Gag] M Ferri – C. Gagliardi, *Crystallization moves.* Pacific J. Math. **100** (1982), 85-103.

[Gar-Jo] M. R. Garey – D. S. Johnson, *Crossing number is NP complete*. SIAM J. Alg. Discrete Math. **4** (1983), 312-316.

[Gu] R. K. Guy, *Crossing numbers of graphs*. In: "Graph theory and its applications", Michigan, 1972 (Alavi-Lick-White editors), Lecture Notes in Math. 303, Springer, Berlin, 1972. Pagg. 111-124.

[Hem] J. Hempel, 3-manifolds. Ann. of Math. Stud. 86, Princeton University Press, Princeton NJ, 1976.

[Hen-We] S. R. Henry, J. R. Weeks, *Symmetry groups of hyperbolic knots and links*. J. Knot Theory Ramifications, **1** (1992), 185-201.

[Ja] W. H. Jaco, Lectures on 3-manifolds topology. Regional Conference Series in Math. 43, Amer. Math. Soc, Providence RI, 1980.

[Ka] L. H. Kauffman, *State models and the Jones polynomial*. Topology **26** (1987), 395-407.

[Ka-Li] L. H. Kauffman – S. Lins, Temperley-Lieb recoupling theory and invariants of 3-manifolds. Princeton University Press, Princeton NJ, 1994.

[Ki] R. Kirby, *A calculus for framed links in* S^3. Invent. Math. **105** (1978), 35-46.

[Li-Man] S. Lins – A. Mandel, *Graph-encoded 3-manifolds*. Disc. Math. **57** (1985), 261-284.

[Mat1] S. V. Matveev, *Special spines of piecewise linear manifolds*. Math. USSR-Sb. **21** (1973), 279-291.

[Mat2] S. V. Matveev, *Universal 3-deformations of special polyehdra*. Russ. Math. Surv. **42** (1987), 226-227.

[Mat3] S. V. Matveev, *Transformations of special spines and the Zeeman conjecture*. Math. USSR-Izv. **31** (1988), 423-434.

[Mat-Fo] S. V. Matveev – A. T. Fomenko, *Constant energy surfaces of Hamiltonian systems, enumeration of three-dimensional manifolds in increasing order of complexity, and computation of volumes of closed hyperbolic manifolds*. Russ. Math. Surv. **43** (1988), 3-25.

[Mi1] J. Milnor, Morse theory. Ann. of Math. Stud. 51, Princeton University Press, Princeton NJ, 1963.

[Mi2] J. Milnor, Lectures on the h-cobordism theorem. Princeton University Press, Princeton NJ, 1965.

[Morg] J. W. Morgan, *On Thurston's uniformization theorem for three-dimensional manifolds.* In: "The Smith conjecture" (Morgan-Bass editors), Academic Press Inc., New York, 1984.

[Mort] H. R. Morton, *Invariants of links and 3-manifolds from skein theory and from quantum groups.* NATO Summer Institute 1992, 1-51.

[Pa] U. Pachner. *P.L. homeomorphic manifolds are equivalent by elementary shellings.* Europ. J. Combinatorics **12** (1991), 129-145.

[Pet] C. Petronio, *An algorithm producing hyperbolicity equations for a link complement in* S^3. Geom. Ded. **44** (1992), 67-104.

[Pi] R. Piergallini, *Standard moves for standard polyhedra and spines.* Rendiconti Circ. Mat. Palermo **37**, suppl. 18 (1988), 391-414.

[Rol] D. Rolfsen, Knots and links. Mathem. Lecture Series 7, Publish or Perish, Berkeley CA, 1976.

[Rou] C. P. Rourke, *A new proof that* Ω_3 *is zero.* J. London Math. Soc. **31** (1985), 373-376.

[Rou-Sa] C. P. Rourke – B. J. Sanderson, An introduction to piecewise linear topology. Ergebn. der Math. Bd. 69, Springer-Verlag, Berlin-Heidelberg-New York, 1982.

[Tho] C. Thomassen, *Planarity and duality of finite and infinite graphs.* J. Comb. Theory **29** (1980), 244-271.

[Thu1] W. P. Thurston, *The geometry and topology of three-manifolds.* Princeton University Mathematics Department (1979).

[Thu2] W. P. Thurston, *Three dimensional manifolds, kleinian groups and hyperbolic geometry.* Bull. Amer. Math. Soc. **6** (1982), 357-381.

[Thu3] W. P .Thurston, *Hyperbolic structures on* 3*-manifolds.* Ann. of Math. **124** (1986), 203-246.

[Tur] V. G. Turaev, Quantum invariants of knots and 3-manifolds. de Gruyter Stud. in Math, Berlin-New York, 1994.

[Tur-Vi] V. G. Turaev – O. Ya. Viro, *State sum invariants of* 3*-manifolds and quantum* $6j$*-symbols.* Topology **31** (1992), 865-902.

[Tut1] W. T. Tutte, *How to draw a graph.* Proc. London Math. Soc. **13** (1963), 743-768.

[Tut2] W. T. Tutte, *Towards a theory of crossing numbers.* J. Combinatorial Theory **8** (1970), 45-63.

[We] J. Weeks, *SNAPPEA.* The hyperbolic structures computer program, 1990.